

# Review of the first W boson mass measurement with the ATLAS Detector

F. Balli, on behalf of the ATLAS collaboration  
CIPANP 2018, Palm Springs

# Outline

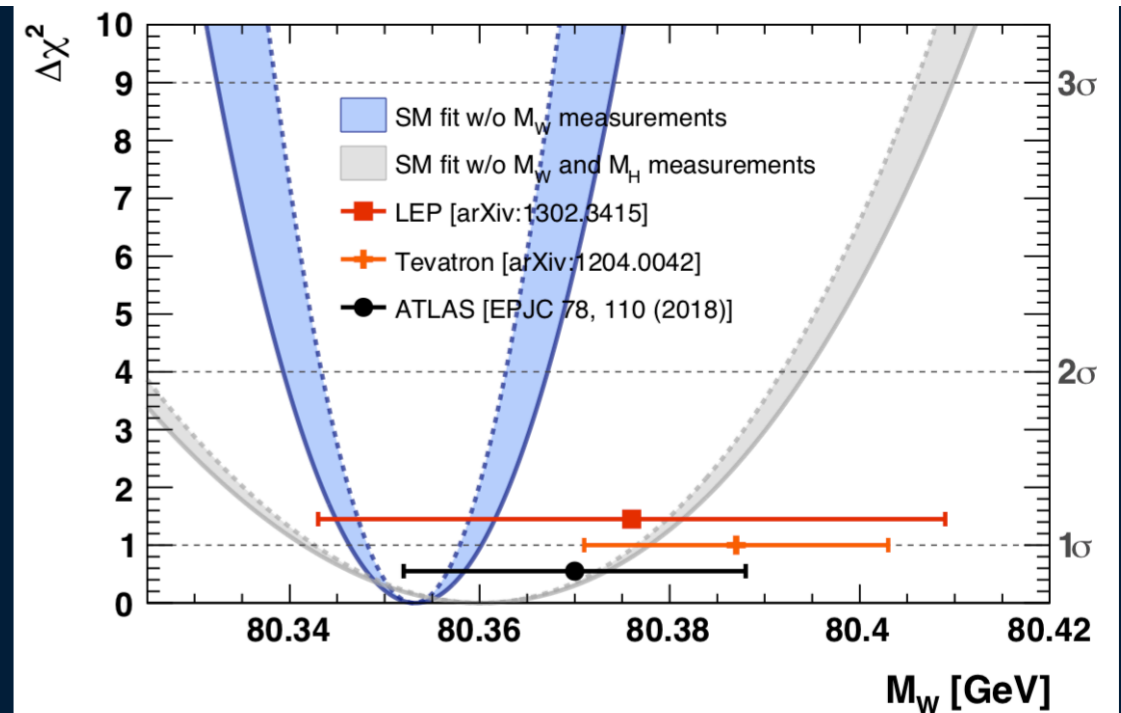
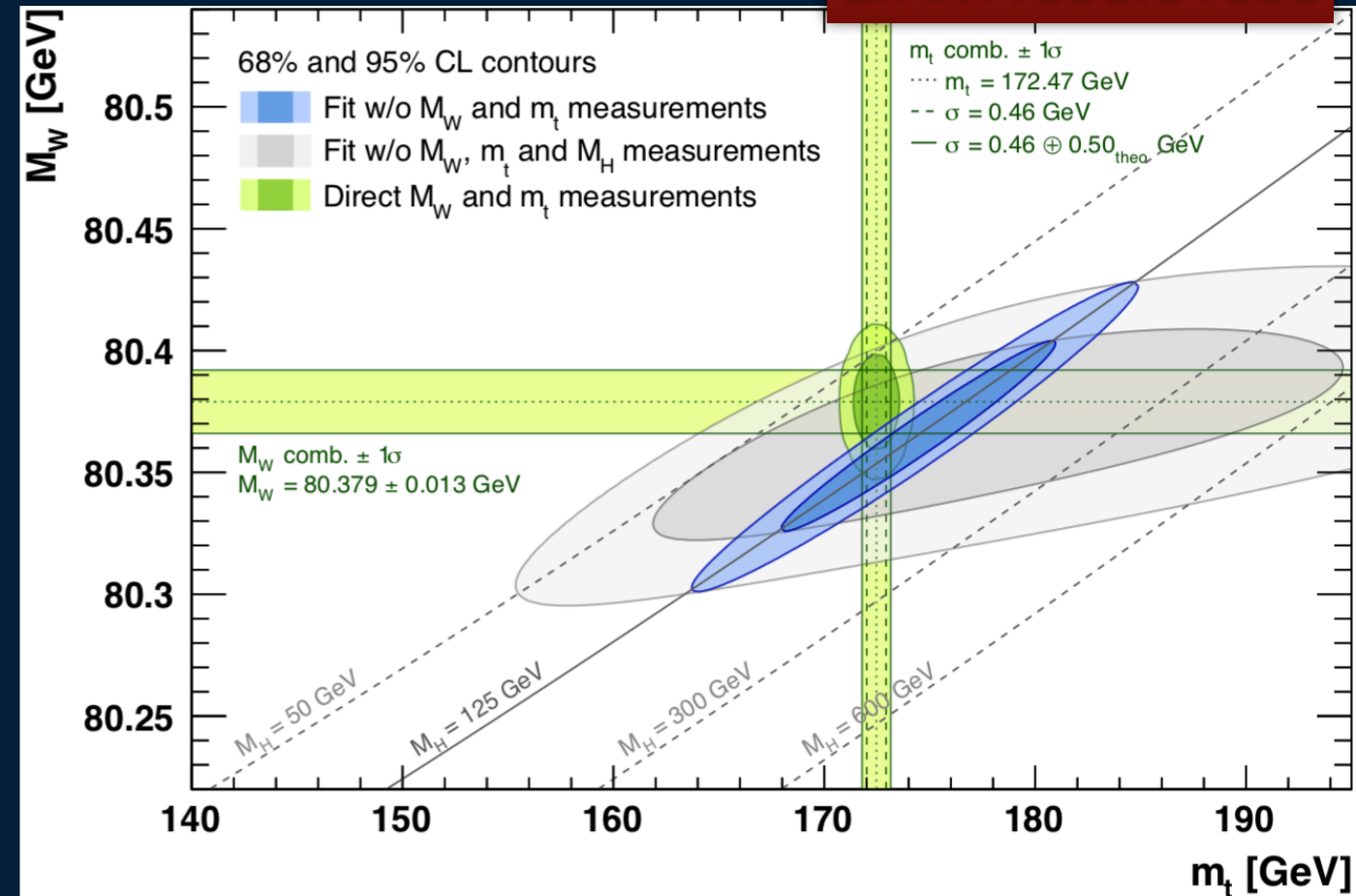
- Introduction
- Modeling aspects
- Experimental aspects
- Conclusion and summary

Eur. Phys. J. C 78 (2018) 110

# Introduction

- Strong physics motivation for high precision W mass measurement (‰)
  - Electroweak fit (allowed  $m_W$  values from SM predictions) : natural goal of 7 MeV
  - Constraints on new physics (NP) — target 5 MeV according to theorists
- Long and steady efforts throughout HEP colliders history to reach the current precision

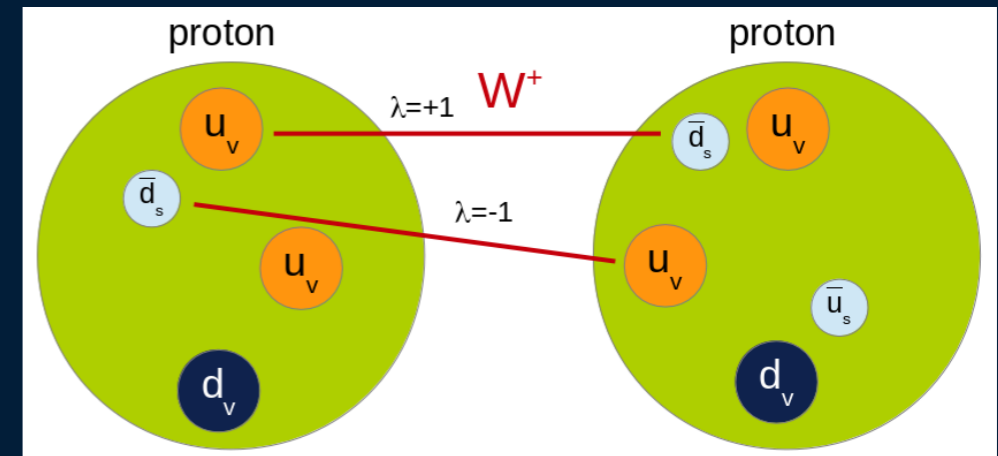
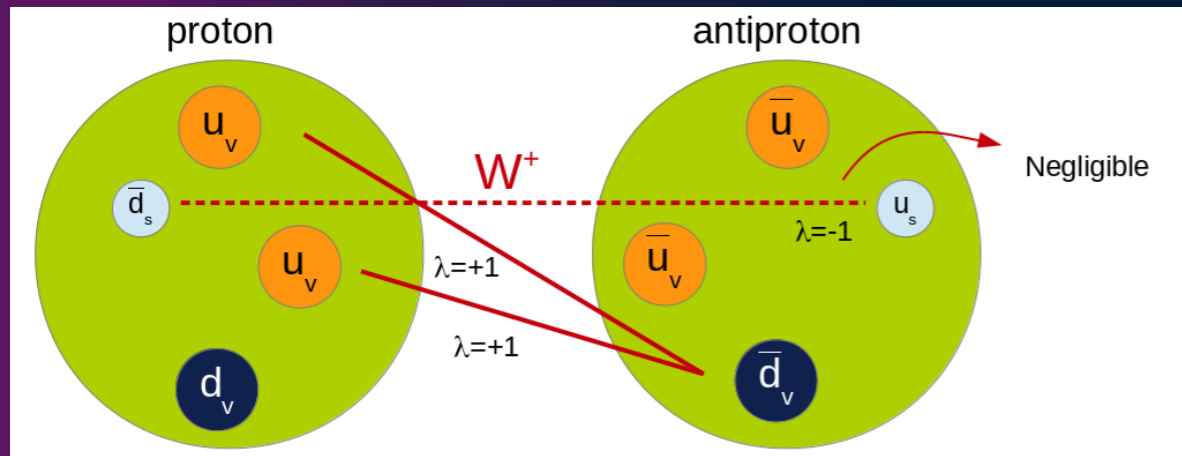
arXiv:1803.01853



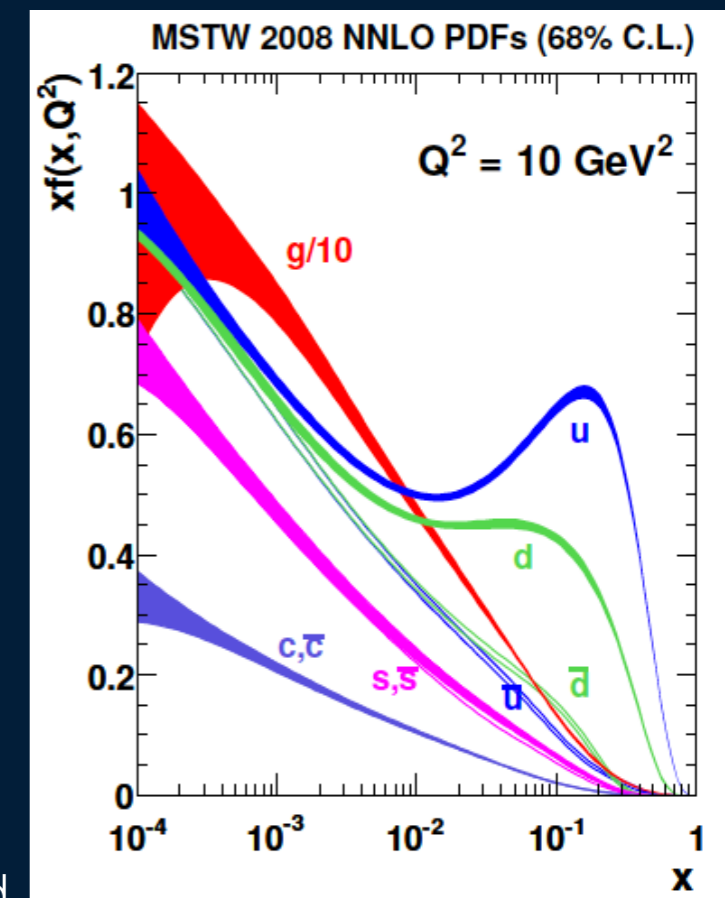
Current world average  
(Tevatron):  
 $m_W = 80.385 \pm 0.015 \text{ GeV}$



# W mass at LHC : more data, larger challenges



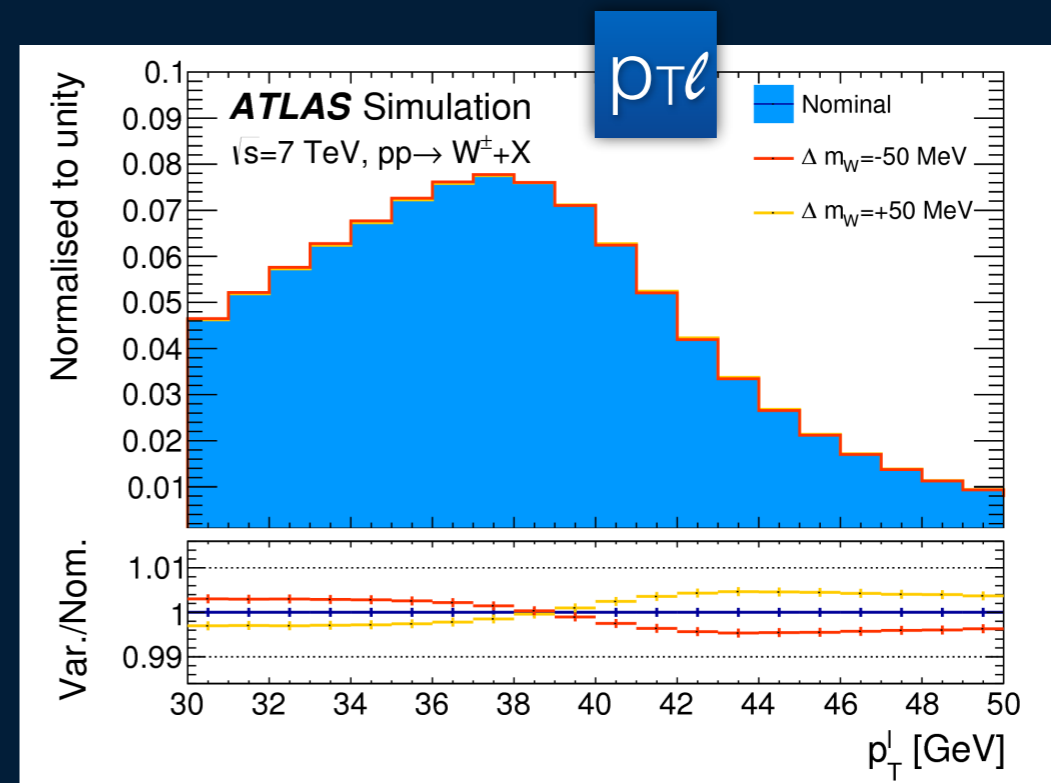
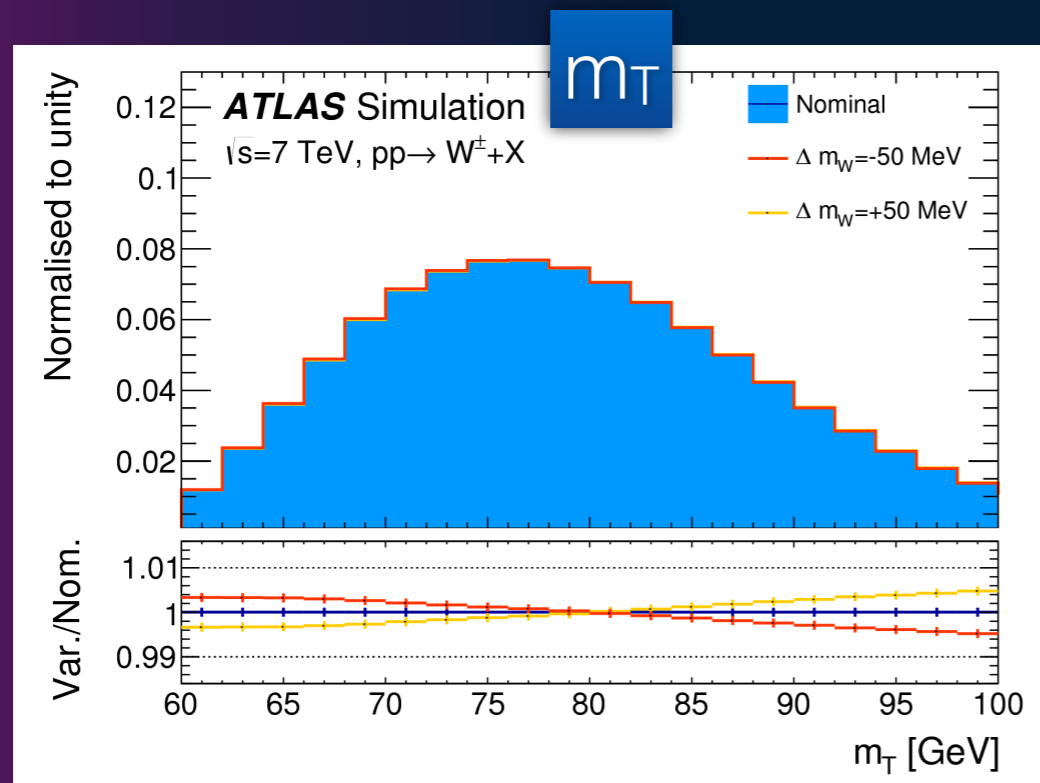
- In  $pp$  (as opposed to  $p\bar{p}$ )  $W^+/W^-$  boson production is asymmetric
  - Different contributions from sea/valence quarks
    - Charge dependence of  $p_T$  spectrum and thus on the measurements observables ( $p_{T\ell}$  and  $m_T$ , see next slide)
- More heavy flavour initiated production (25% of the W production is induced by at least one second generation quark s or c)
- $W^+$ ,  $W^-$  and Z are produced by different light flavour fractions
  - W measurements rely heavily on Z measurements
- Larger gluon-induced W production
- Large PDF-induced W-polarisation uncertainty (valence vs sea quarks)
- Strange quark pdf uncertainty  $\rightarrow$  uncertainty on the relative fraction of charm-initiated W boson  $\rightarrow$  alter the balance between valence quark and sea quark





# Analysis strategy

- Measurement's methodology :
  - obtain predictions with simulated events for signal and background (except data-driven multijet background)
  - to extract the result, compare data and predictions for distributions sensitive to  $m_W$  (lepton  $p_T$ , transverse W mass  $m_T$ ) by performing a template  $\chi^2$  fit
- Very simple in principle, but extremely challenging in practice as it requires at the 1/10,000 level :
  - Accurate theoretical description of W production and decay kinematics in the simulation
  - Precise calibration of the detector
- Fully reconstructed mass in Z-boson sample to validate the analysis and to provide significant experimental and theoretical constraints (ancillary measurements)



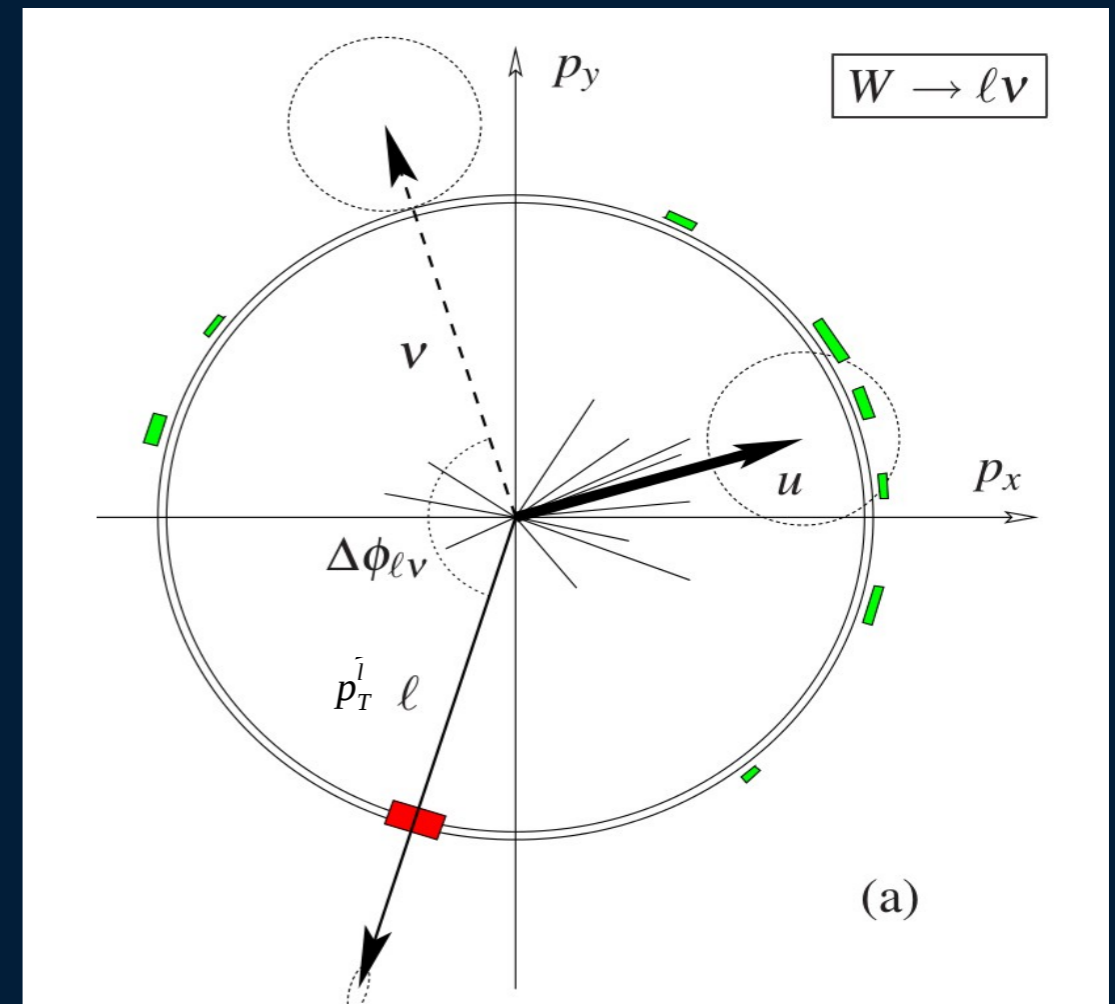
# Measurement's categories

Decay channel	$W \rightarrow e\nu$	$W \rightarrow \mu\nu$
Kinematic distributions	$p_T^\ell, m_T$	$p_T^\ell, m_T$
Charge categories	$W^+, W^-$	$W^+, W^-$
$ \eta_\ell $ categories	[0, 0.6], [0.6, 1.2], [1.8, 2.4]	[0, 0.8], [0.8, 1.4], [1.4, 2.0], [2.0, 2.4]

- Measurement performed in 2 channels, using 2 observables, 2 charge categories, 3 (4)  $|\eta(\text{lepton})|$  bins in the electron (muon) channel
  - In total, 28 different values of  $m_W$  are extracted
  - Allows to :
    - Thoroughly validate the physics modelling
    - benefit from different sensitivities to systematic uncertainties

# Event selection

- Lepton selection
  - muon :  $p_T > 30 \text{ GeV}$ ,  $|\eta| < 2.4$ , track-based isolation
  - electron :  $p_T > 30 \text{ GeV}$ ,  $|\eta| < 1.2$  or  $1.8 < |\eta| < 2.4$ , track and calorimeter-based isolation
- Recoil :  $u_T < 30 \text{ GeV}$
- $m_T > 60 \text{ GeV}$ ,  $p_T^{\text{miss}} > 30 \text{ GeV}$



$\vec{u}_T$  : vector sum of calorimeter deposits excluding lepton deposits

$$\vec{p}_T^{\text{miss}} = -(\vec{u}_T + \vec{p}_{T\ell})$$

$$m_T = \sqrt{[2 p_{T\ell} p_T^{\text{miss}} (1 - \cos\Delta\phi)]}$$



# MODELING ASPECTS

# Introduction to the modeling

- Factorisation of cross-section under 4 terms
  - Approximation checked and valid at 2 MeV level for  $m_W$

spherical harmonics

$$\frac{d\sigma}{dp_1 dp_2} = \left[ \frac{d\sigma(m)}{dm} \right] \left[ \frac{d\sigma(y)}{dy} \right] \left[ \frac{d\sigma(p_T, y)}{dp_T dy} \left( \frac{d\sigma(y)}{dy} \right)^{-1} \right] \left[ (1 + \cos^2 \theta) + \sum_{i=0}^7 A_i(p_T, y) P_i(\cos \theta, \phi) \right]$$

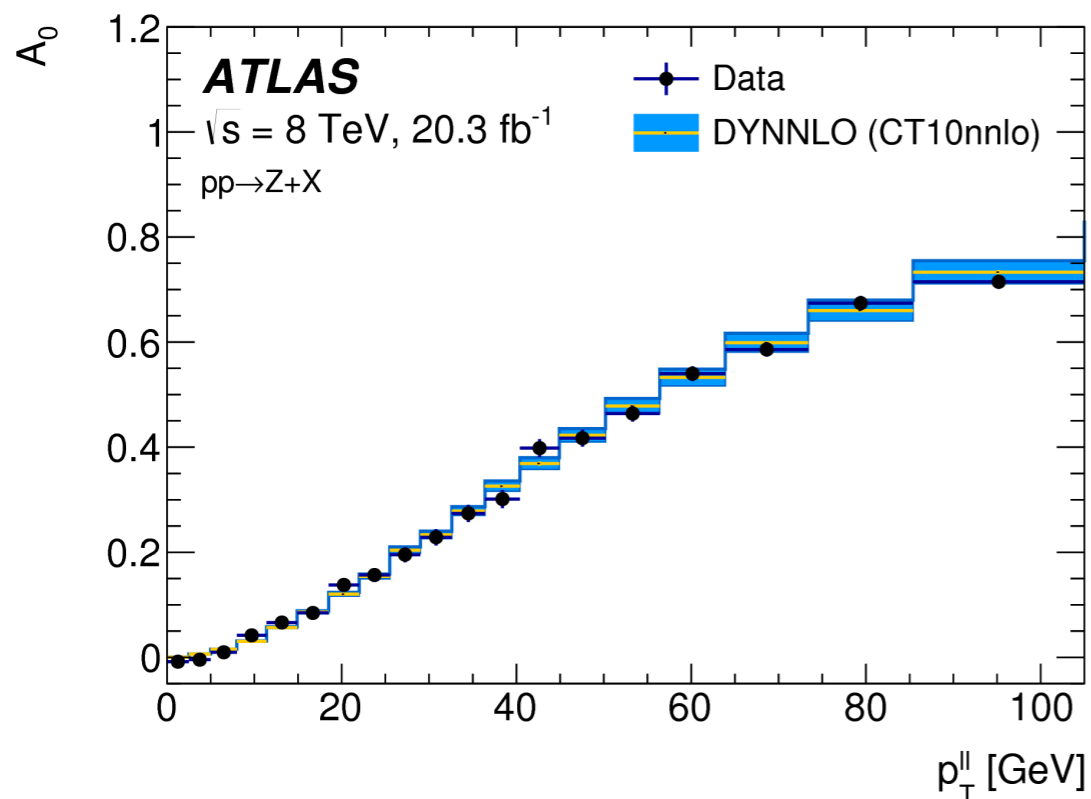
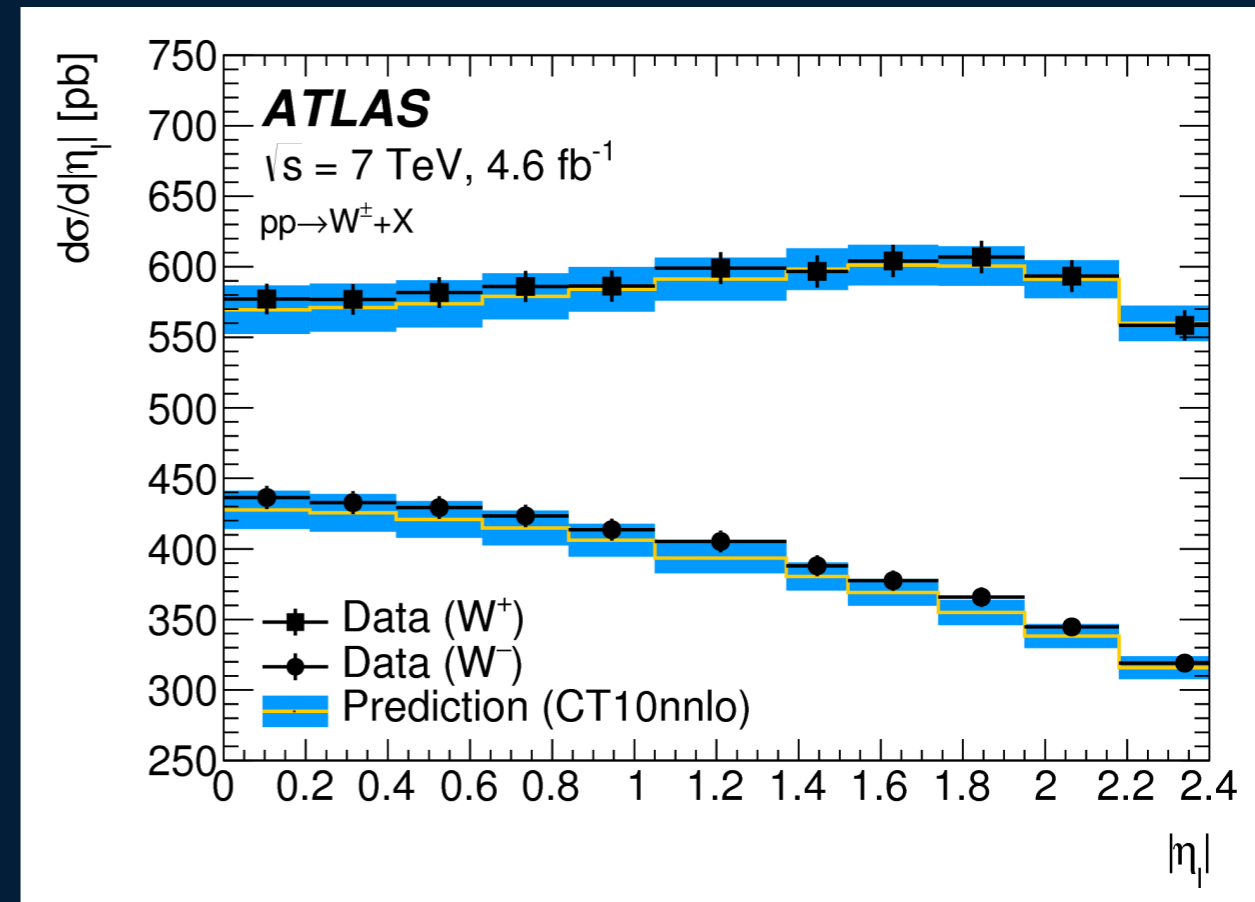
- Baseline MC is Powheg+Pythia8
- $d\sigma(m)/dm$  modeled with Breit Wigner
- Other terms : reweight baseline MC according to various predictions
  1.  $d\sigma(y)/dy$  : fixed-order NNLO prediction from DYNNLO
  2.  $p_T$  at a given  $y$  : Pythia8 AZ
  3. polarisation  $A_i$  : fixed-order NNLO prediction from DYNNLO

# Polarisation and rapidity

- Use of DYNNLO (Fixed-order NNLO)
- Validate against 7 TeV ATLAS W, Z cross-section measurements

Eur. Phys. J. C 77 (2017) 367

- PDF : CT10nnlo (best agreement), MMHT14nnlo and CT14nnlo used for uncertainties (others disfavoured by the data)



- Polarisation : describes the kinematics of vector boson decay products
- ATLAS Z polarisation measurement validates fixed-order prediction

JHEP 08 (2016) 159

- uncertainties propagated from Z to W

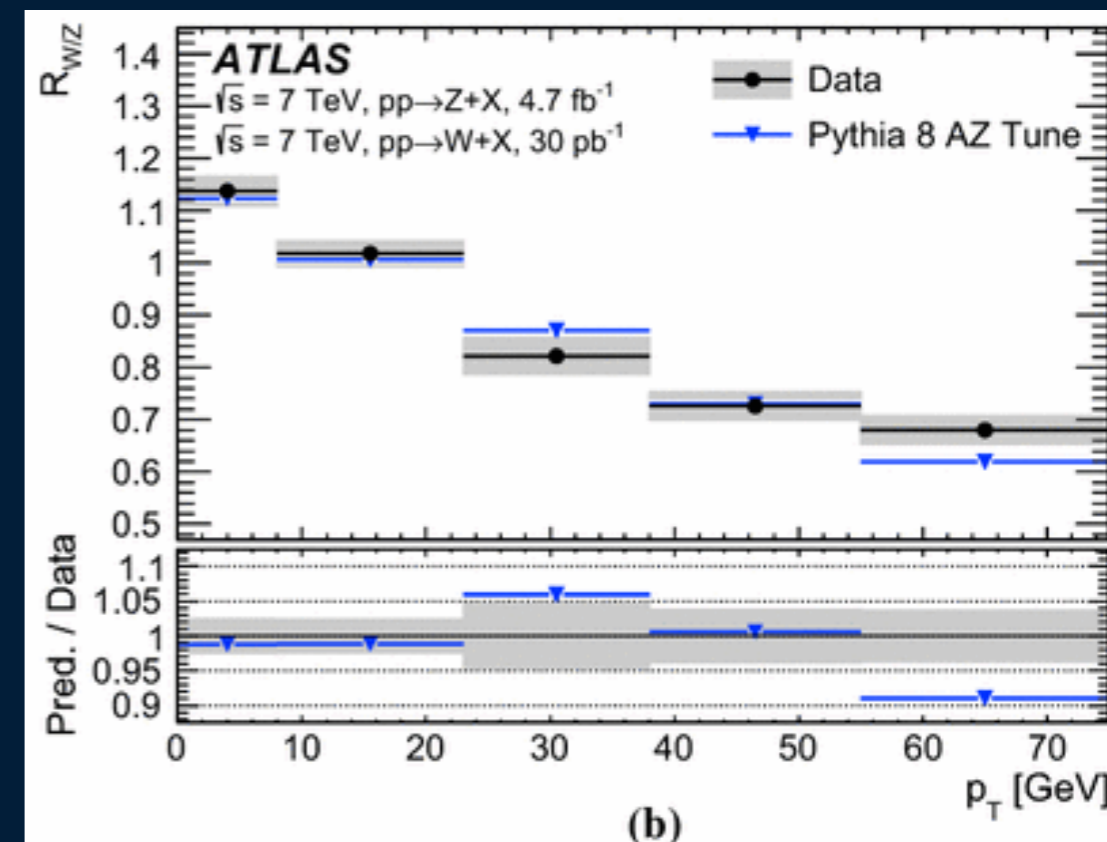
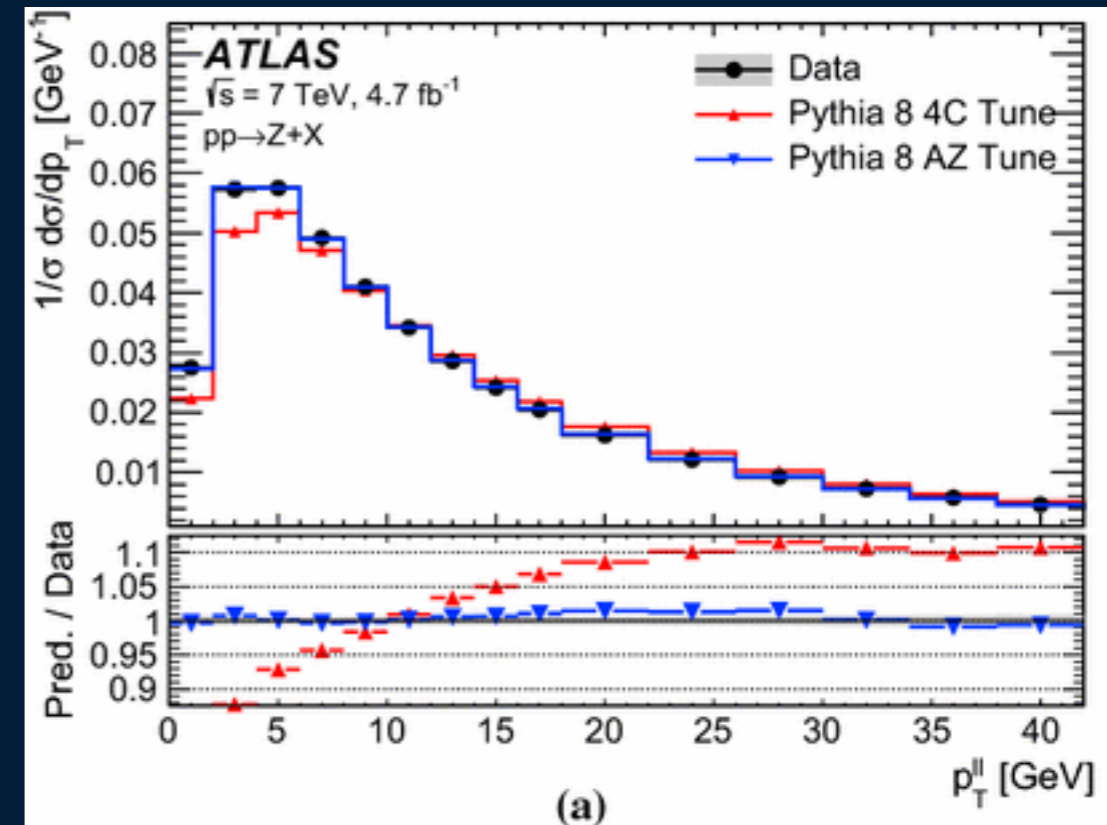


# Boson transverse momentum

- Use Pythia8 AZ tuned on Z p<sub>T</sub>  
ATLAS data **JHEP 09 (2014) 145**
- Good agreement for

$$R_{W/Z}(p_T) = \left( \frac{1}{\sigma_W} \cdot \frac{d\sigma_W(p_T)}{dp_T} \right) \left( \frac{1}{\sigma_Z} \cdot \frac{d\sigma_Z(p_T)}{dp_T} \right)^{-1}$$

- Uncertainties on PS include
  - tune uncertainties
  - c and b masses uncertainties
  - factorisation scale variation
  - LO PS PDF uncertainty



# Electroweak and QCD uncertainties

- QED/EW effects : mainly FSR photons, implemented with Photos
  - NLO EW corrections from Winhac — taken as uncertainty
  - FSR pair production impact checked with Photos and Sanc

Decay channel	$W \rightarrow e\nu$		$W \rightarrow \mu\nu$	
	$p_T^\ell$	$m_T$	$p_T^\ell$	$m_T$
$\delta m_W$ [MeV]				
FSR (real)	< 0.1	< 0.1	< 0.1	< 0.1
Pure weak and IFI corrections	3.3	2.5	3.5	2.5
FSR (pair production)	3.6	0.8	4.4	0.8
Total	4.9	2.6	5.6	2.6

- PDFs uncertainties to NNLO predictions are dominant : may do better in the future with profiled sets (incorporating parton shower)

$W$ -boson charge	$W^+$		$W^-$		Combined			
	$p_T^\ell$	$m_T$	$p_T^\ell$	$m_T$	$p_T^\ell$	$m_T$		
$\delta m_W$ [MeV]								
Fixed-order PDF uncertainty			13.1	14.9	12.0	14.2	8.0	8.7
AZ tune			3.0	3.4	3.0	3.4	3.0	3.4
Charm-quark mass			1.2	1.5	1.2	1.5	1.2	1.5
Parton shower $\mu_F$ with heavy-flavour decorrelation			5.0	6.9	5.0	6.9	5.0	6.9
Parton shower PDF uncertainty			3.6	4.0	2.6	2.4	1.0	1.6
Angular coefficients			5.8	5.3	5.8	5.3	5.8	5.3
Total			15.9	18.1	14.8	17.2	11.6	12.9



# EXPERIMENTAL ASPECTS

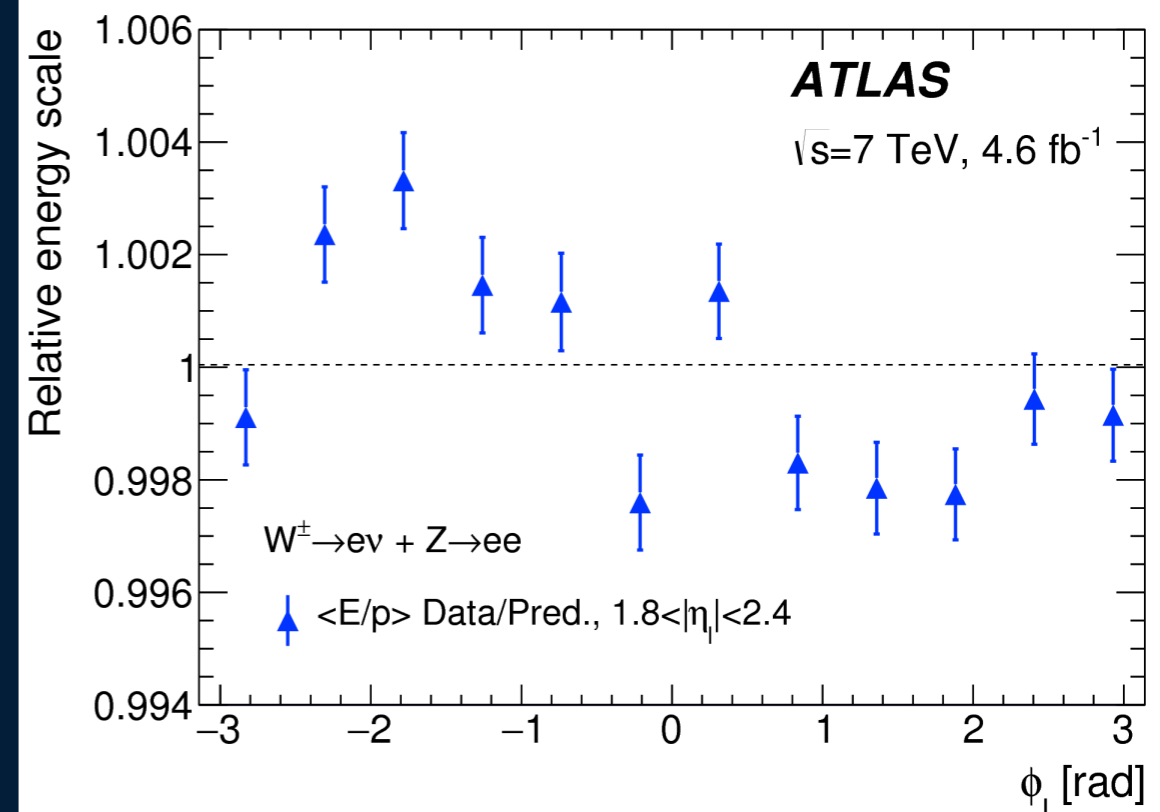
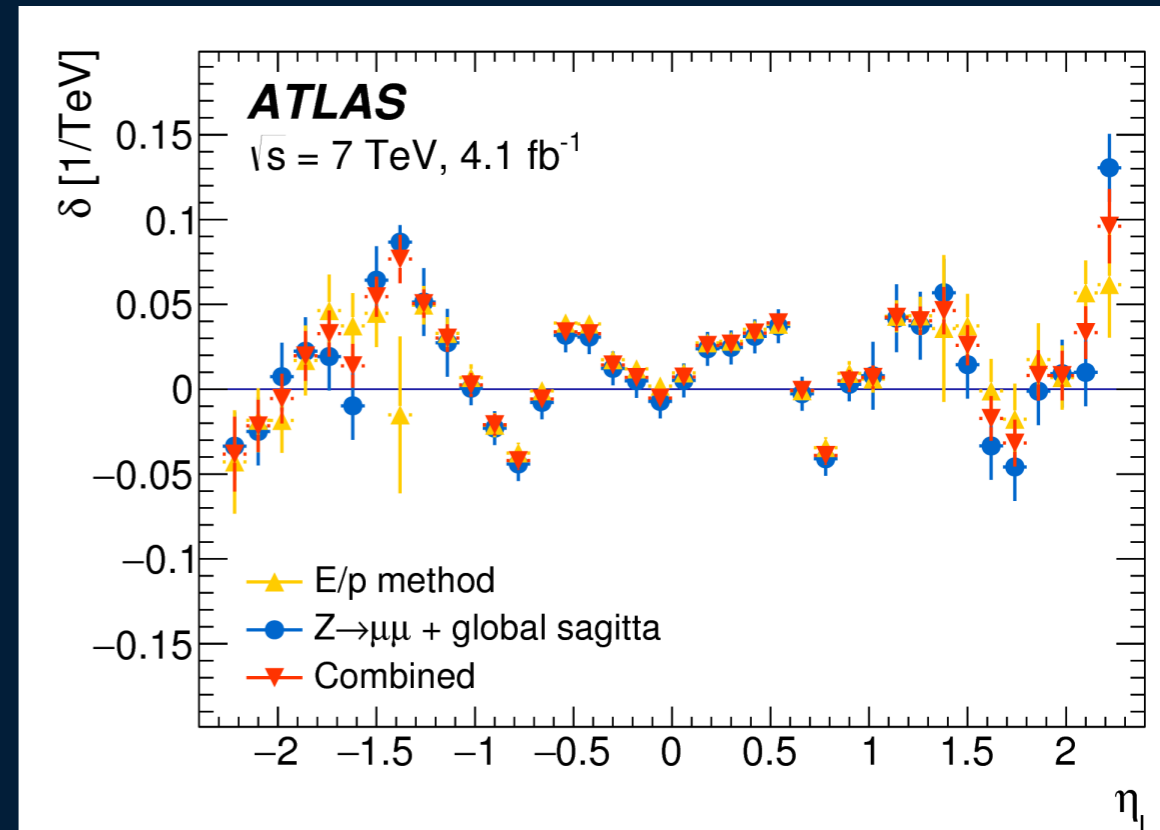


# Lepton calibration

- muon momentum scale calibration using Z, extrapolation to W using  $p_{T\ell}(W)$  calibration residual dependence
- muon sagitta bias calibration uses W events (E/p) and Z events

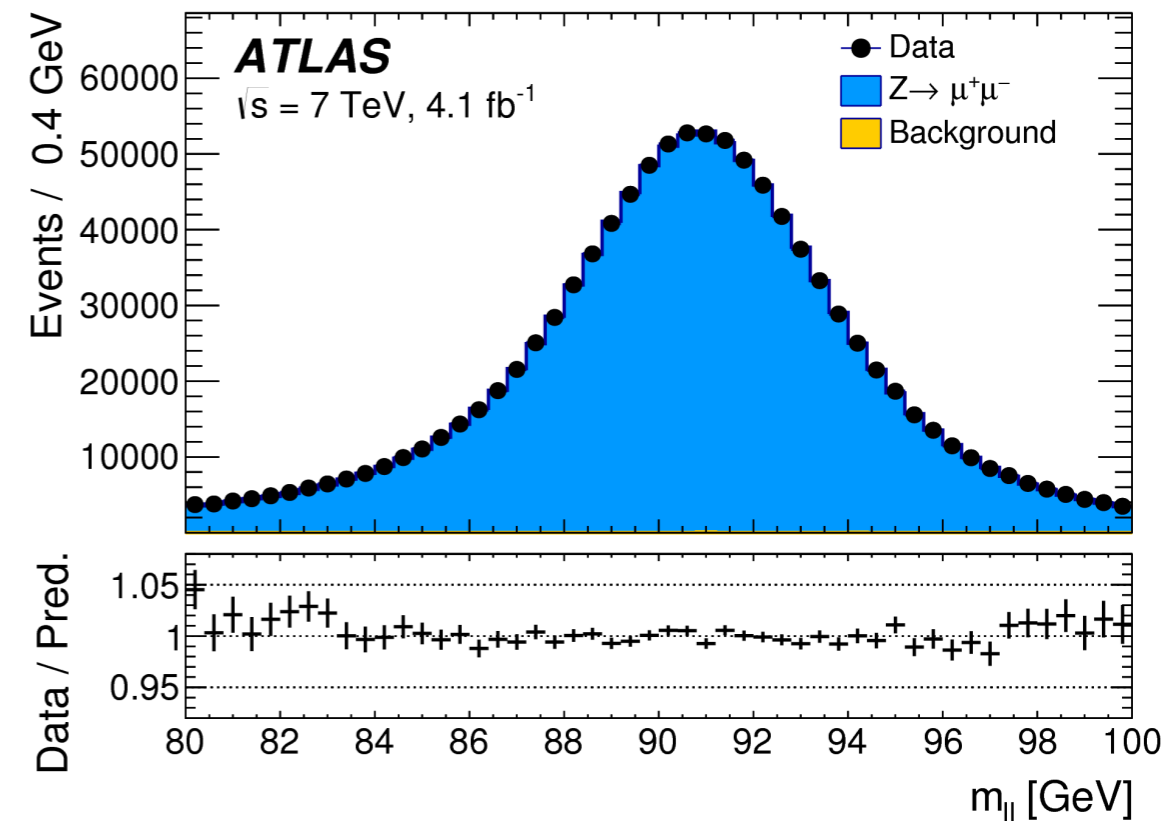
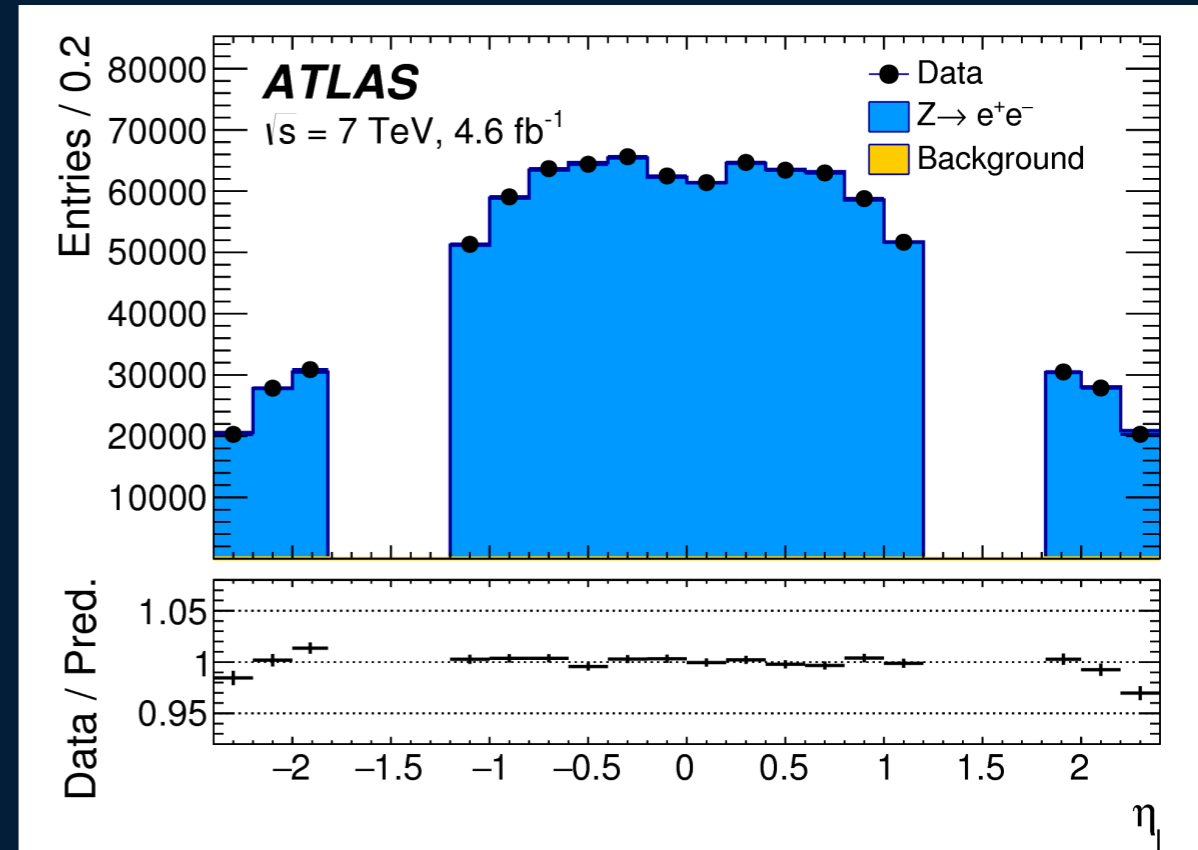
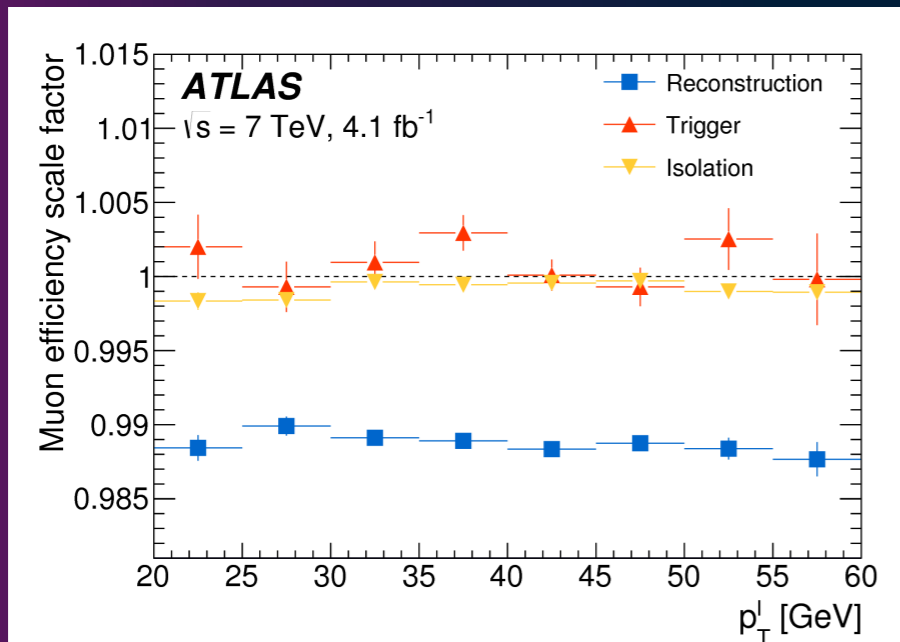
$$p_{T}^{\text{data,corr}} = \frac{p_{T}^{\text{data}}}{1 + q \cdot \delta(\eta, \phi) \cdot p_{T}^{\text{data}}}$$

- electron calibration uses Z events
  - Overall average relative uncertainty  $9.4 \times 10^{-5}$
  - $\phi$  modulation due to mechanical deformation under gravity corrected with W and Z events



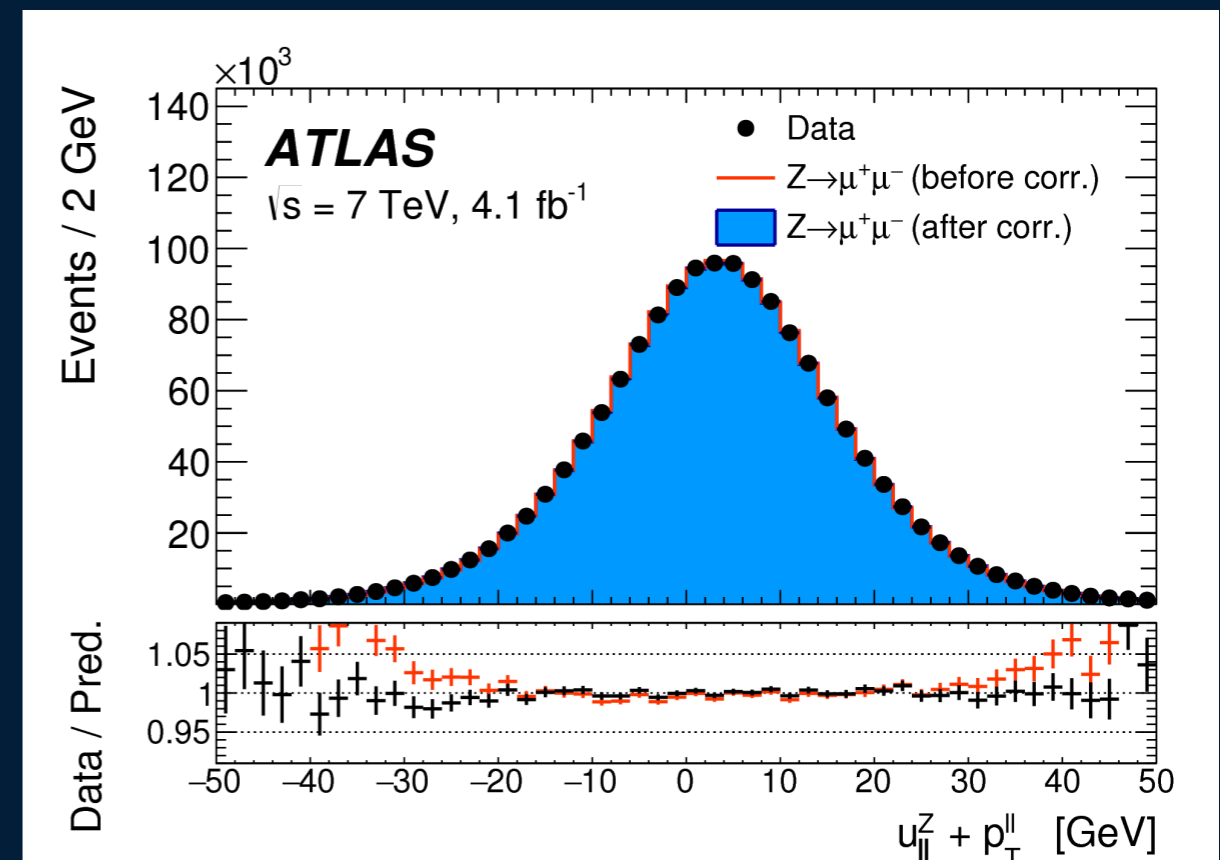
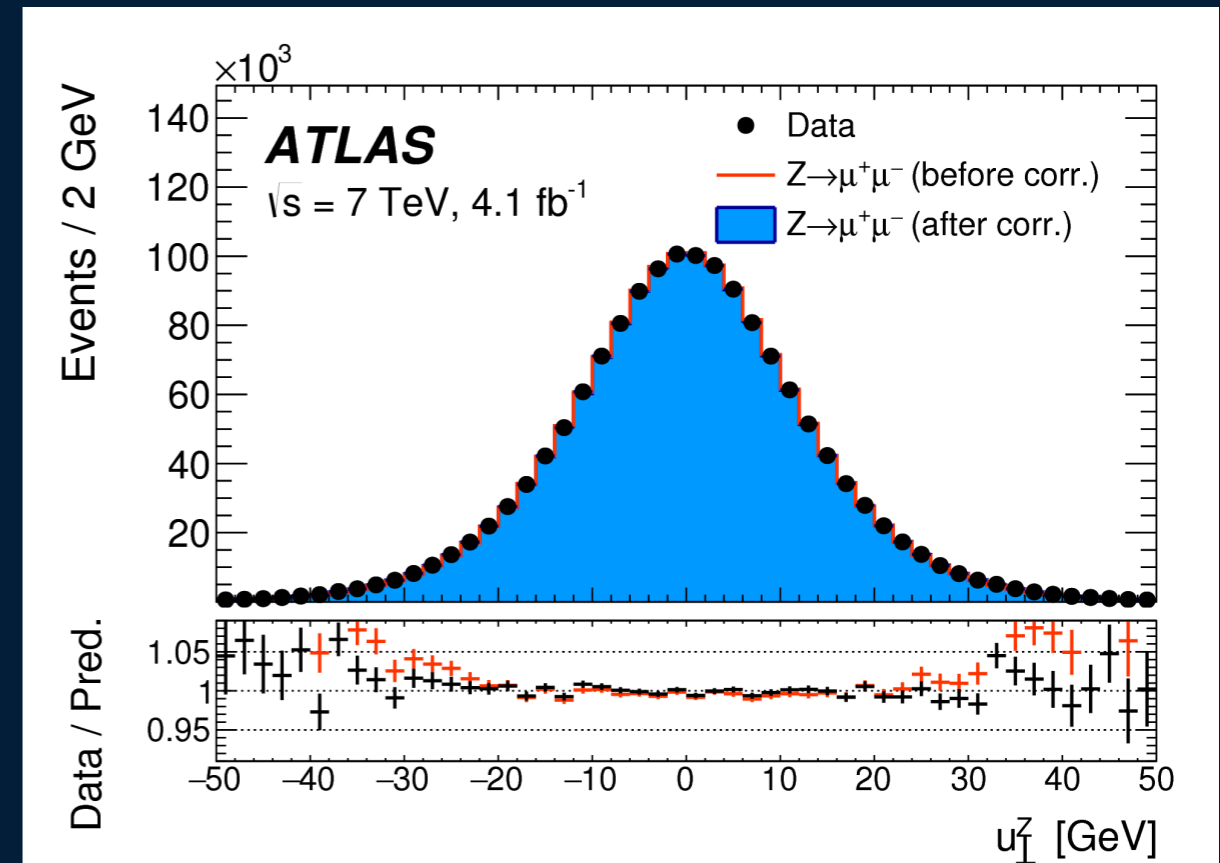
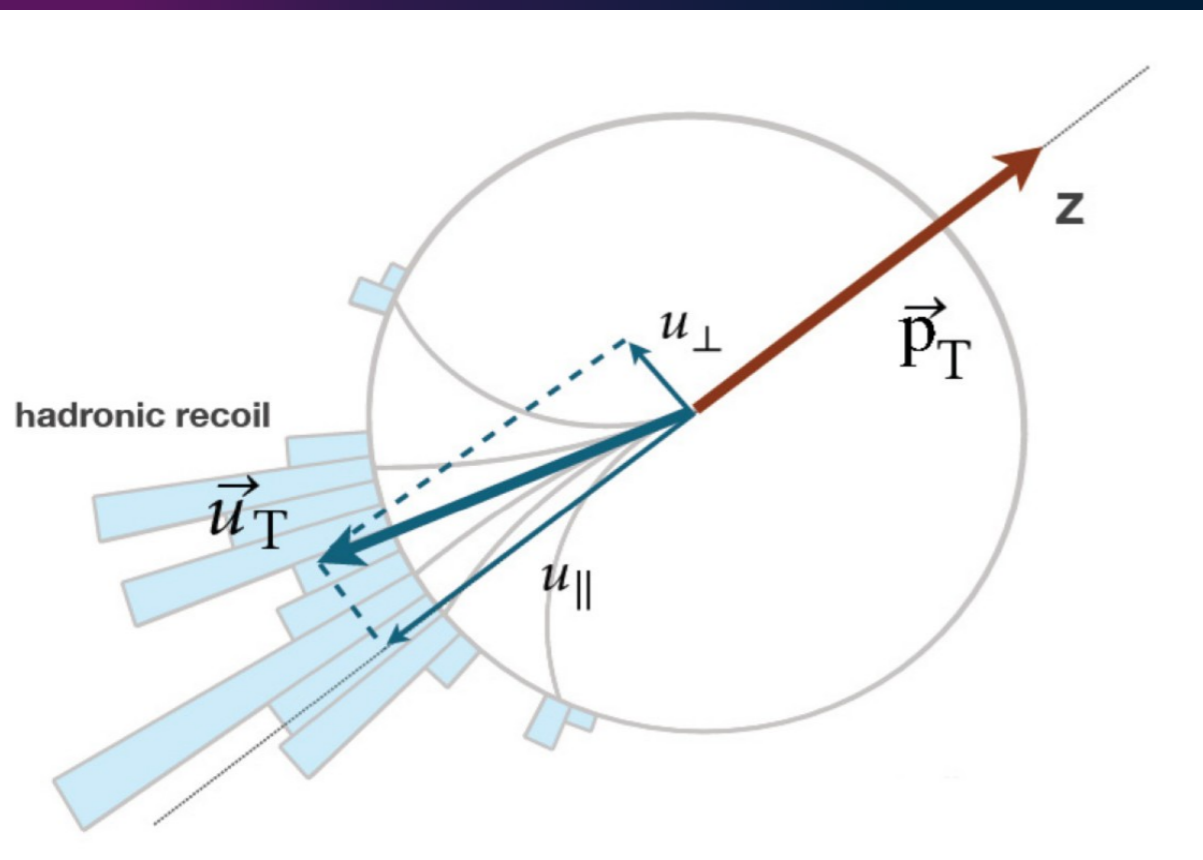
# Lepton calibration

- Selection efficiencies for reconstruction, identification, trigger, isolation  $\sim 10(8)$  MeV for  $p_{T\ell}(m_{T\ell})$  fit
- use tag-and-probe methods for the scale factors and uncertainties
- Total lepton uncertainty  $\sim 10$  MeV (muon) and 14 MeV (electron)



# Hadronic recoil calibration

- 2-step procedure :
  - Correct the modeling of the overall activity in the simulation
  - Correct residual discrepancy in the recoil response and resolution using  $Z \rightarrow \ell\ell$  events
- 2.6/13.0 MeV uncertainty on  $p_{T\ell}/m_T$  fit

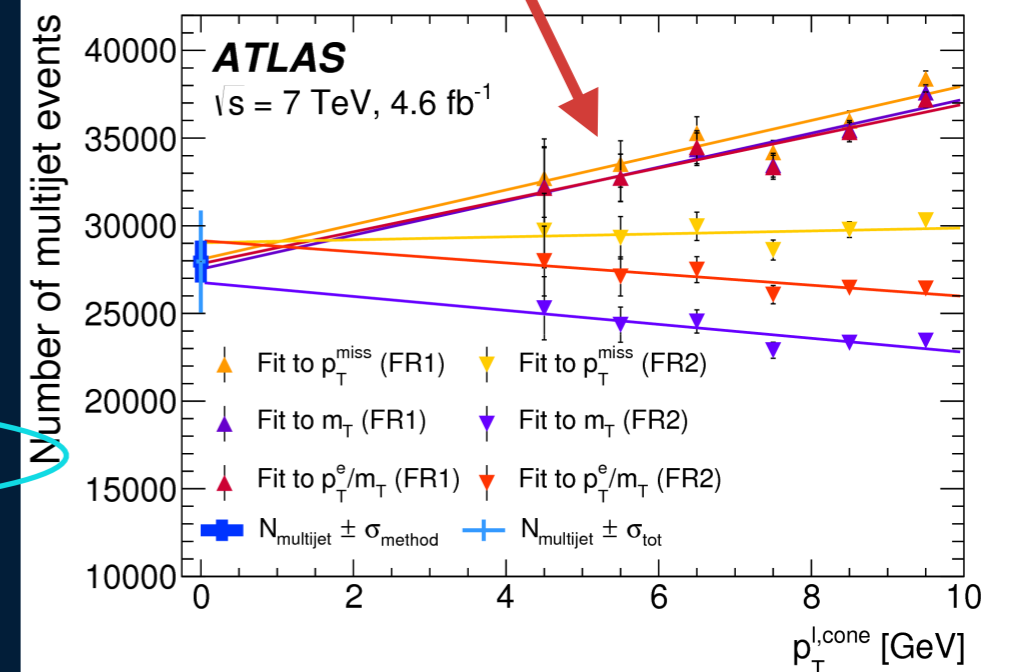
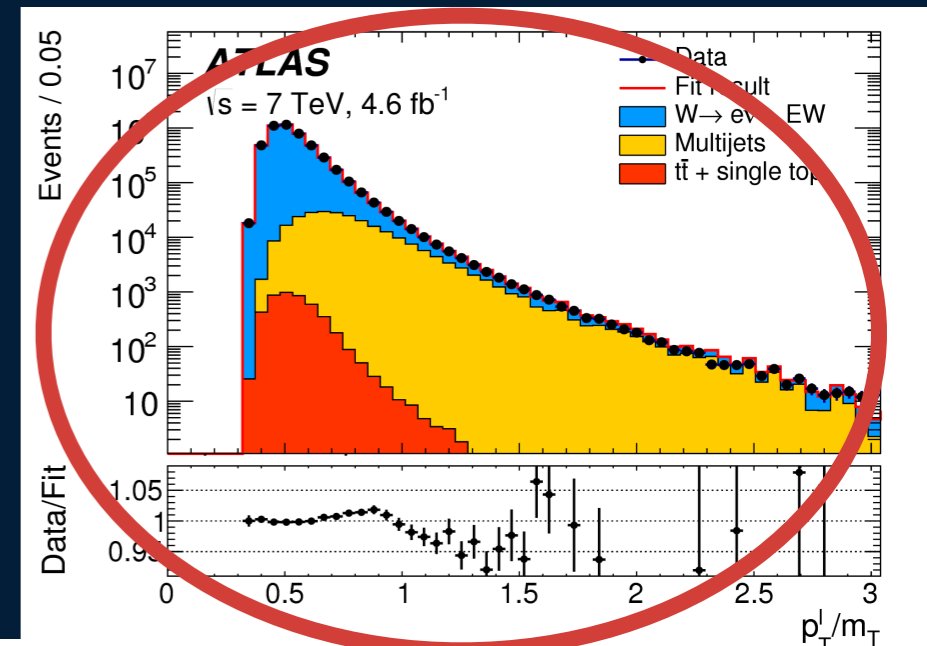




# Multijet background

- data-driven technique :
  - 2 different background enriched regions to fit multijet fraction
    - EW and top contamination subtracted with MC estimation
  - 3 different observables :  $m_T$ ,  $p_{T\ell}/m_T$ ,  $p_T^{\text{miss}}$
  - scan in isolation variable
  - linear extrapolation to signal region

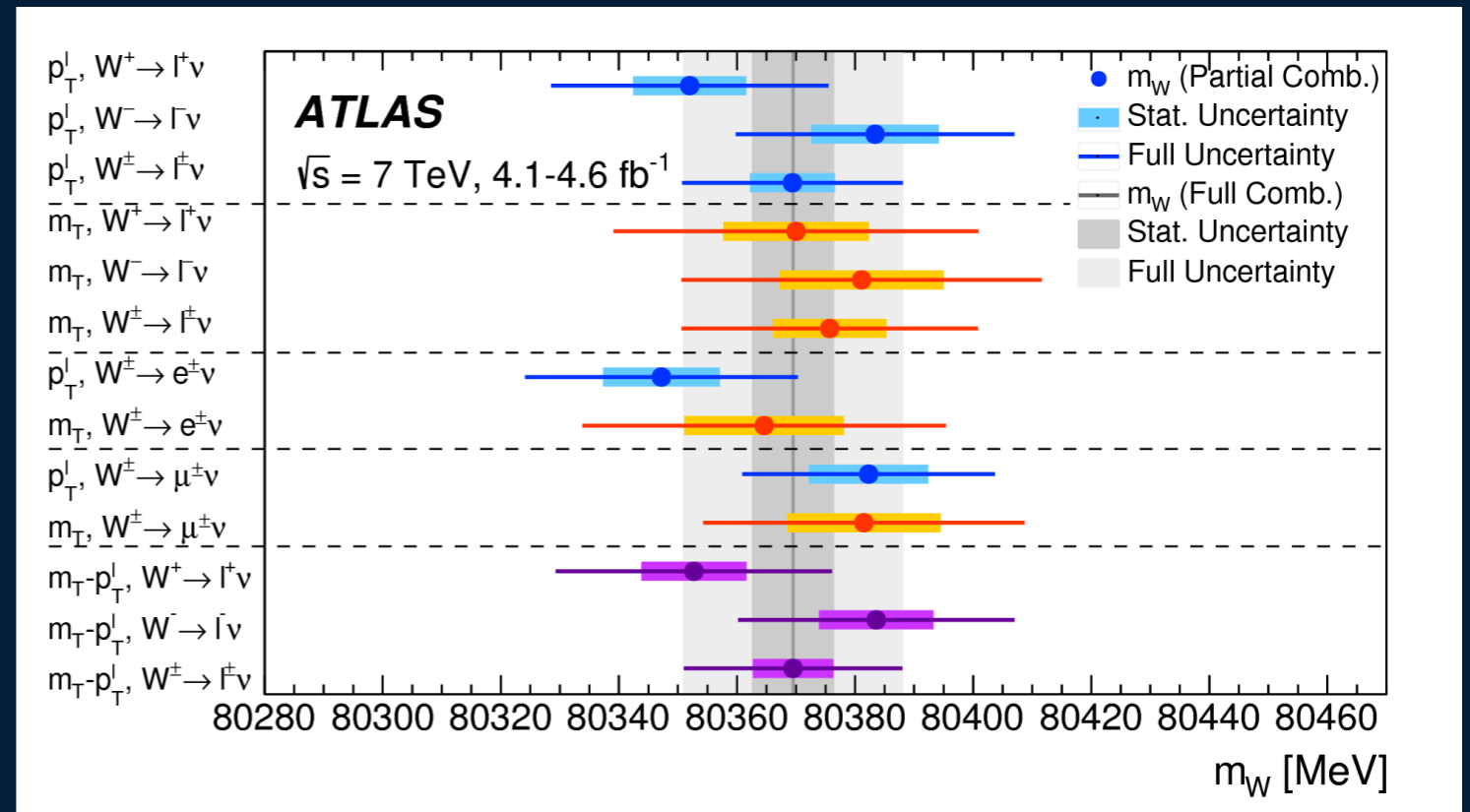
0.6 - 1.7 % (e channel)  
0.5 - 0.7 % (mu channel)



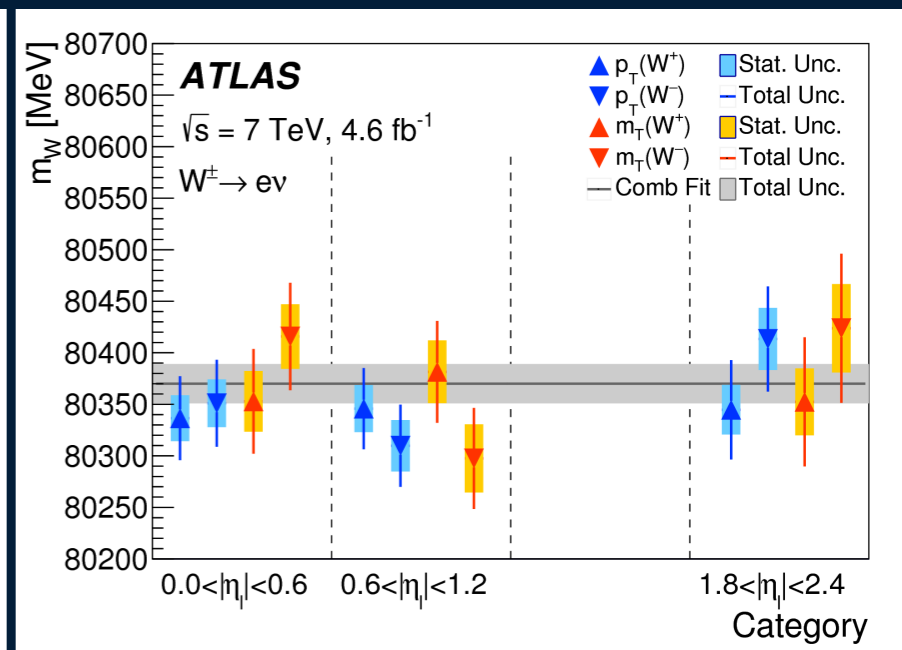
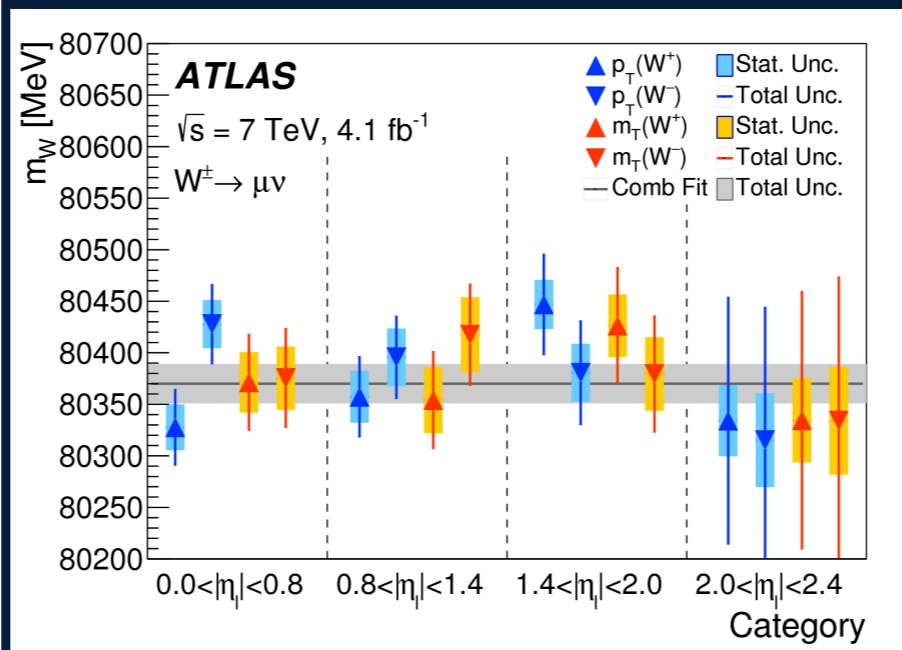
Kinematic distribution Decay channel W-boson charge	$p_T^\ell$				$m_T$				
	$W \rightarrow e\nu$		$W \rightarrow \mu\nu$		$W \rightarrow e\nu$		$W \rightarrow \mu\nu$		
	$W^+$	$W^-$	$W^+$	$W^-$	$W^+$	$W^-$	$W^+$	$W^-$	
$\delta m_W$ [MeV]									
$W \rightarrow \tau\nu$ (fraction, shape)	0.1	0.1	0.1	0.2	0.1	0.2	0.1	0.3	
$Z \rightarrow ee$ (fraction, shape)	3.3	4.8	–	–	4.3	6.4	–	–	
$Z \rightarrow \mu\mu$ (fraction, shape)	–	–	3.5	4.5	–	–	4.3	5.2	
$Z \rightarrow \tau\tau$ (fraction, shape)	0.1	0.1	0.1	0.2	0.1	0.2	0.1	0.3	
$WW, WZ, ZZ$ (fraction)	0.1	0.1	0.1	0.1	0.4	0.4	0.3	0.4	
Top (fraction)	0.1	0.1	0.1	0.1	0.3	0.3	0.3	0.3	
Multijet (fraction)	3.2	3.6	1.8	2.4	8.1	8.6	3.7	4.6	
Multijet (shape)	3.8	3.1	1.6	1.5	8.6	8.0	2.5	2.4	
Total	6.0	6.8	4.3	5.3	12.6	13.4	6.2	7.4	

# $m_W$ extraction

- $\chi^2$  template fit to the data in each category (distribution, charge, lepton channel,  $\eta_\ell$  bin)
- All categories give consistent result  $\rightarrow$  strength of detector calibration and physics modelling
- combination using BLUE method



Combination	Weight
Electrons	0.427
Muons	0.573
$m_T$	0.144
$p_T^l$	0.856
$W^+$	0.519
$W^-$	0.481



# CONCLUSION AND SUMMARY

$$m_W = 80370 \pm 7 \text{ (stat.)} \pm 11 \text{ (exp. syst.)} \pm 14 \text{ (mod. syst.) MeV}$$

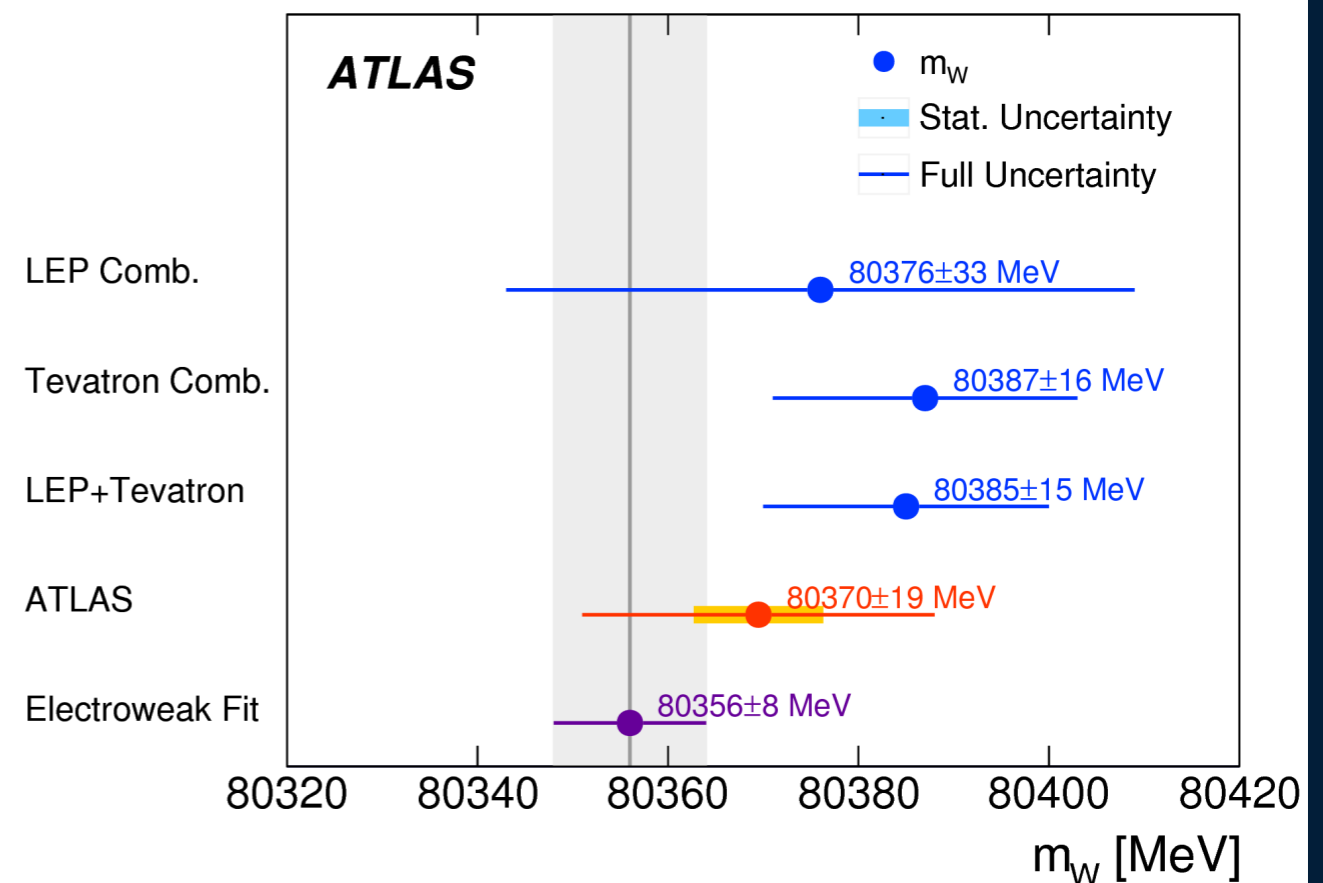
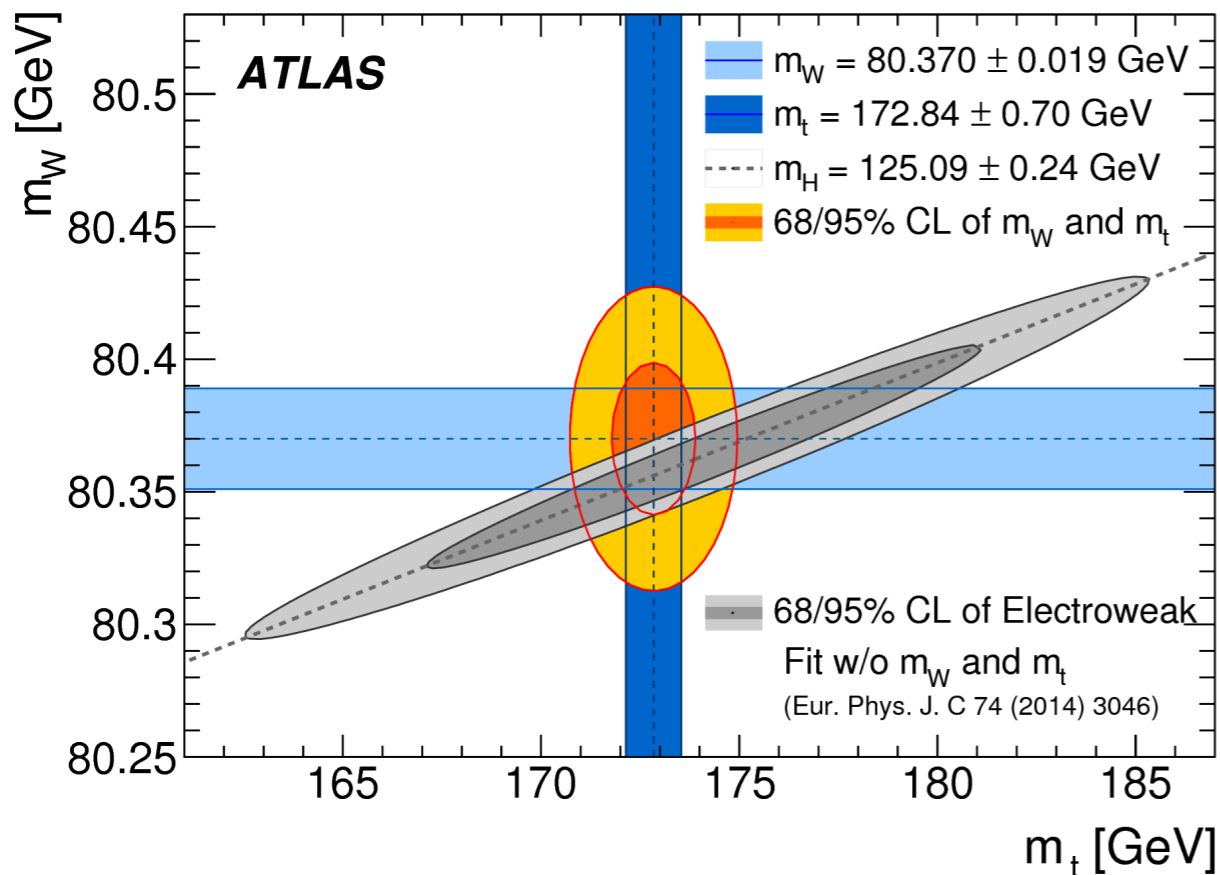
$$= 80370 \pm 19 \text{ MeV,}$$

$$m_{W^+} - m_{W^-} = -29 \pm 28 \text{ MeV}$$



Standard Model RAYEN WINS

Combined categories	Value [MeV]	Stat. Unc.	Muon Unc.	Elec. Unc.	Recoil Unc.	Bckg. Unc.	QCD Unc.	EW Unc.	PDF Unc.	Total Unc.	$\chi^2/\text{dof}$ of Comb.
$m_{T-p_T^\ell}, W^\pm, e-\mu$	80369.5	6.8	6.6	6.4	2.9	4.5	8.3	5.5	9.2	18.5	29/27



# What's next ?

- What can be done to improve the precision in the coming years ?
  - **measurement at different center of mass energies**
    - PDF sensitivity is different (interesting for combinations)
  - special LHC runs with lower pile-up : reduces hadronic recoil uncertainties, gives more weight to  $m_T$  measurement, renders some precise ancillary measurements possible, *e.g.*  $p_T(W)$
  - Increase the precision on PDFs : more LHC data in fits, more constraints at high  $\eta$  (HL-LHC)...
  - More progress on theory side for W  $p_T$  : new or improved generators including resummation techniques
  - Experimental innovations : *e.g.* pile-up mitigation techniques
  - Combinations with existing measurements (*e.g.* Tevatron)



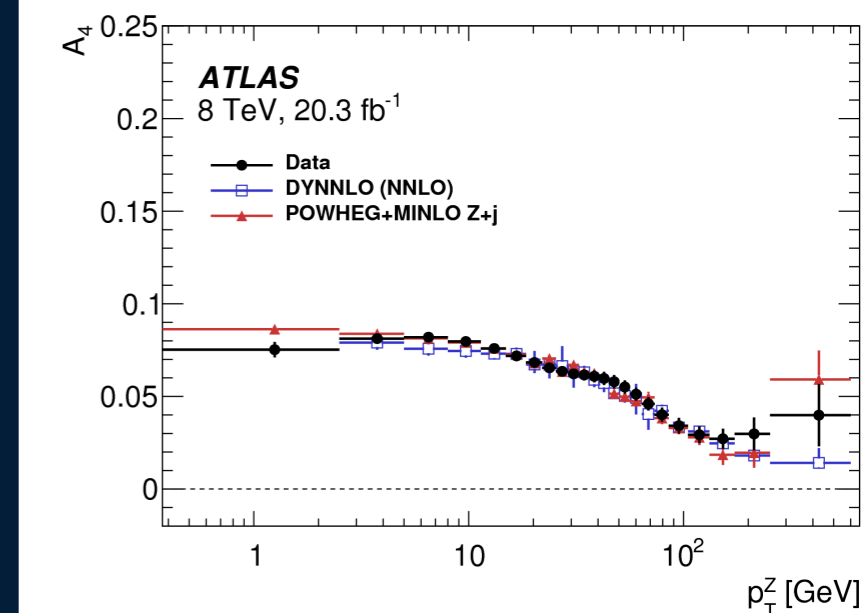
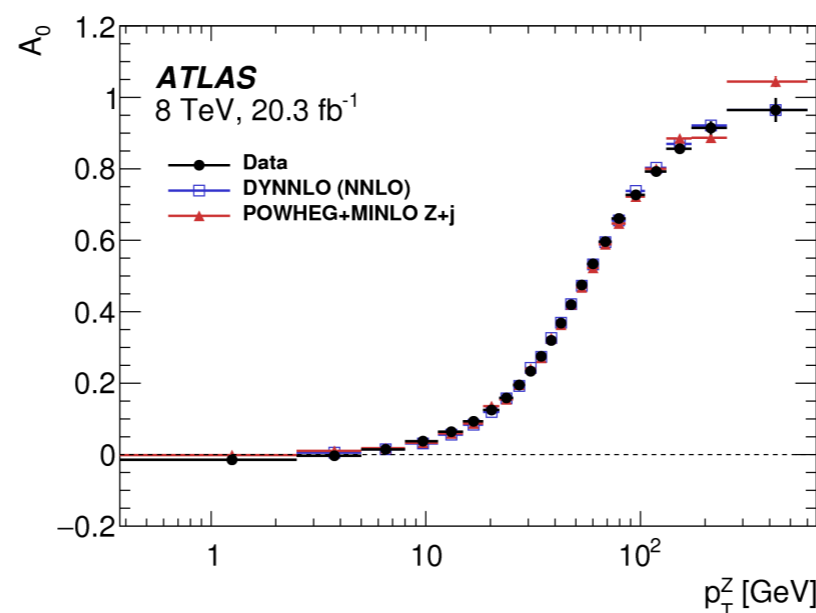
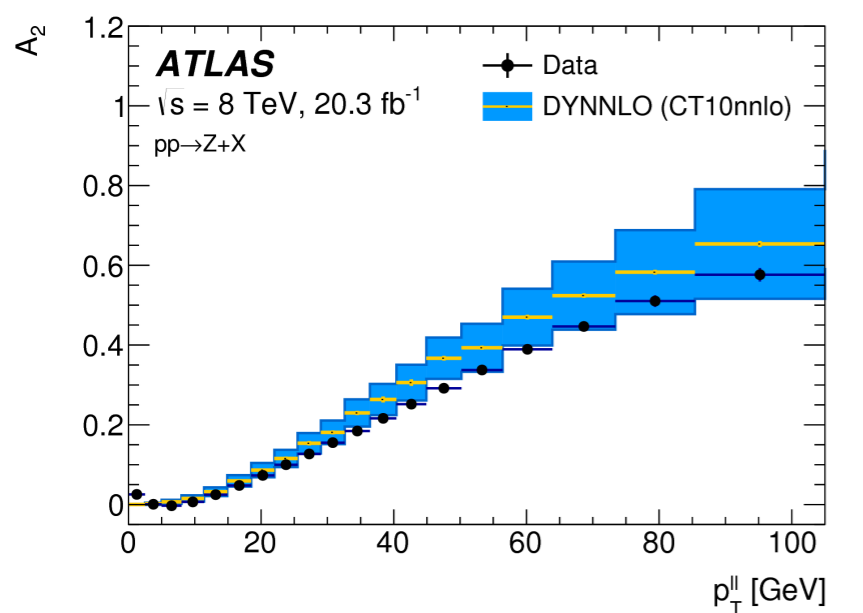
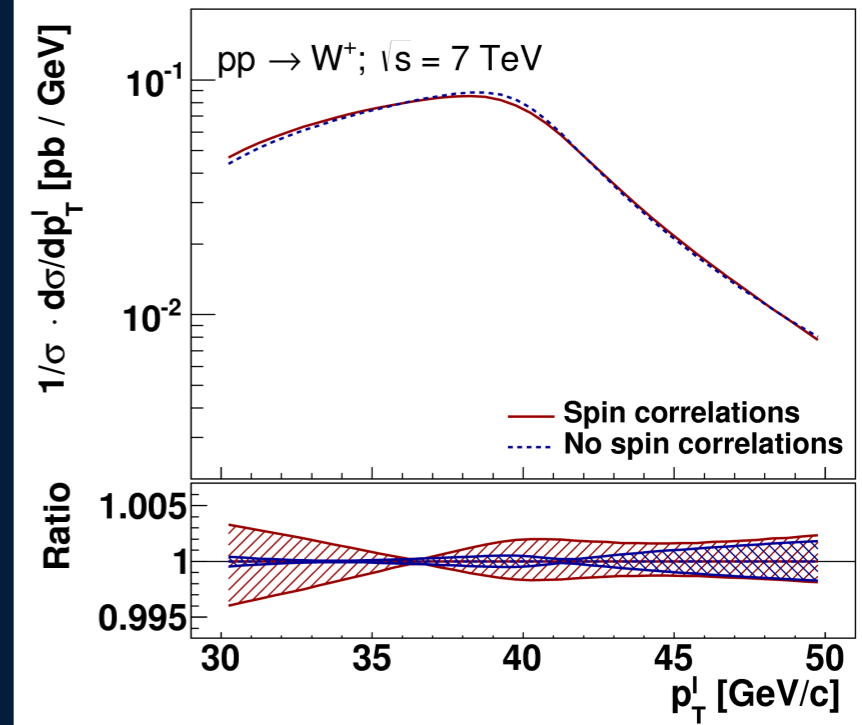
Thank you for your  
attention!!

# BACKUP

# Polarisation

ATLAS-PHYS-PUB-2014-015

- Crucial to get right in  $pp$  collisions, otherwise miss some effects
- ATLAS measurement of Z angular coefficients validates fixed-order pQCD NNLO prediction
  - except for  $A_2$  : additional uncertainty
    - data/prediction difference is added to the uncertainty ; pseudo-experiments show no correlation with other coefficients
- Uncertainties on the Z measurement are propagated to the W



JHEP 08 (2016) 159

# W boson transverse momentum

- Pythia8 tuned on Z p<sub>T</sub> ATLAS data (AZ tune)

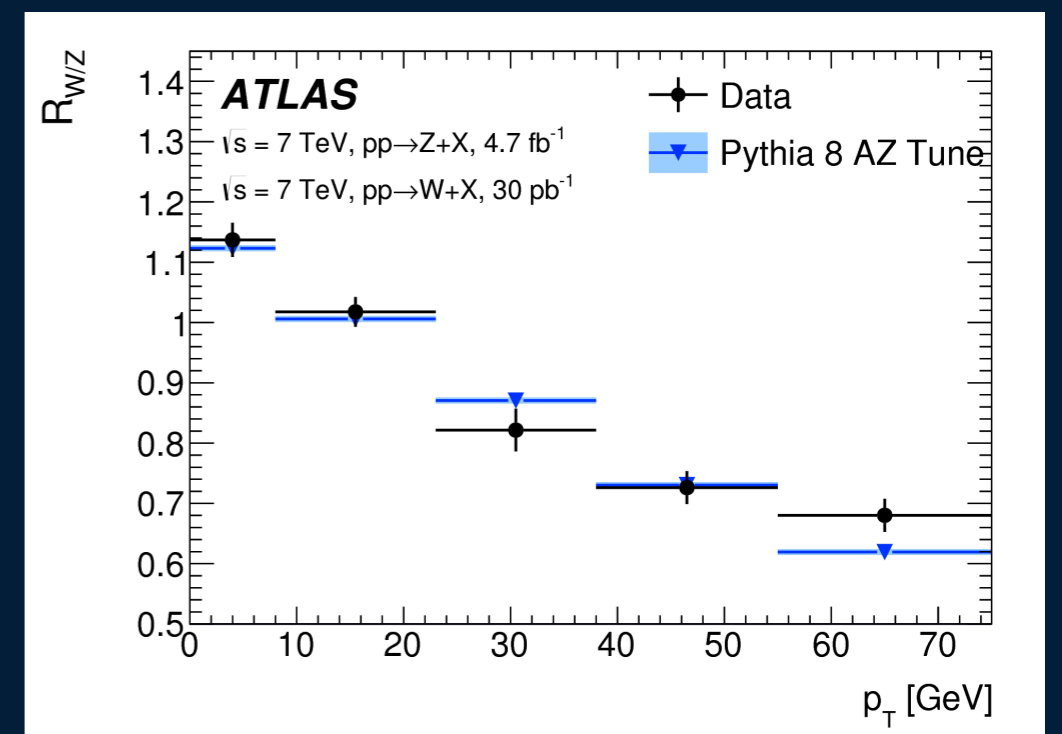
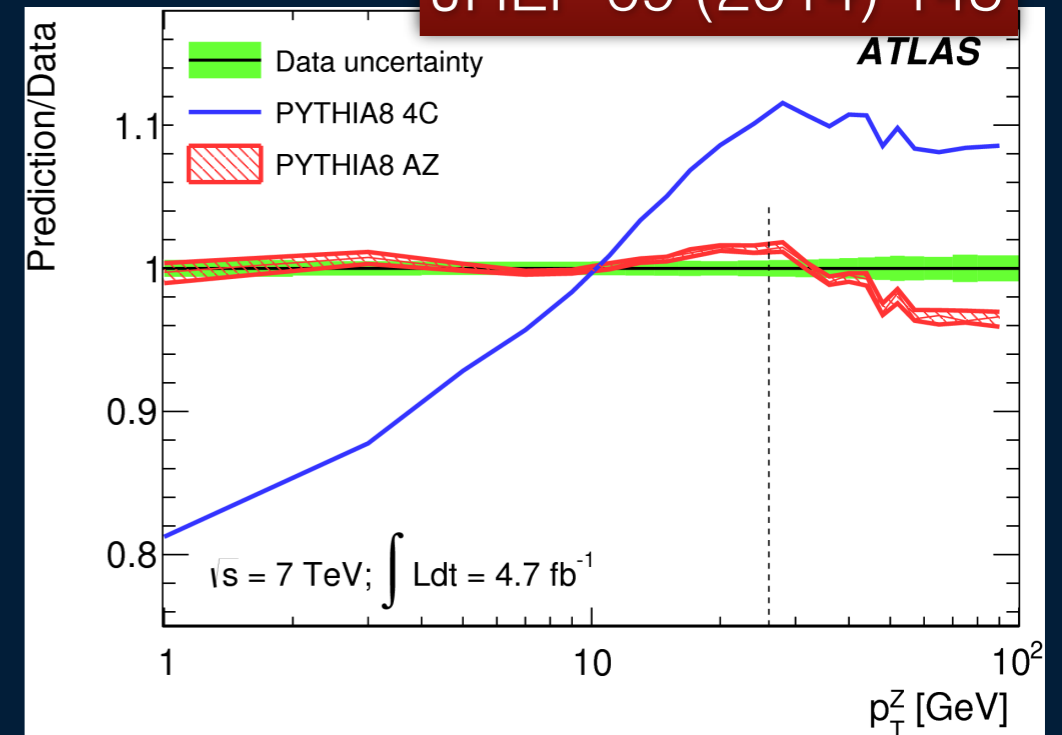
PYTHIA8	
Tune Name	AZ
Primordial k <sub>T</sub> [GeV]	1.71 ± 0.03
ISR α <sub>S</sub> <sup>ISR</sup> (m <sub>Z</sub> )	0.1237 ± 0.0002
ISR cut-off [GeV]	0.59 ± 0.08
χ <sub>min</sub> <sup>2</sup> /dof	45.4/32

- Good agreement is obtained for the ratio of differential cross-sections using this tune:

$$R_{W/Z}(p_T) = \left( \frac{1}{\sigma_W} \cdot \frac{d\sigma_W(p_T)}{dp_T} \right) \left( \frac{1}{\sigma_Z} \cdot \frac{d\sigma_Z(p_T)}{dp_T} \right)^{-1}$$

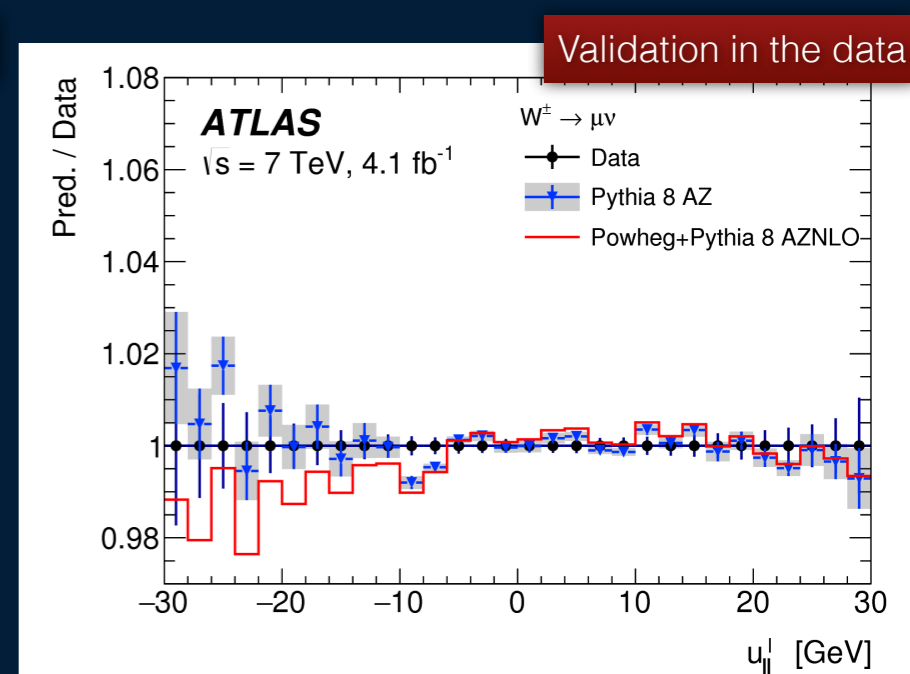
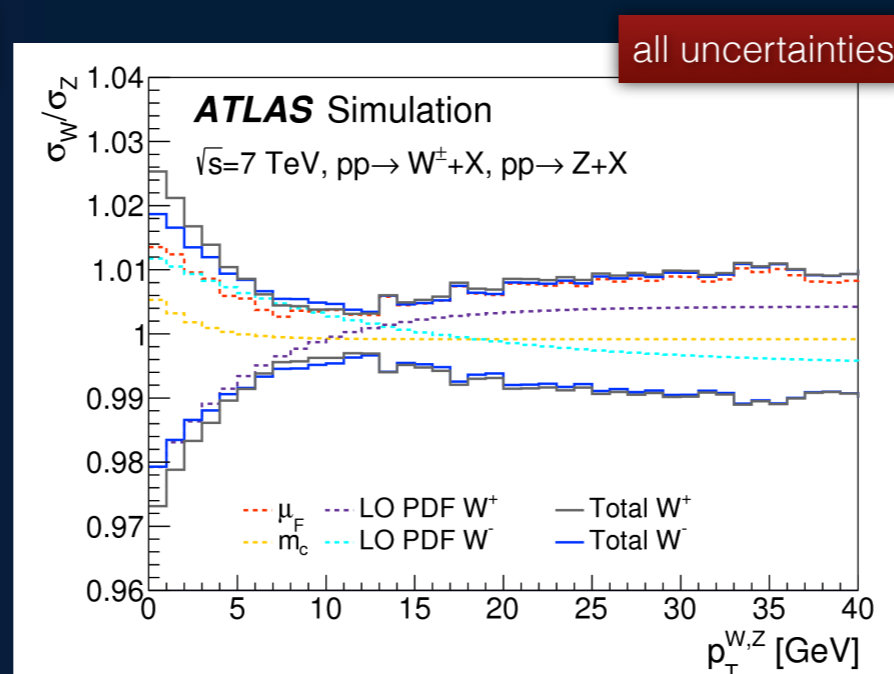
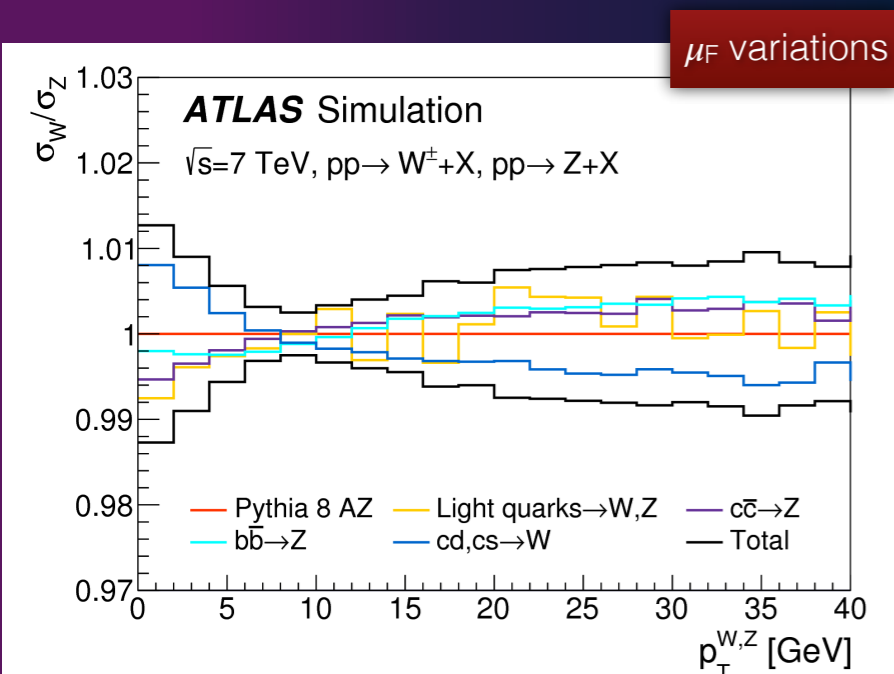
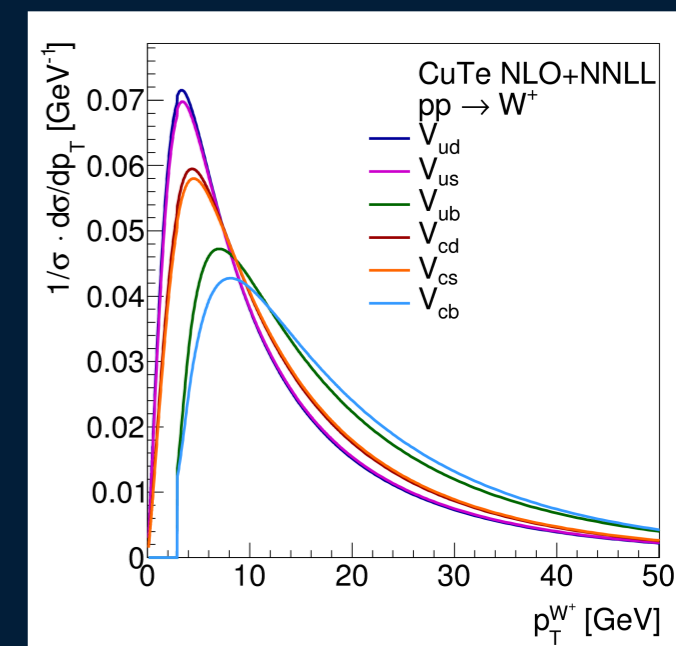
- p<sub>T</sub>(W) is obtained via the product of this ratio and the experimental Z p<sub>T</sub> spectrum
  - The total uncertainty being the sum in quadrature of these two components, ~1-2%

JHEP 09 (2014) 145



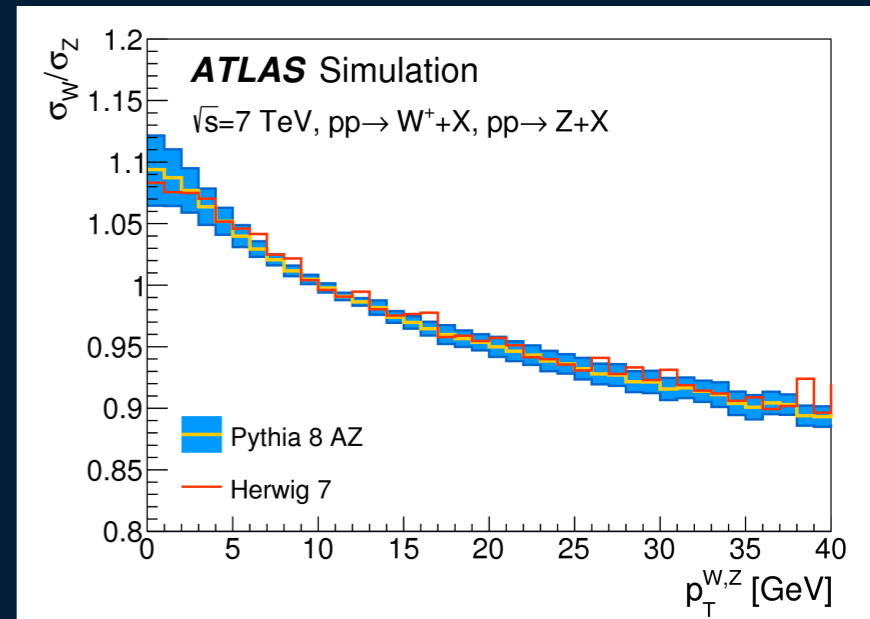
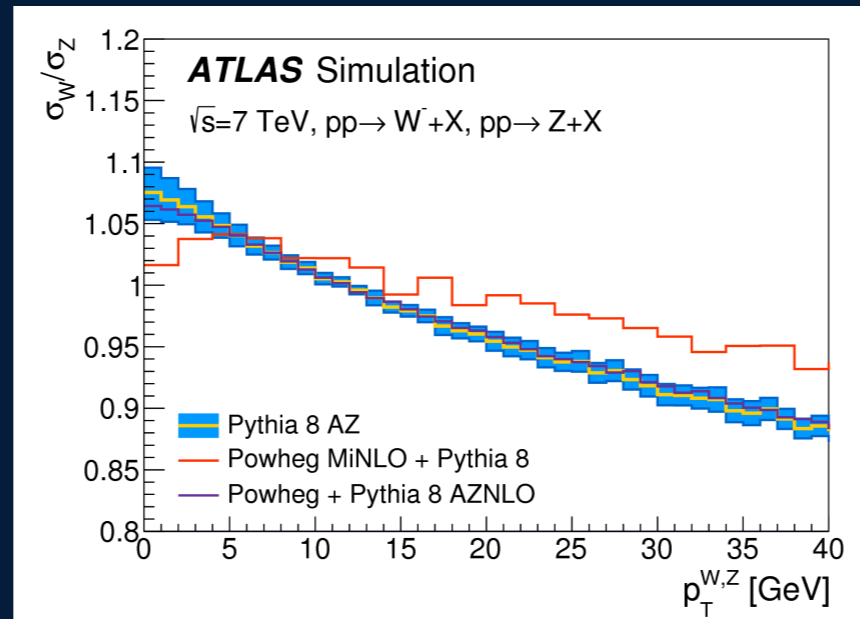
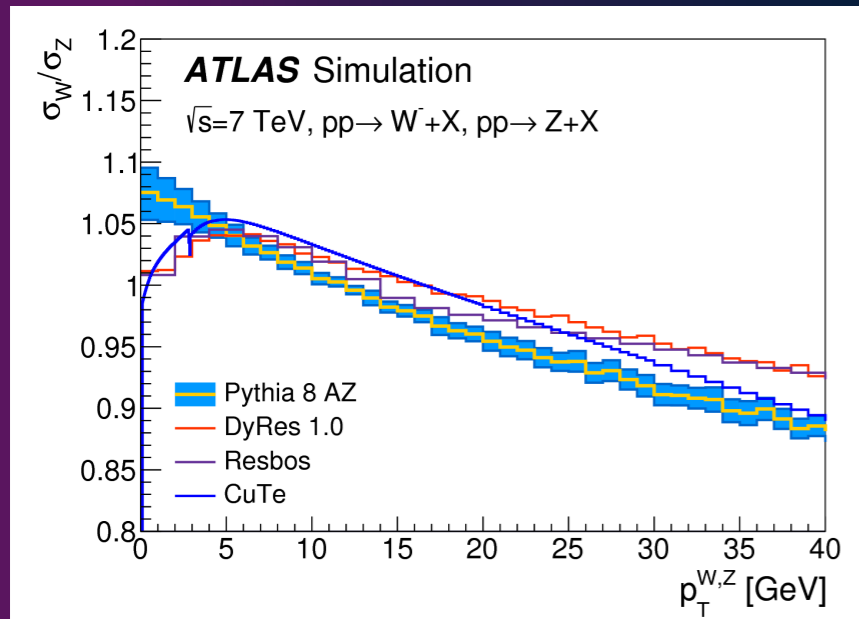
# Uncertainties to $p_T(W)$

- Only modelling uncertainties which are uncorrelated between Z and W give sizeable uncertainties on the measurement
  - Induced by heavy flavour initiated production : 6/3% of cc/bb for Z, 20% of cs for W production
- Missing higher orders in QCD ISR : factorisation scale ( $\mu_F$ ) variations taken as correlated between W and Z for light quark, independently for heavy quarks
- other sources : uncertainty on  $m_c$ , choice of parton shower LO PDF
- Central prediction and uncertainty well validated with the recoil distribution in the data

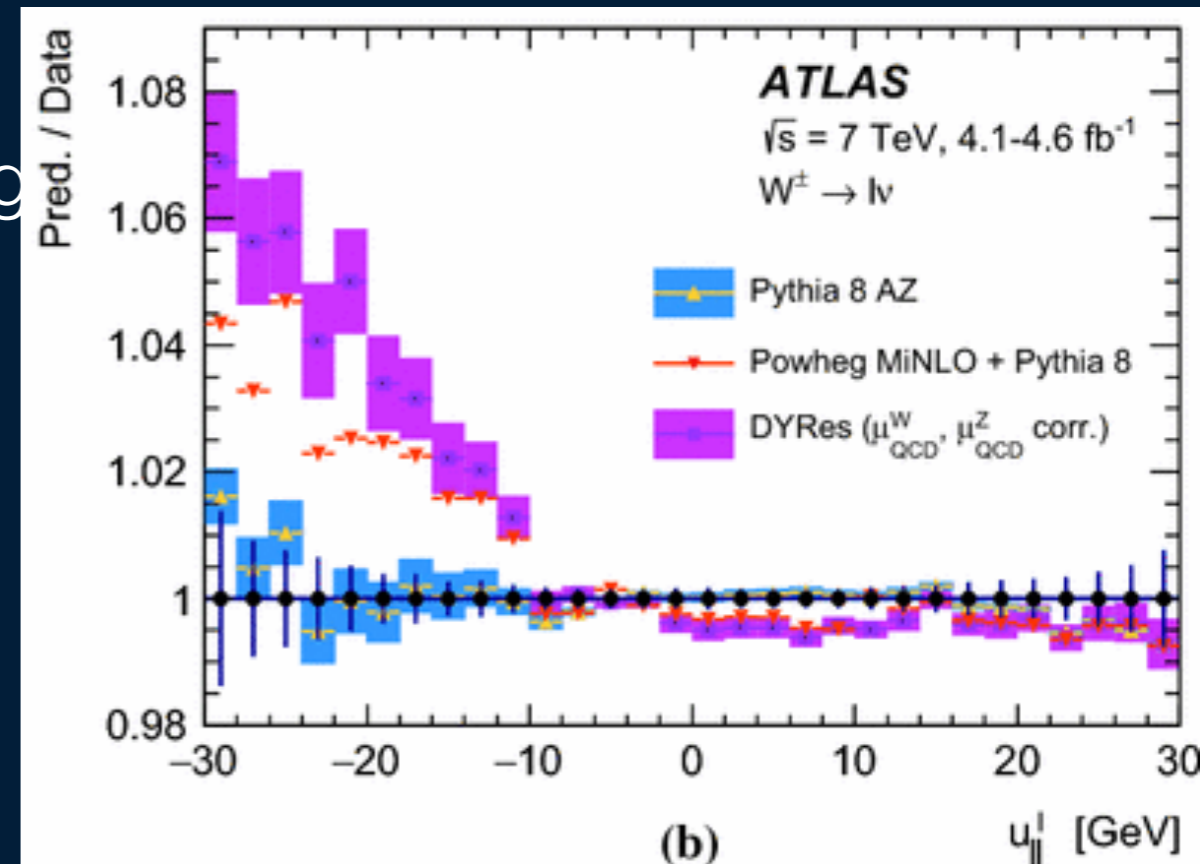




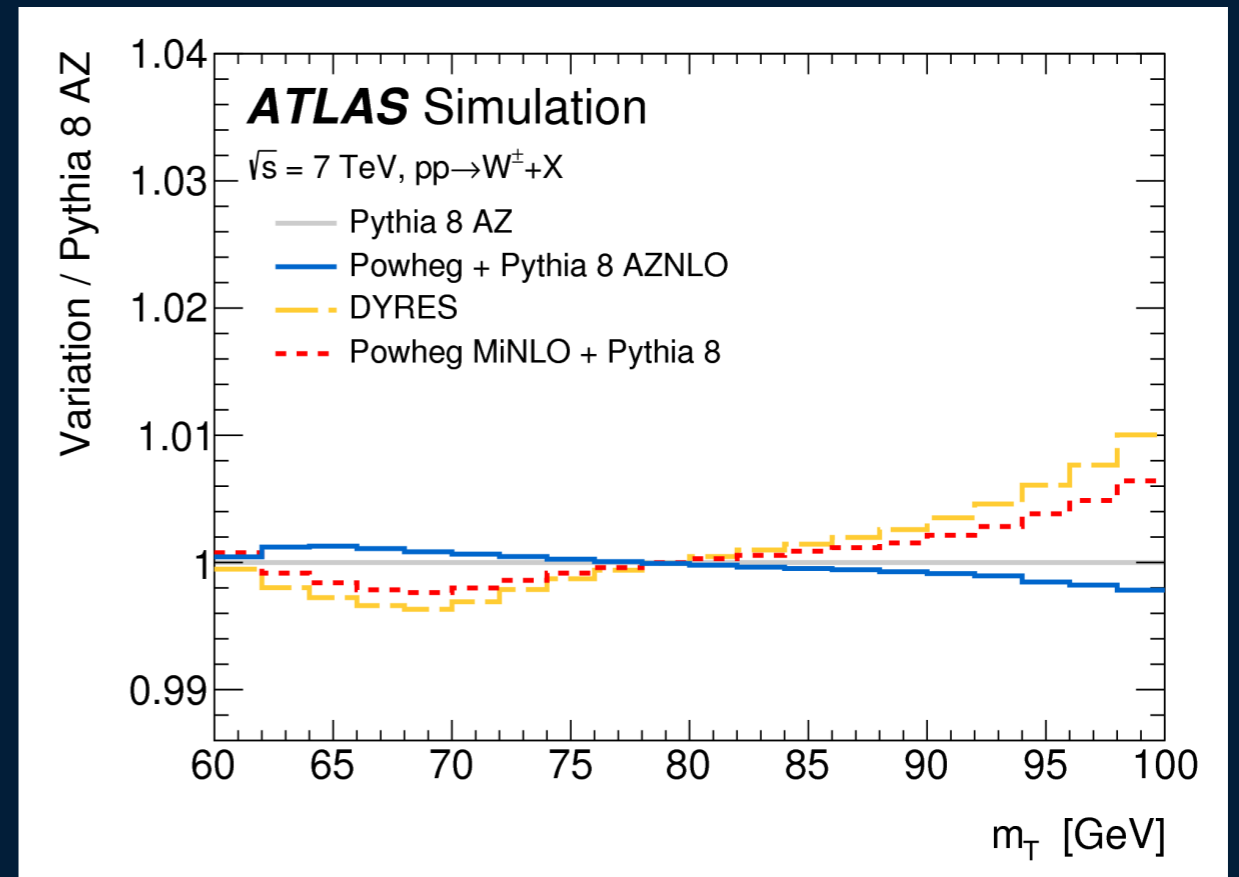
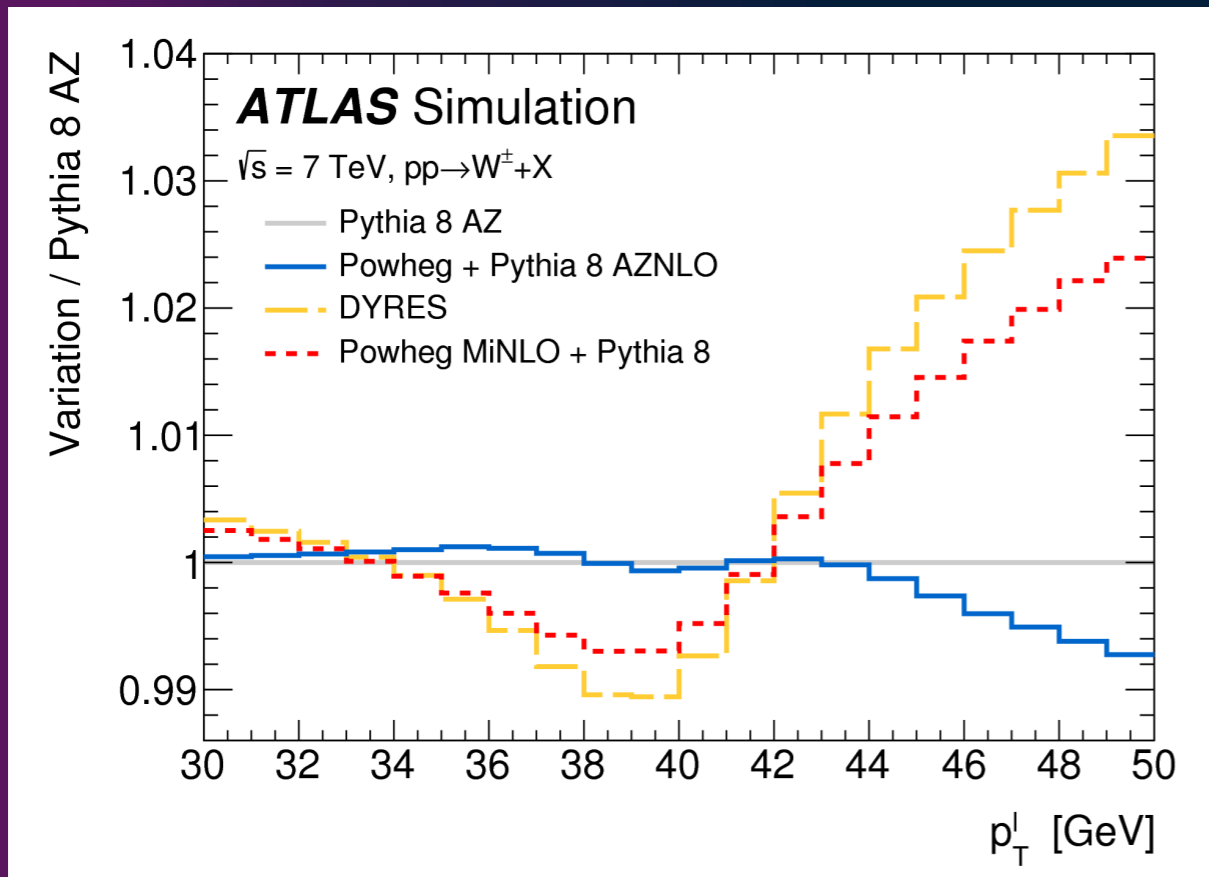
# $p_T$ modeling strategy



- Very different prediction of  $p_T(W)/p_T(Z)$  ratio from resummed technique or Powheg MiNLO with respect to Pythia 8 AZ
- Pythia8 AZ is validated by the data ( $u_{||}$ ) contrary to other predictions
- Negligible impact of the parton shower model (Herwig 7)

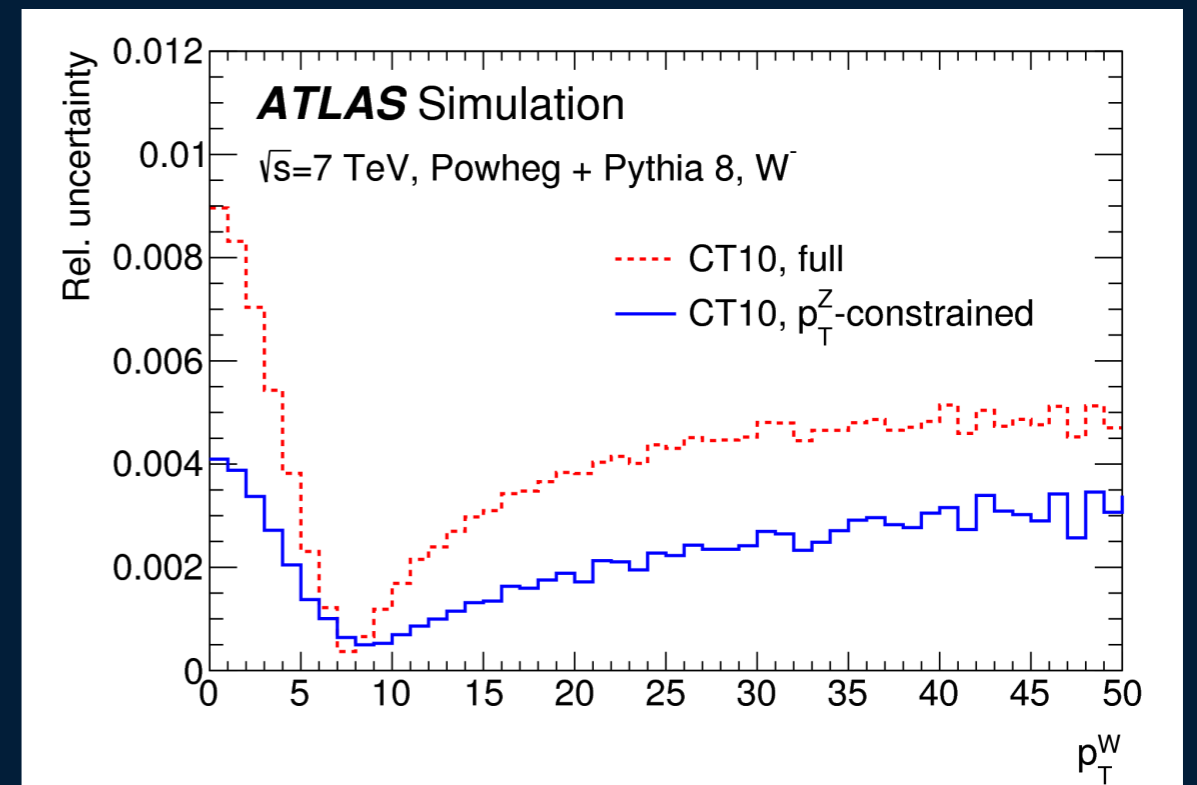
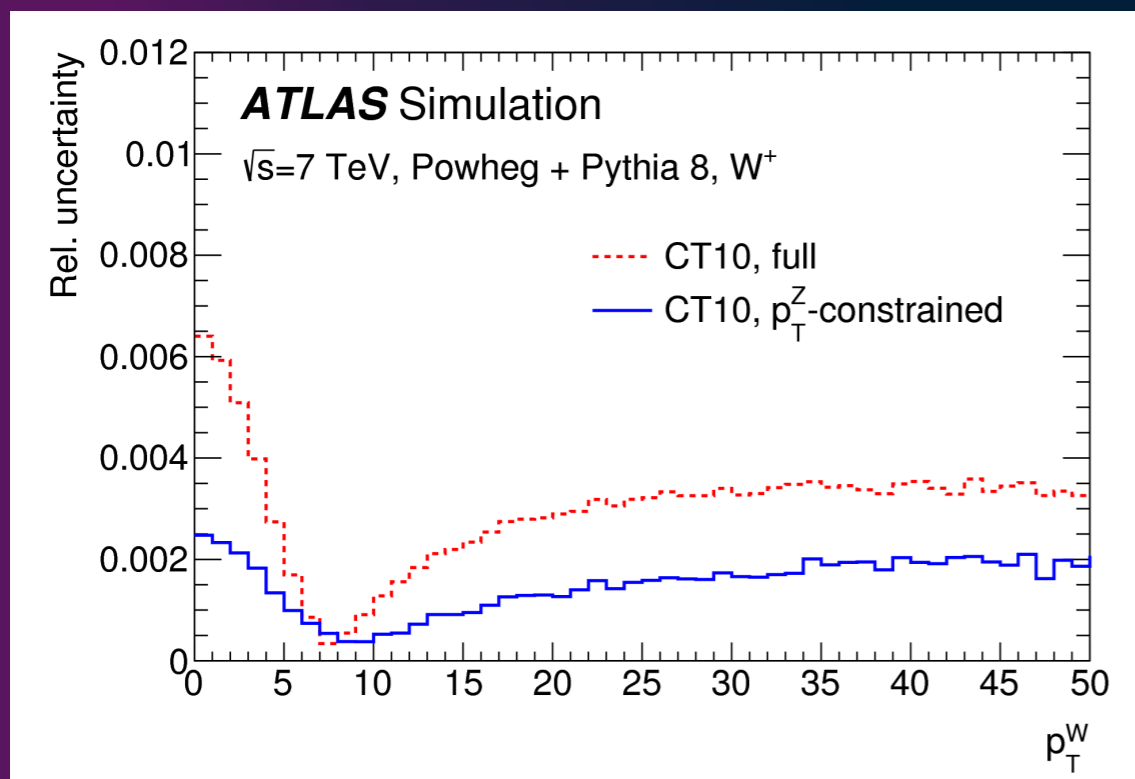
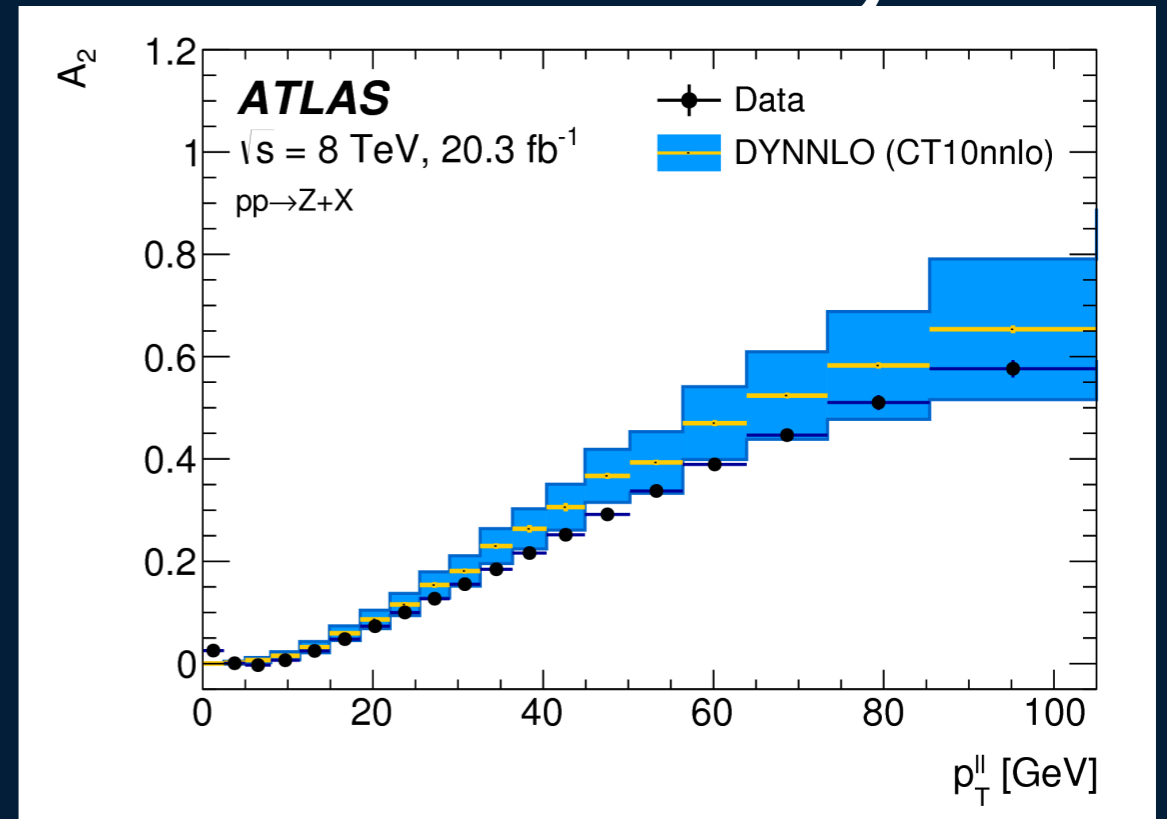


# $p_T$ modeling strategy

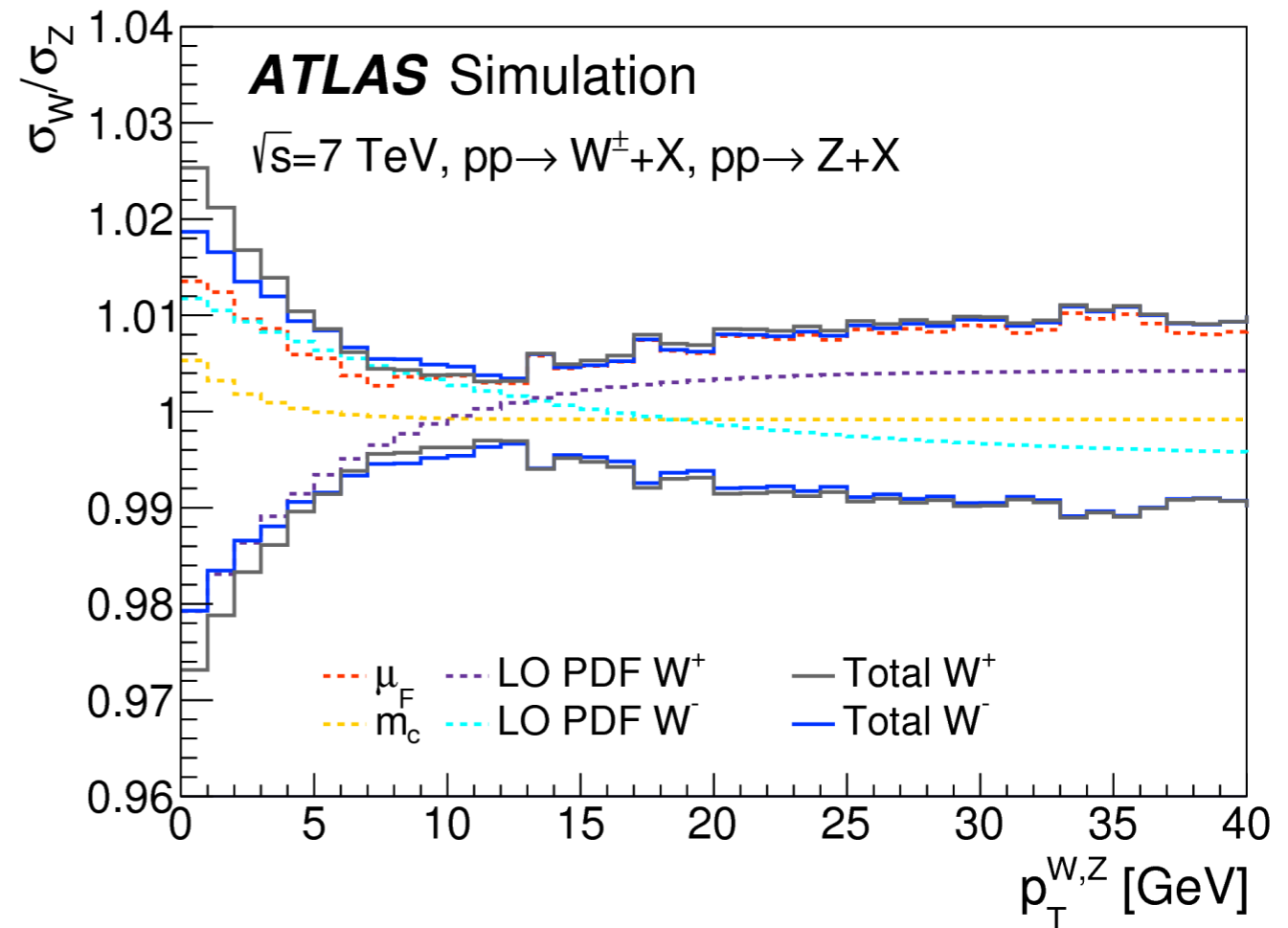
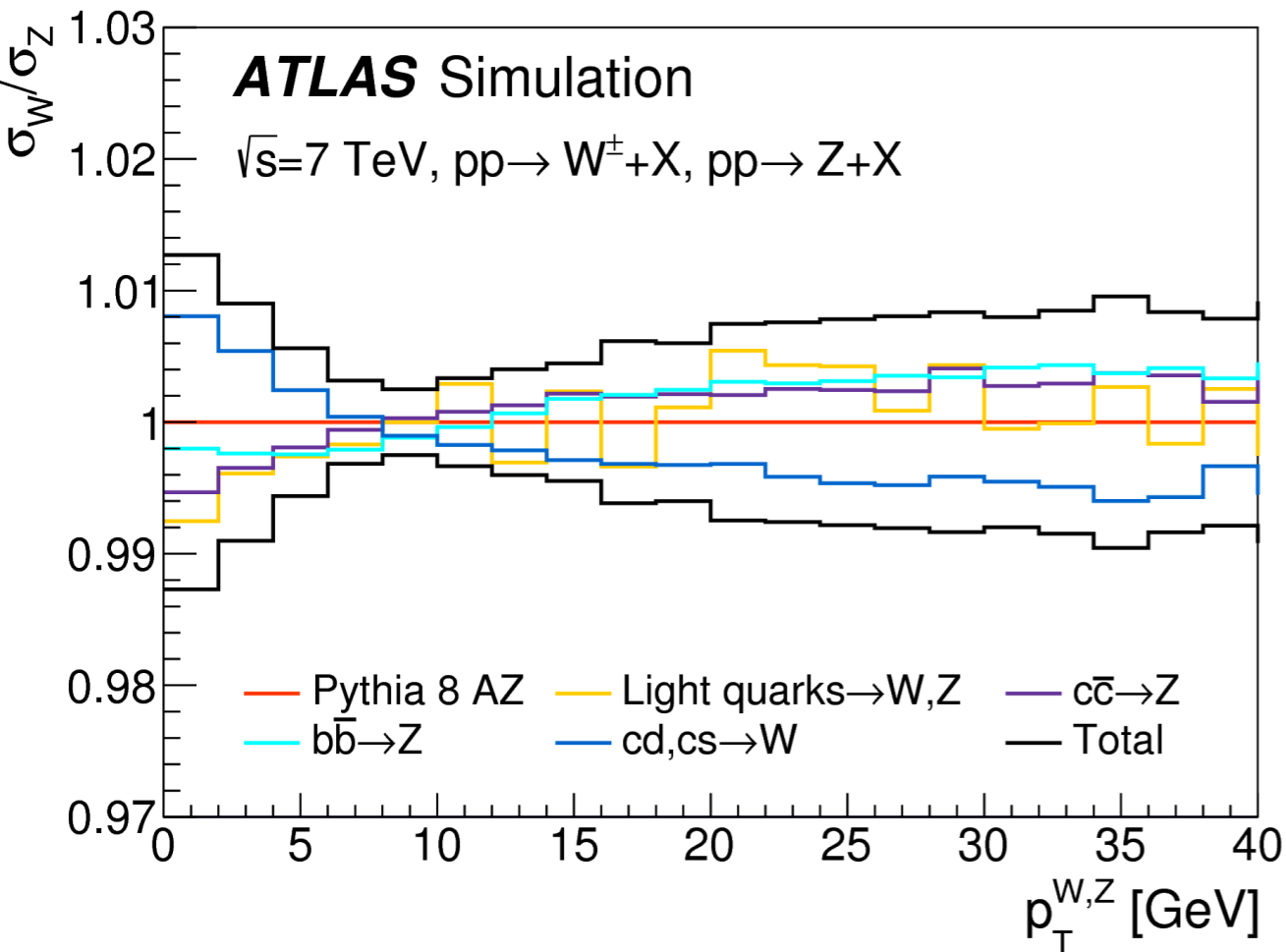


# fixed-order uncertainty

- Experimental polarisation uncertainties from Z measurement propagated to W, additional uncertainty for  $A_2$  (disagreement with DYNNLO)
- CT10nnlo relative variations of  $p_T^W$  and  $p_T^Z$  are considered

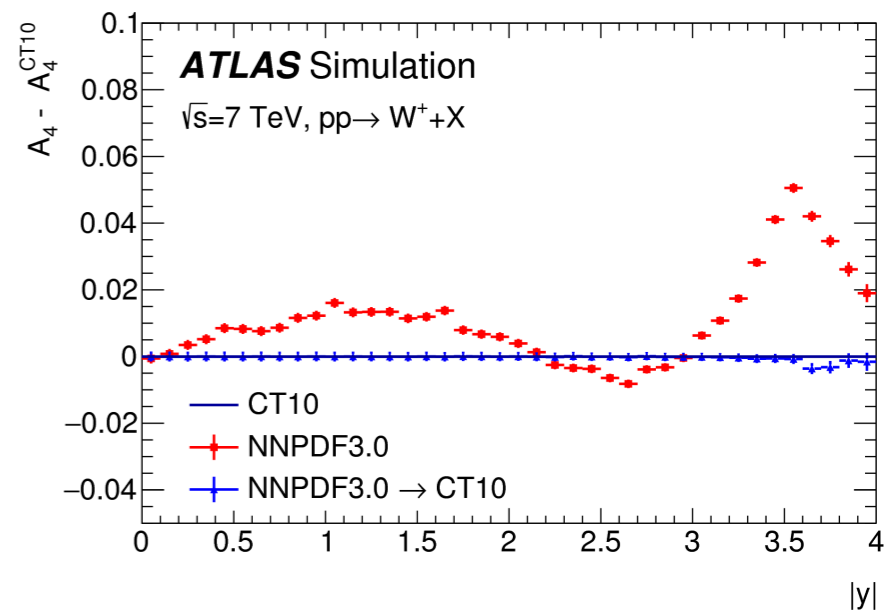
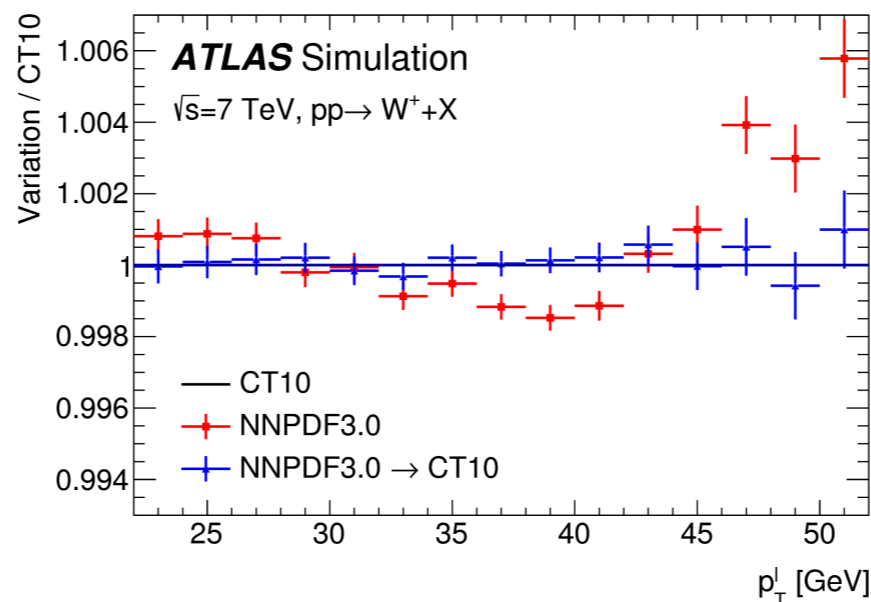
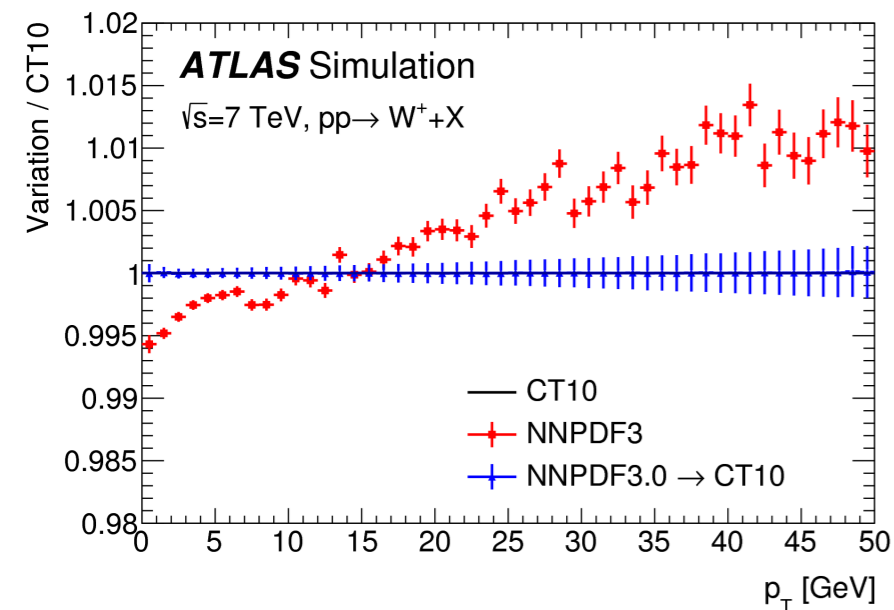
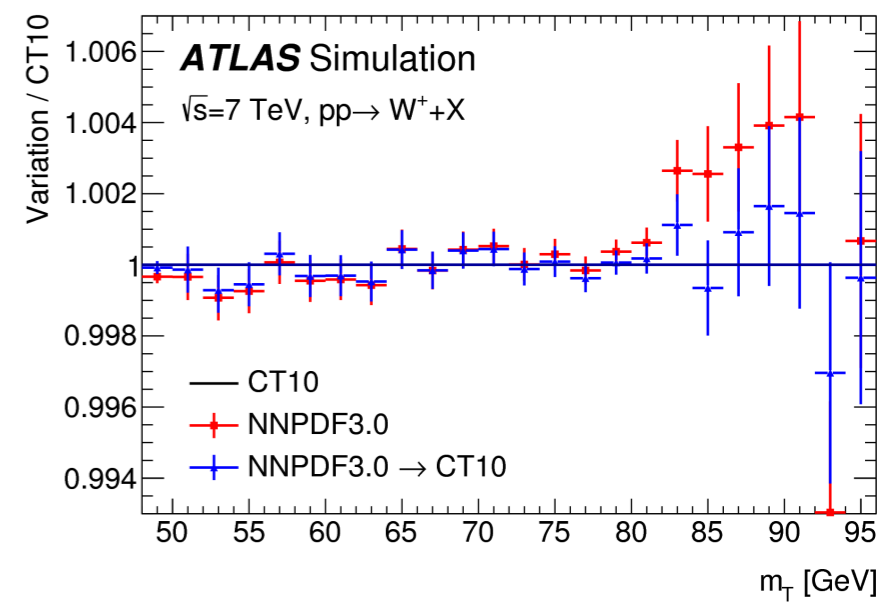
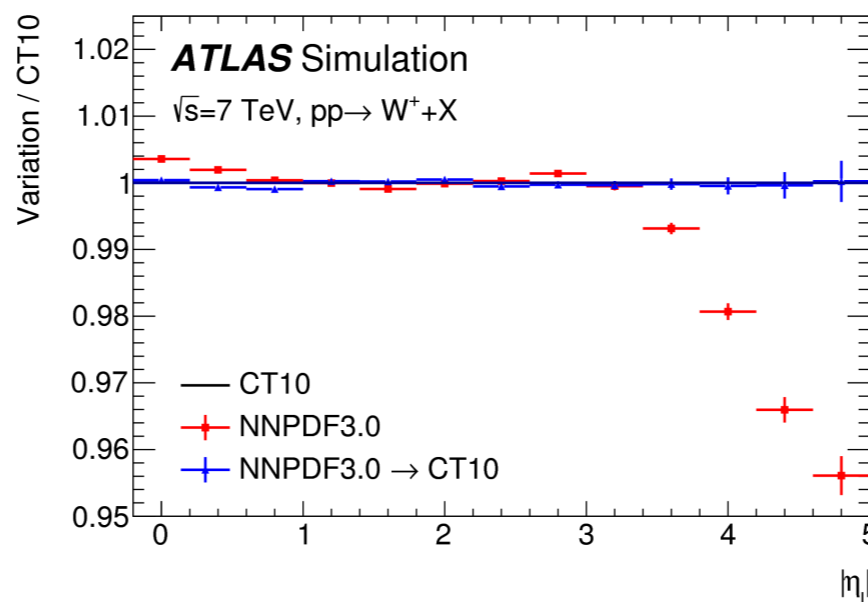
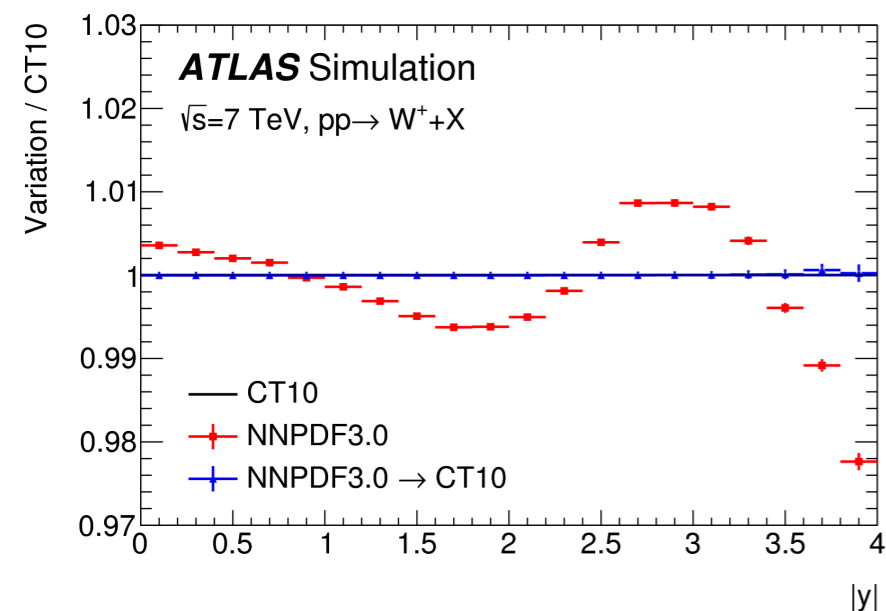


# Parton shower uncertainty



- factorisation scale variations correlated between W/Z for light quark, uncorrelated for heavy quarks
- other sources :  $m_c$ , parton shower LO PDF

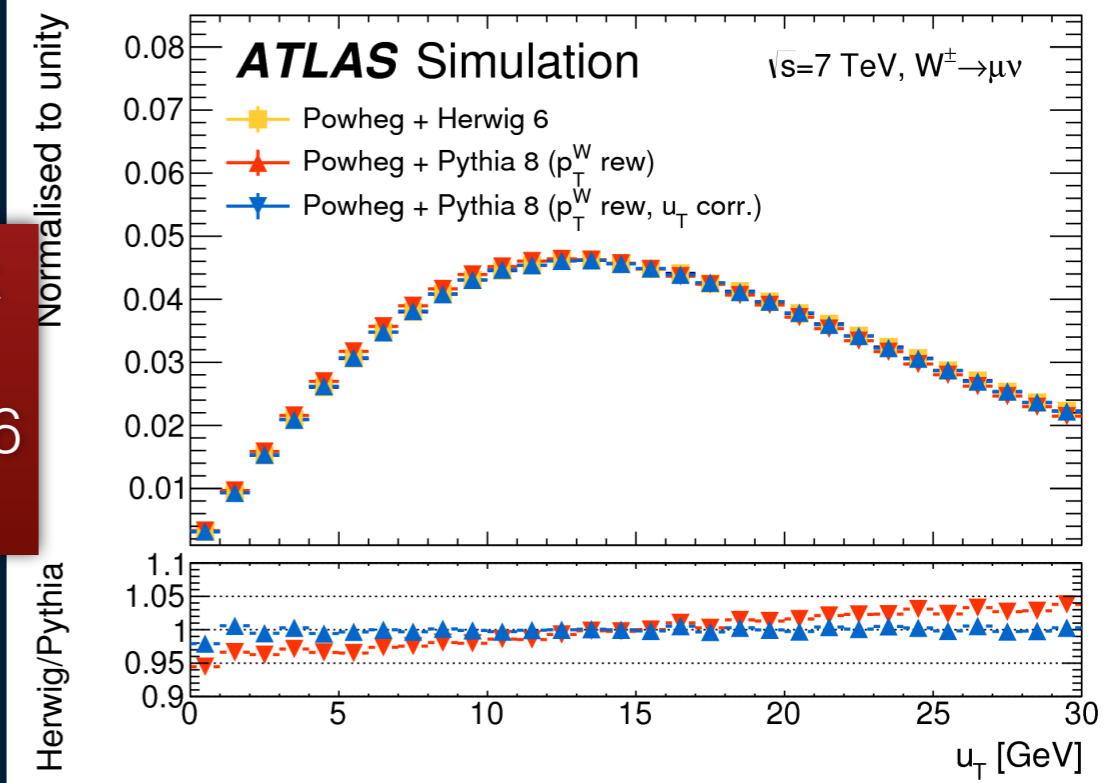
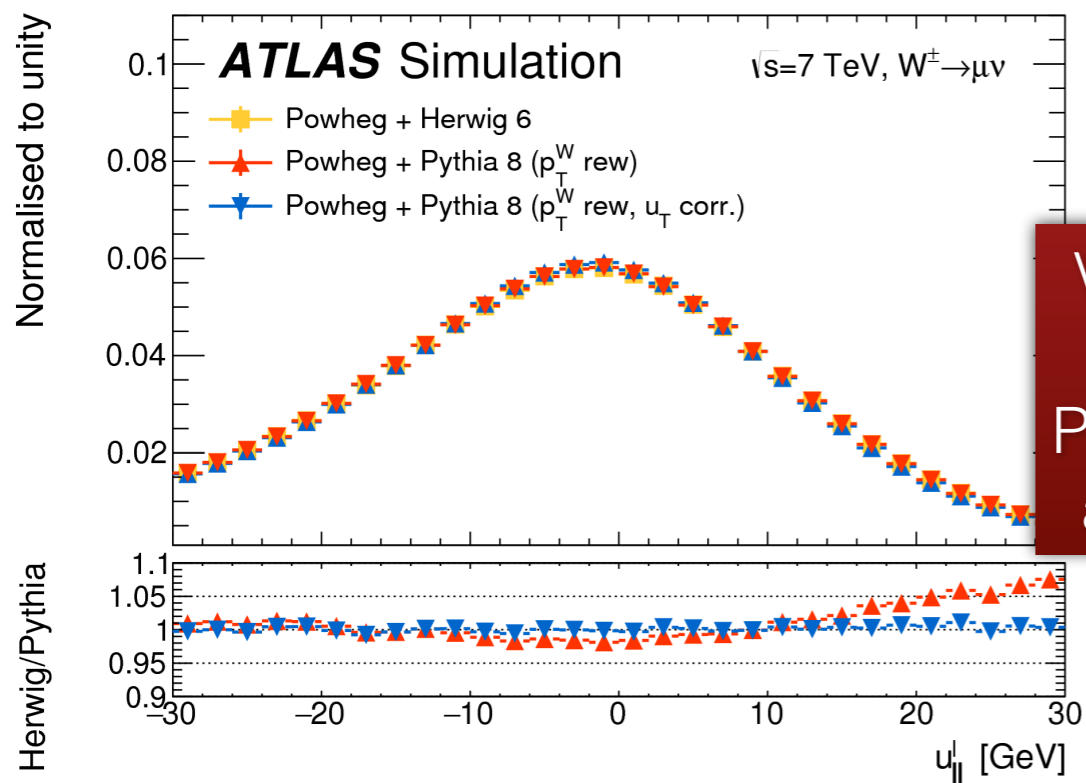
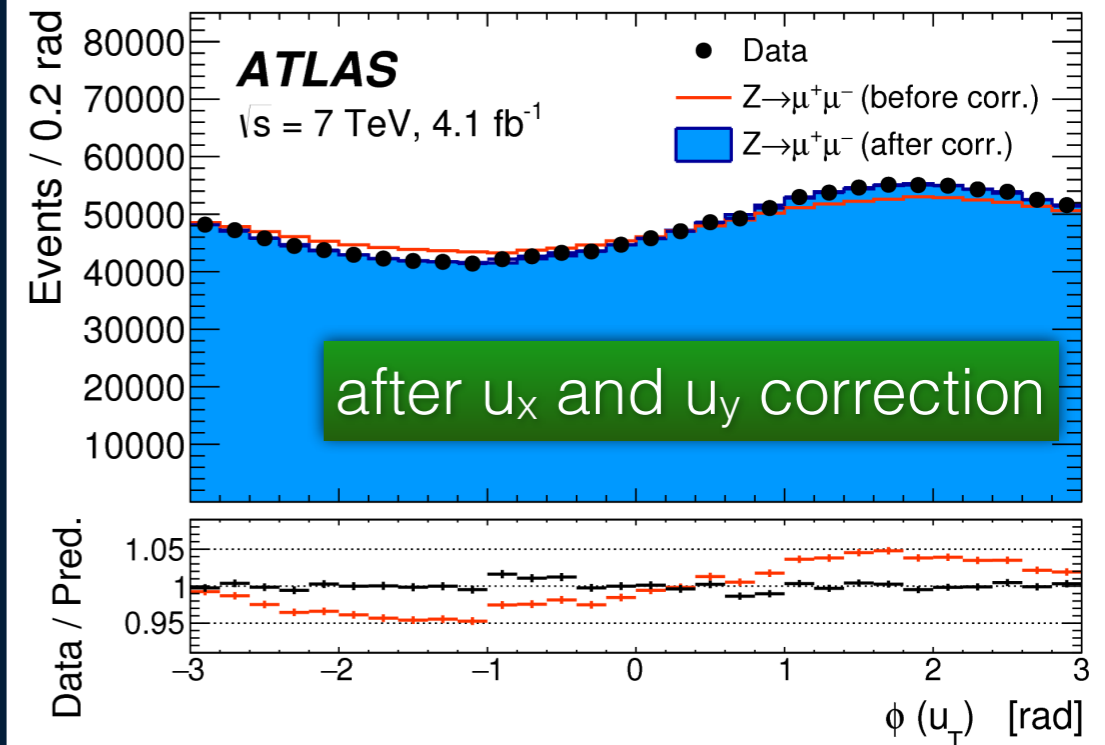
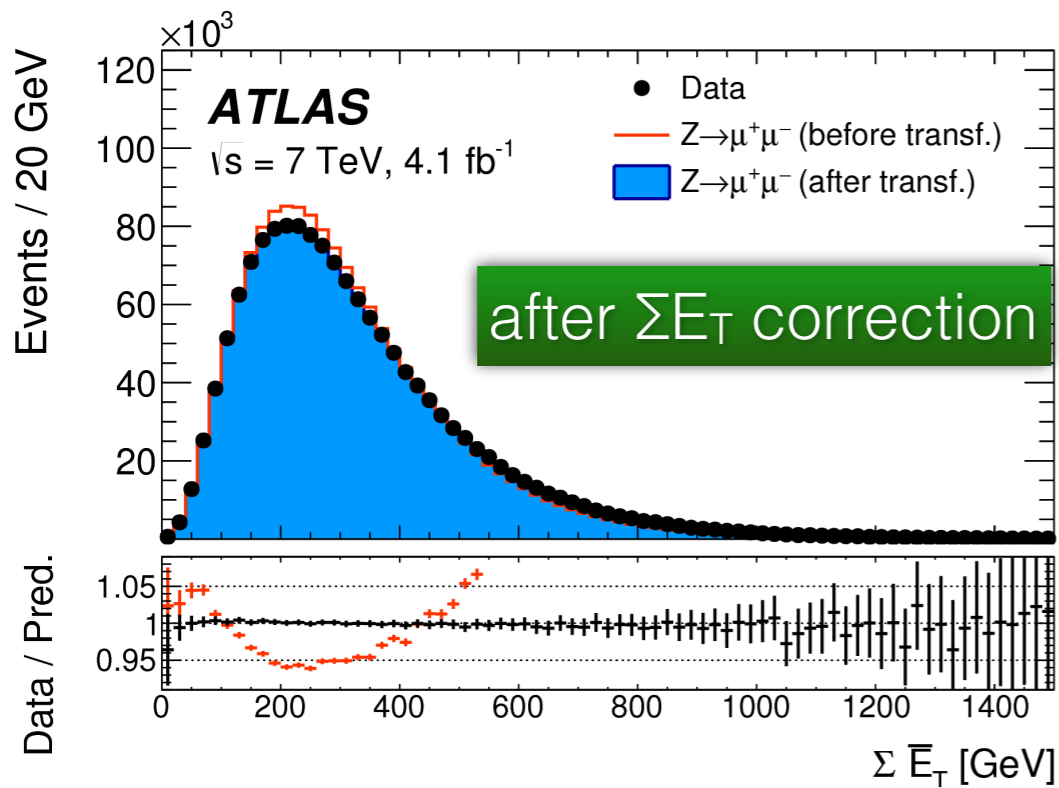
# Modeling tests



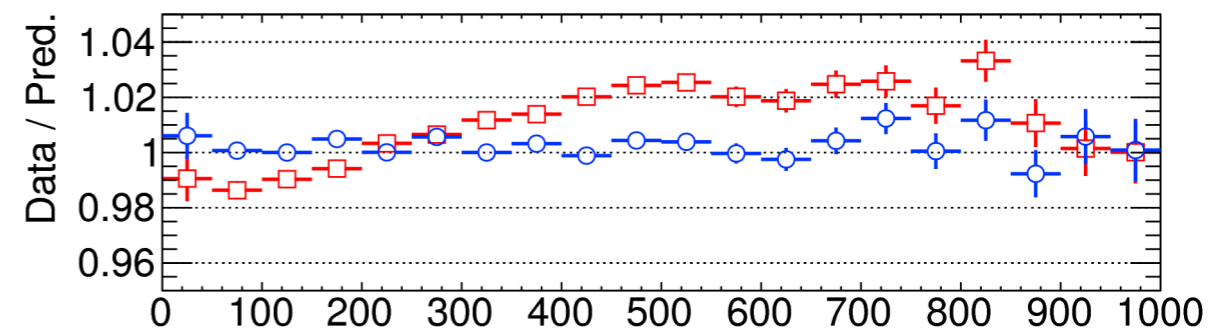
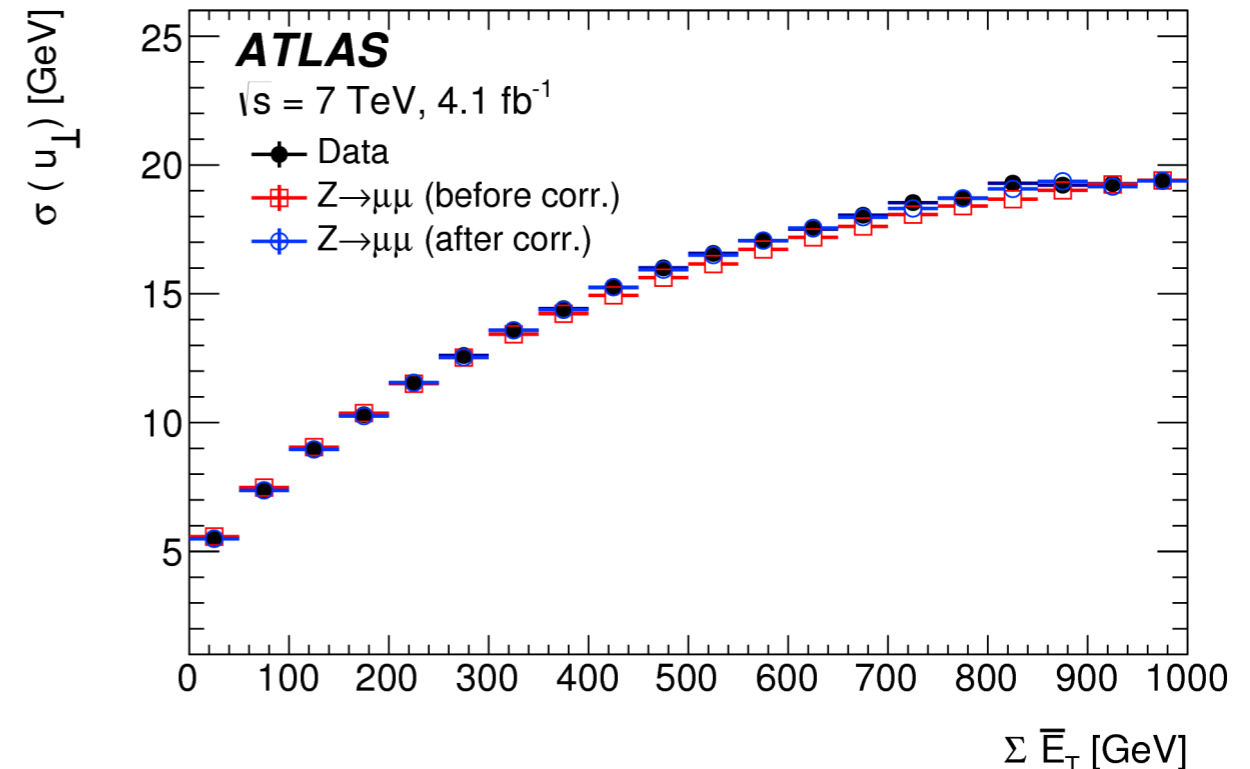
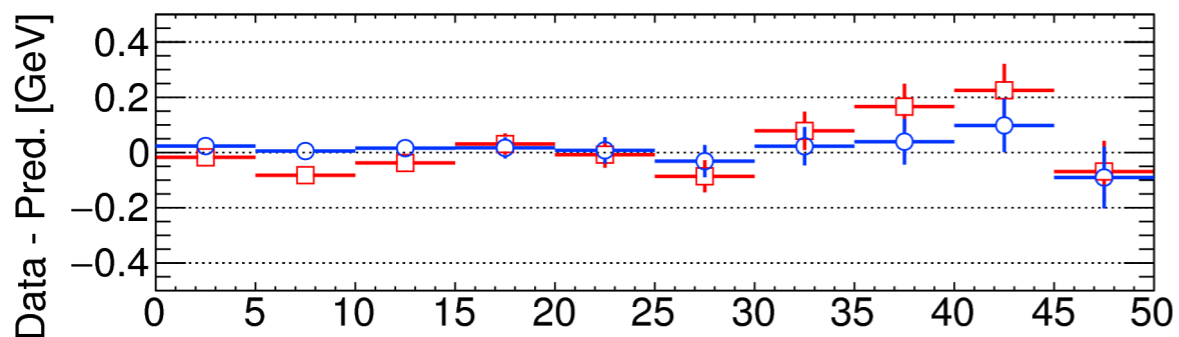
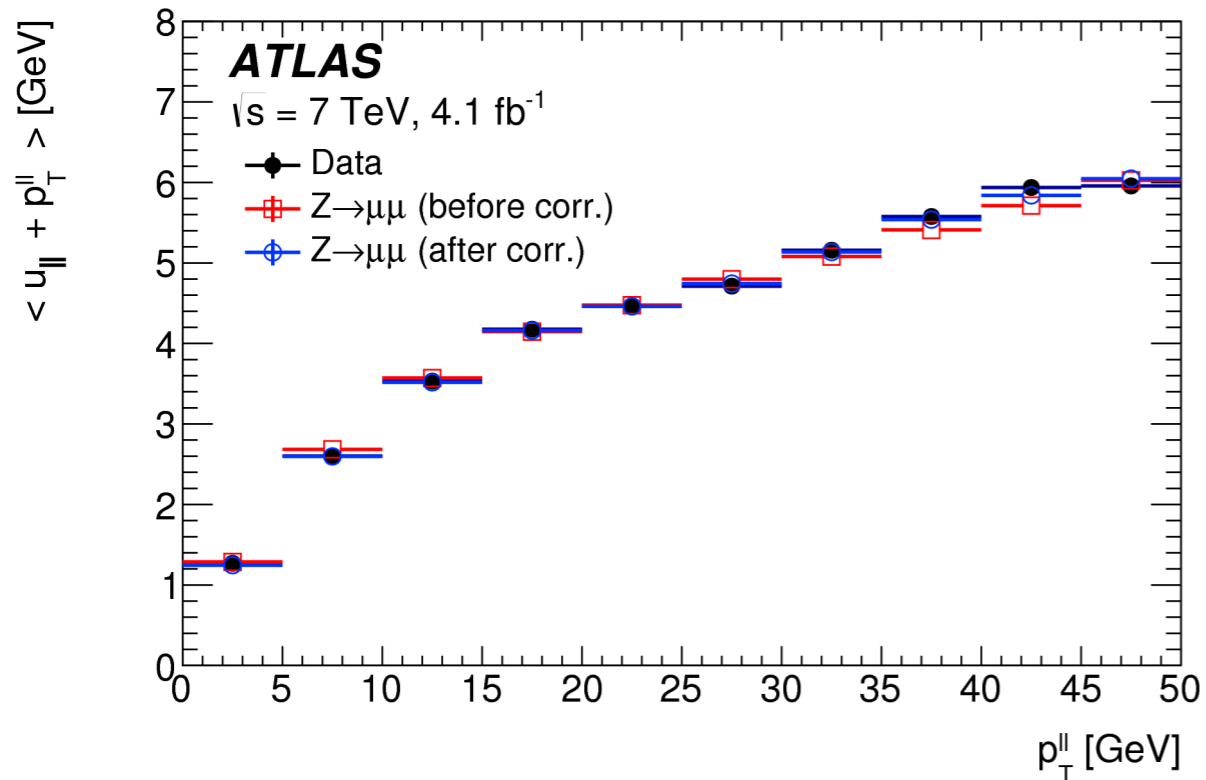
Use NNPDF3 prediction as pseudo-data, perform the various reweightings ( $y$ ,  $p_T$ , polarisation) to CT10 sample : strongly validates the modeling procedure  $\Delta m_W = 1.5 \pm 2.0$  MeV



# Recoil calibration



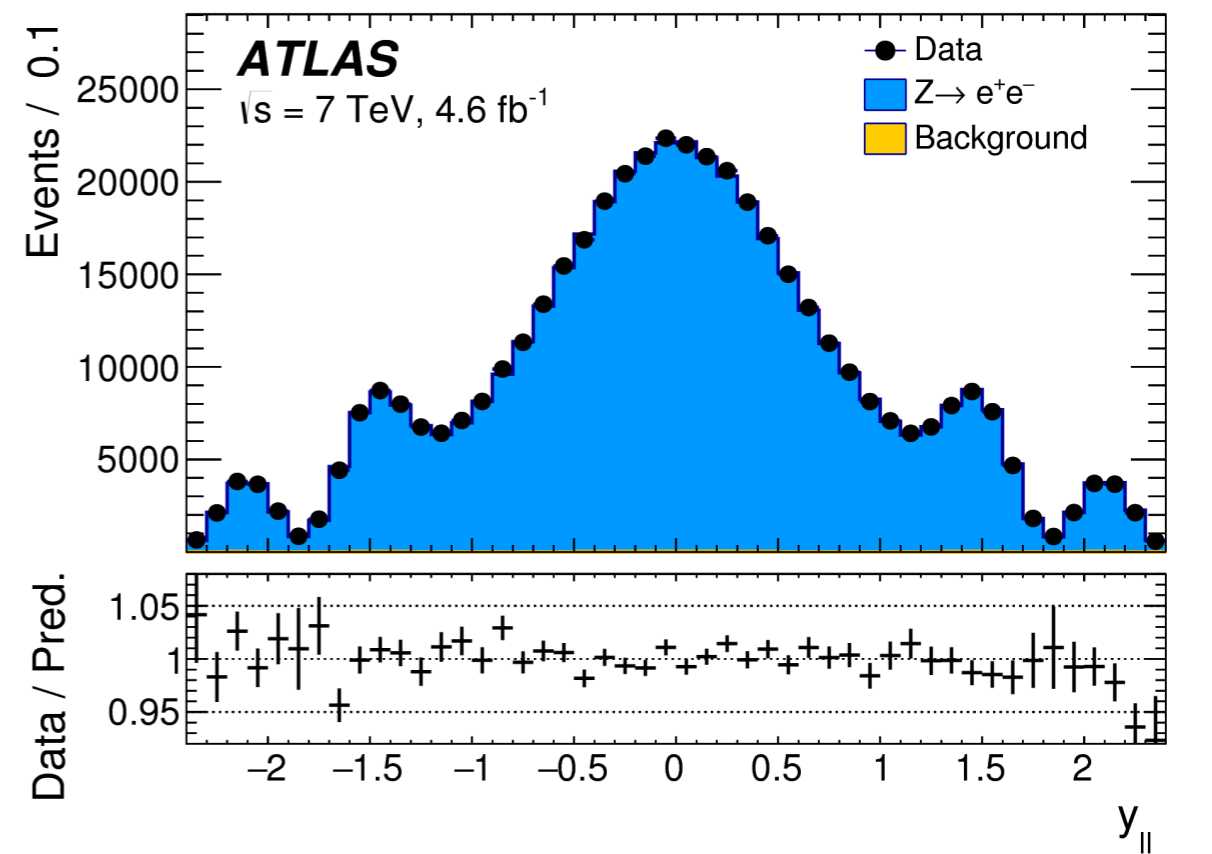
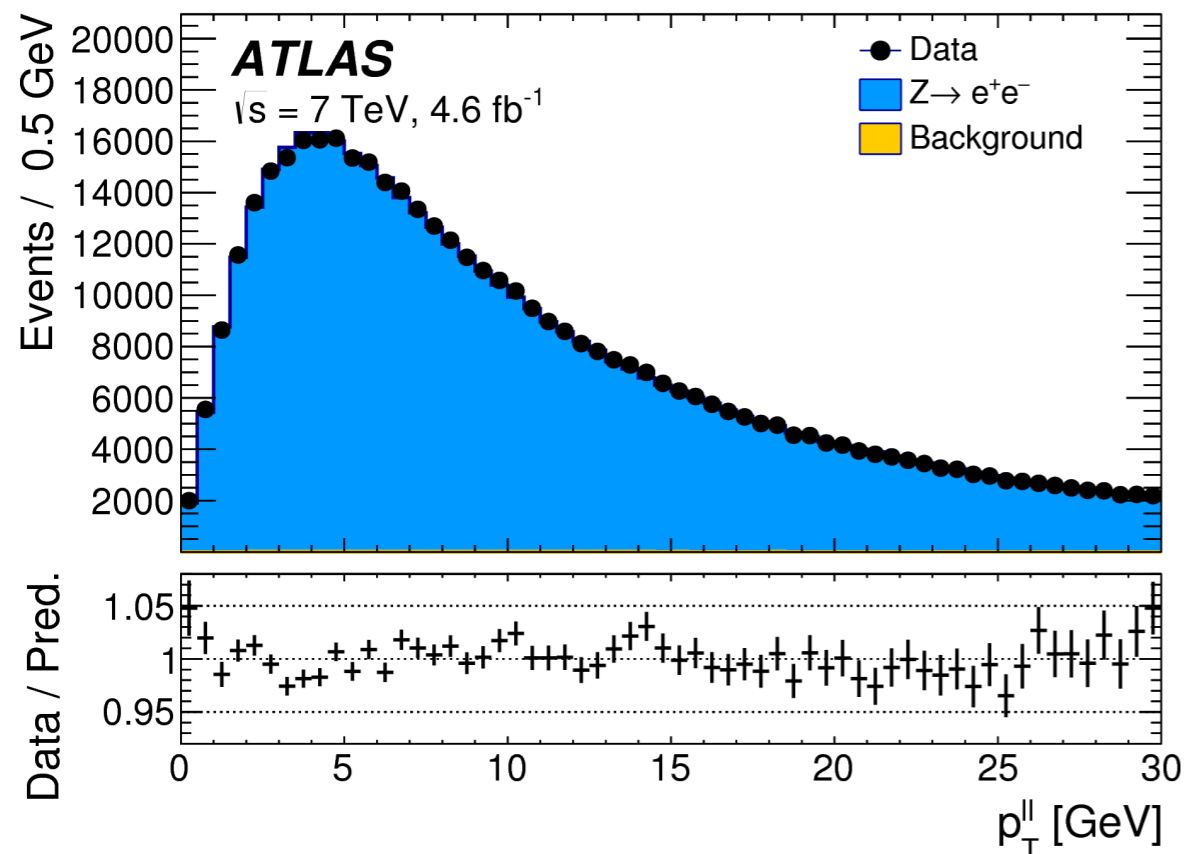
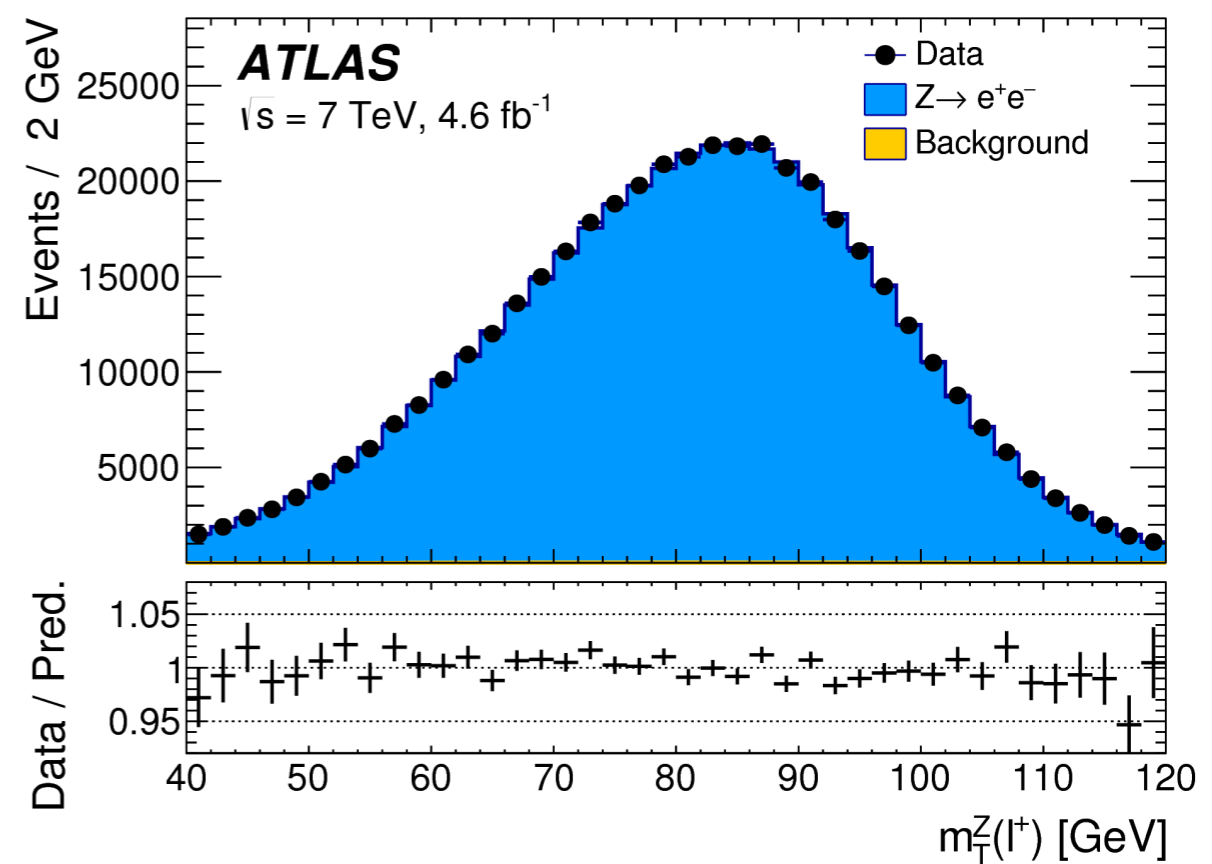
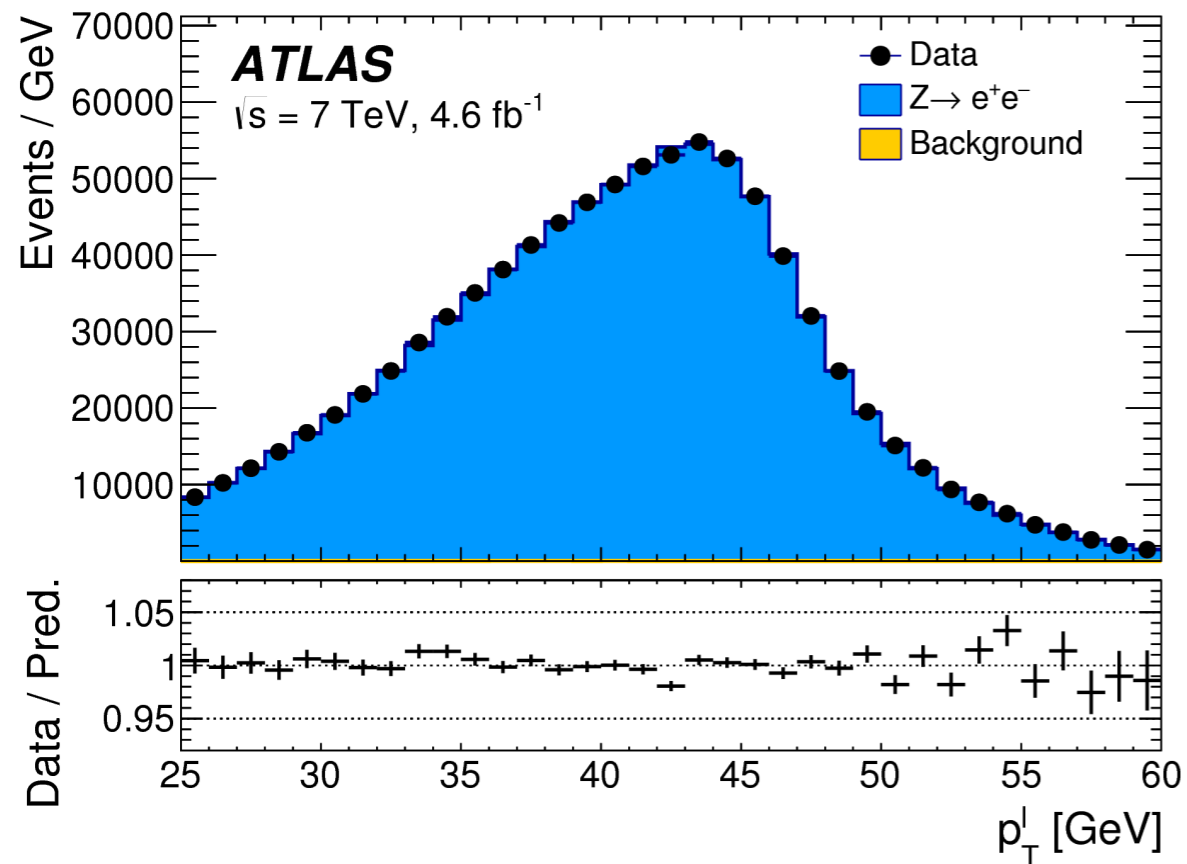
# Recoil calibration



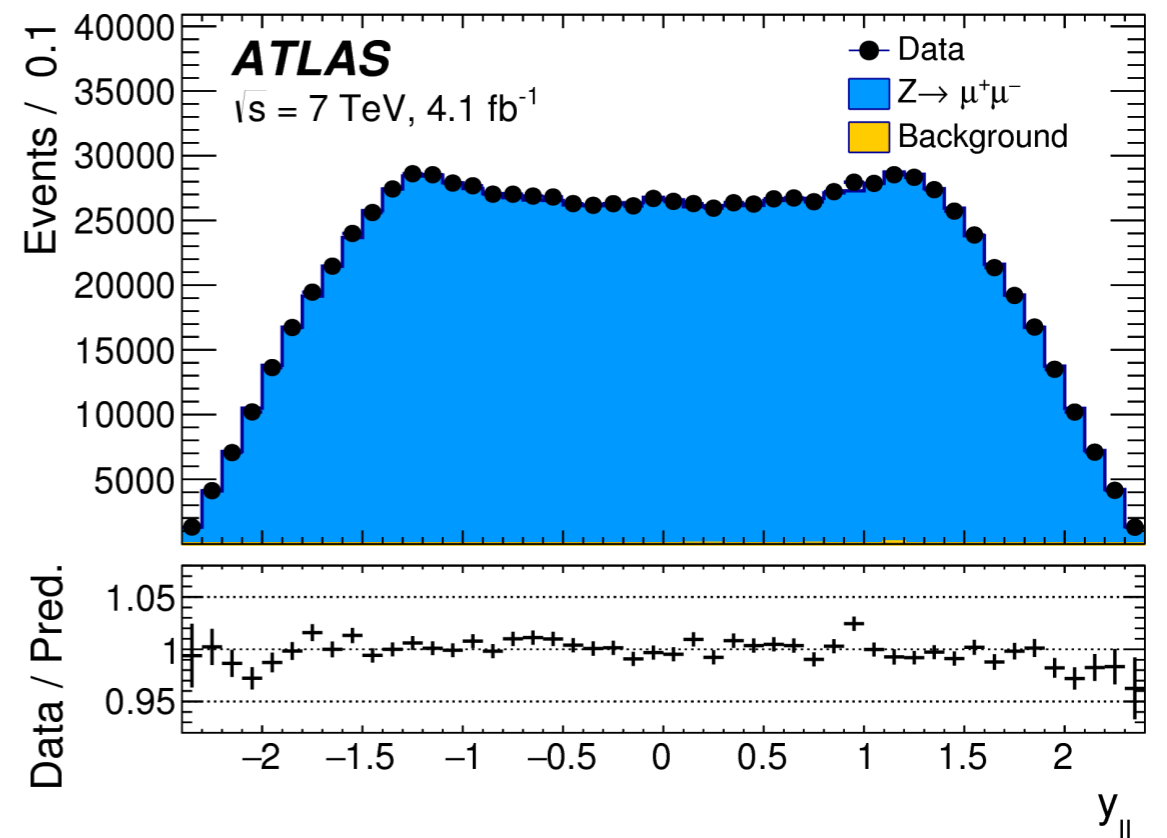
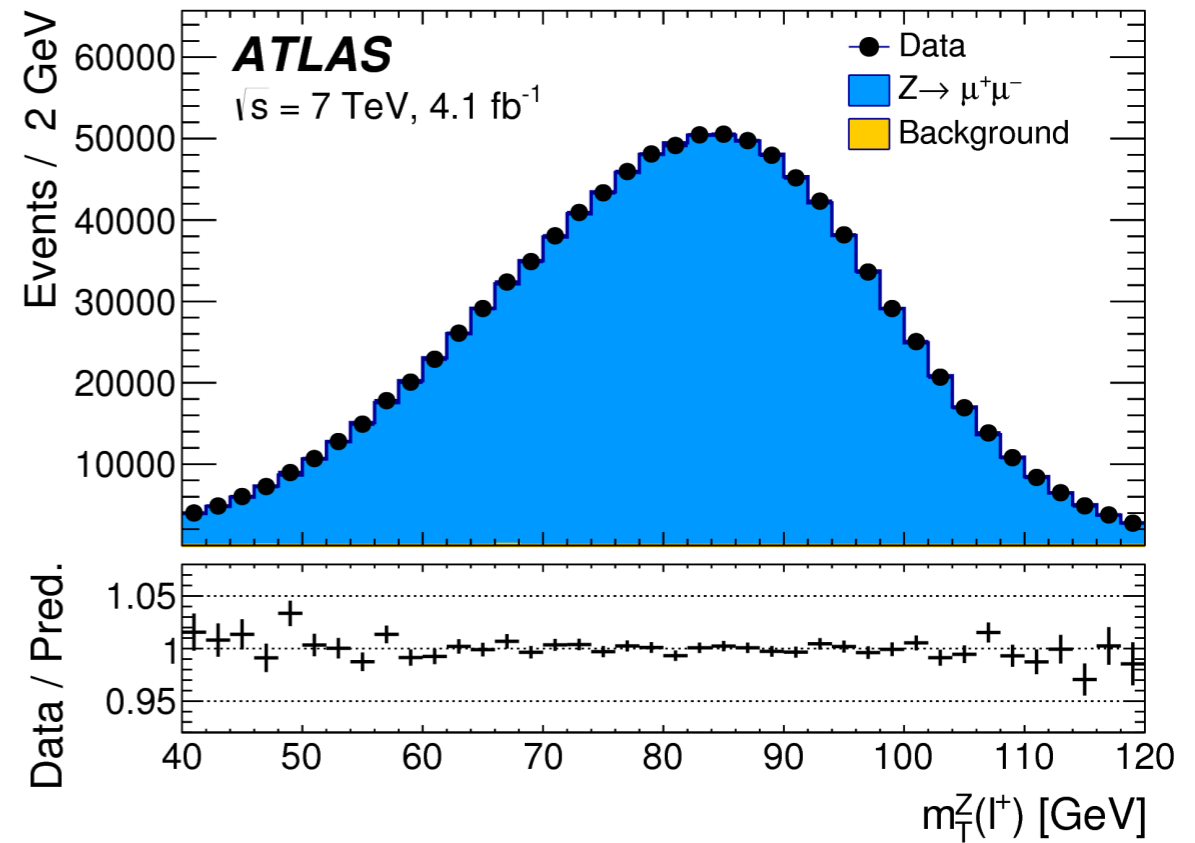
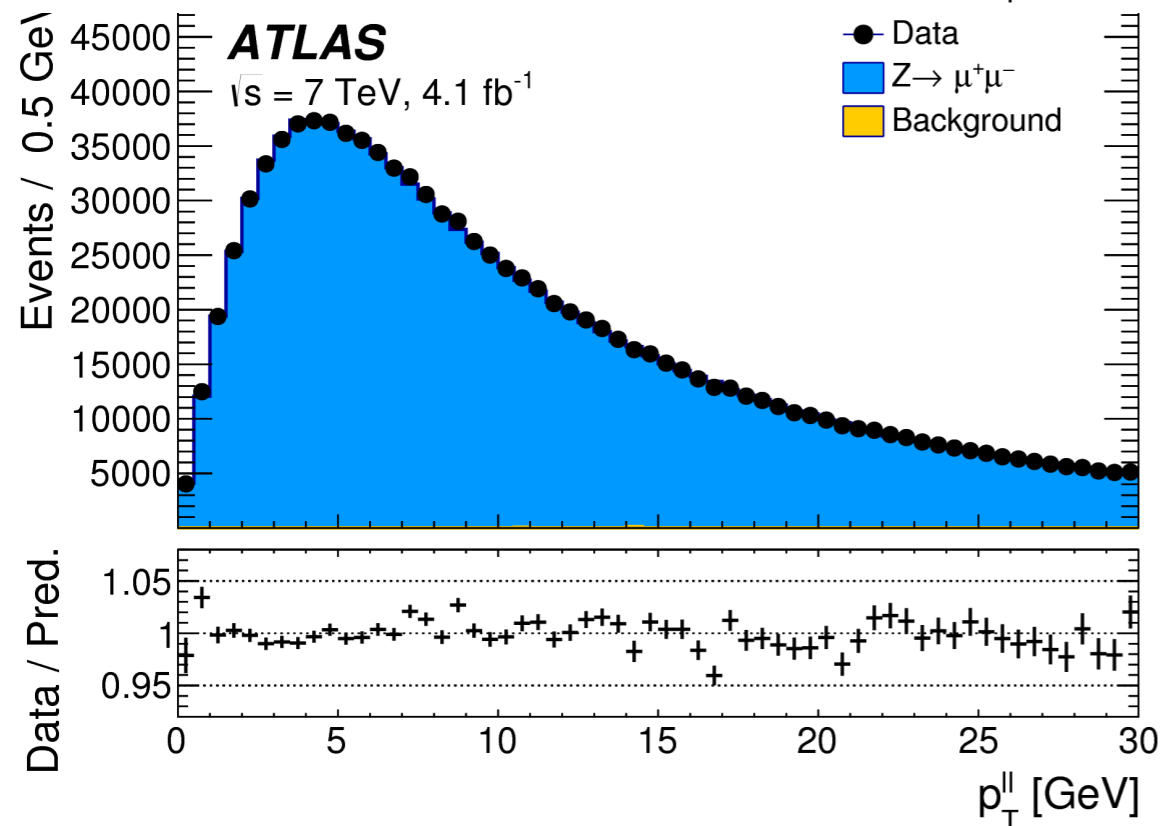
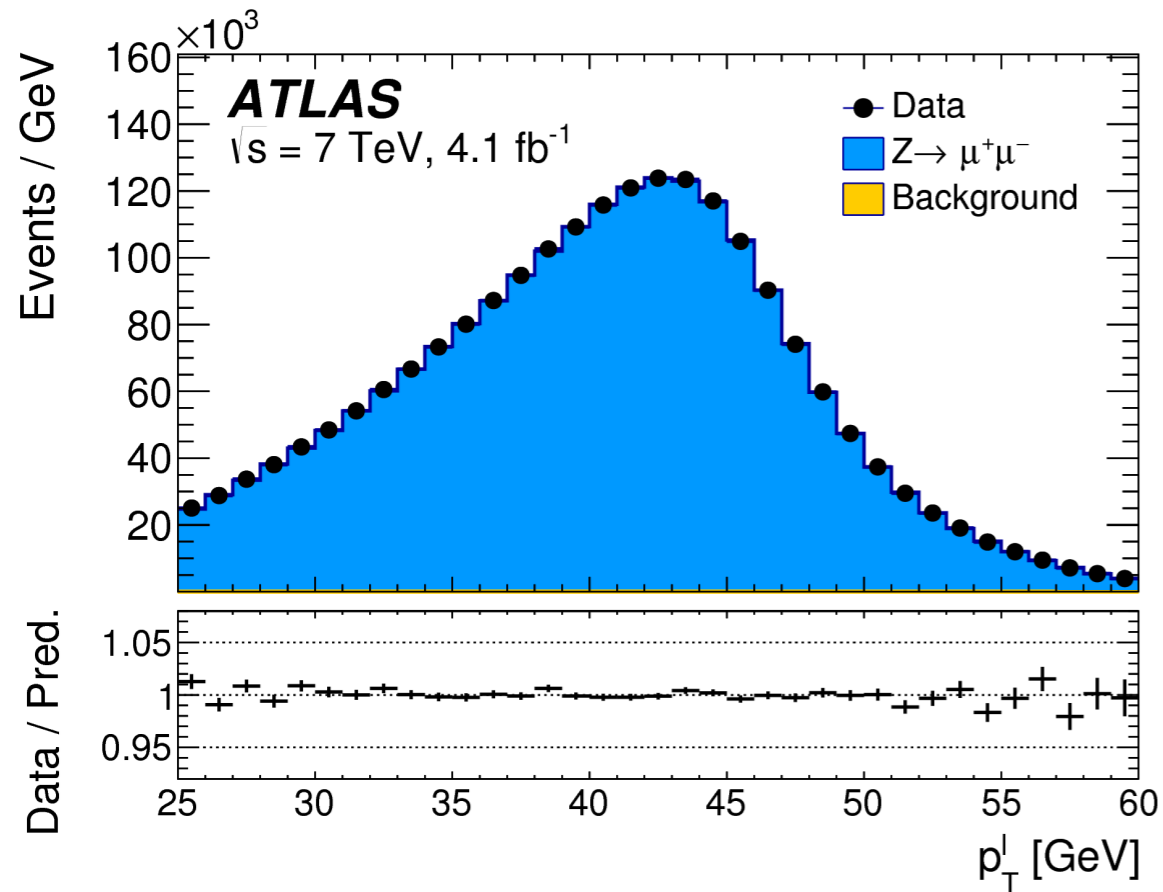
Recoil bias vs  $p_{\parallel}^Z$

Recoil resolution vs  $\Sigma \bar{E}_{\perp}$

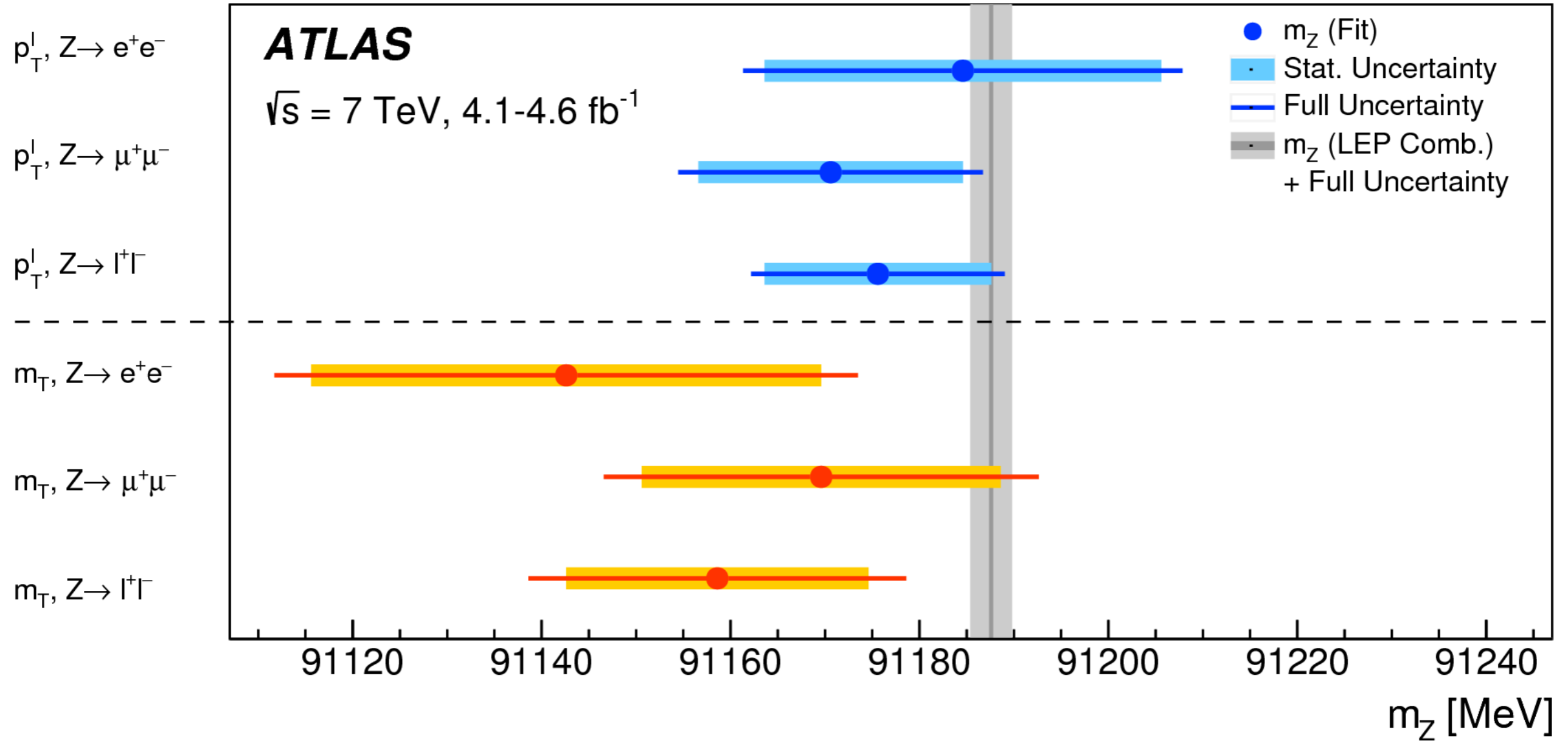
# Z ee plots after all corrections



# Z $\mu\mu$ plots after all corrections

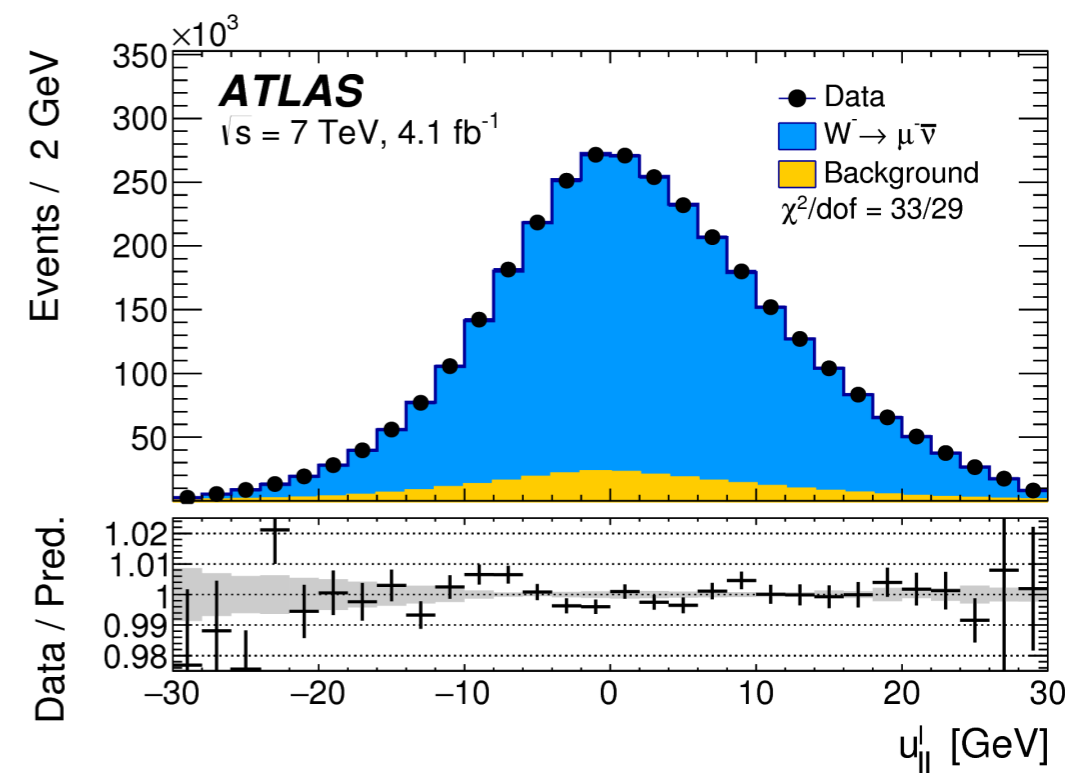
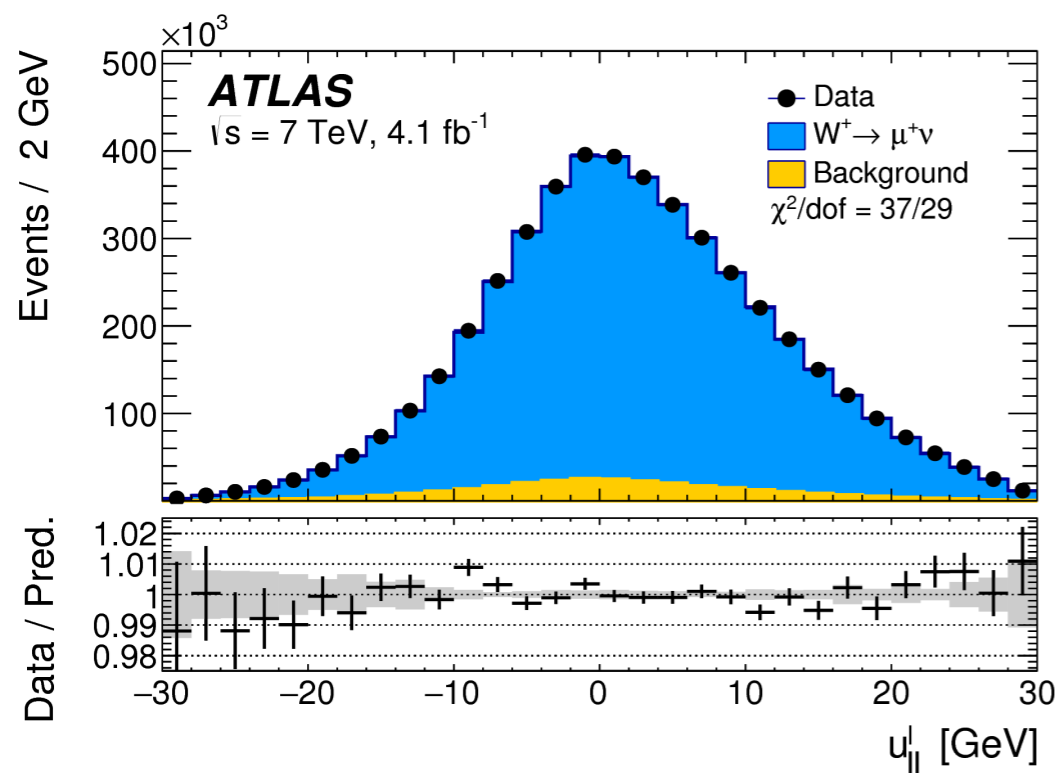
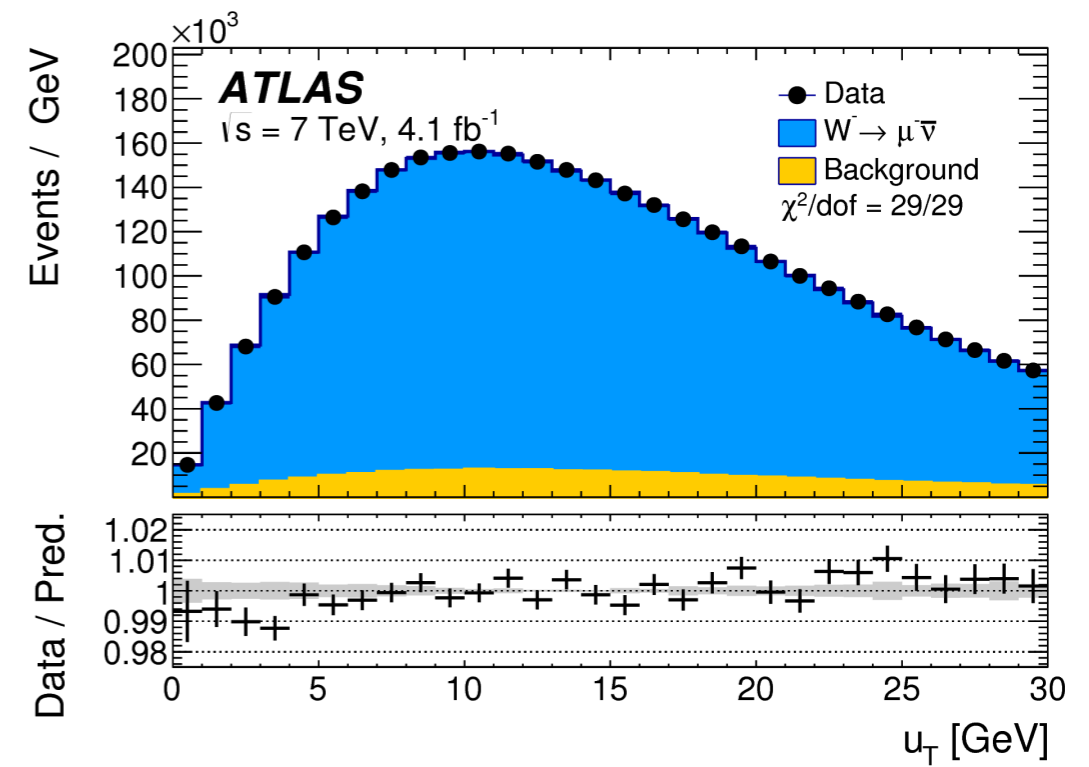
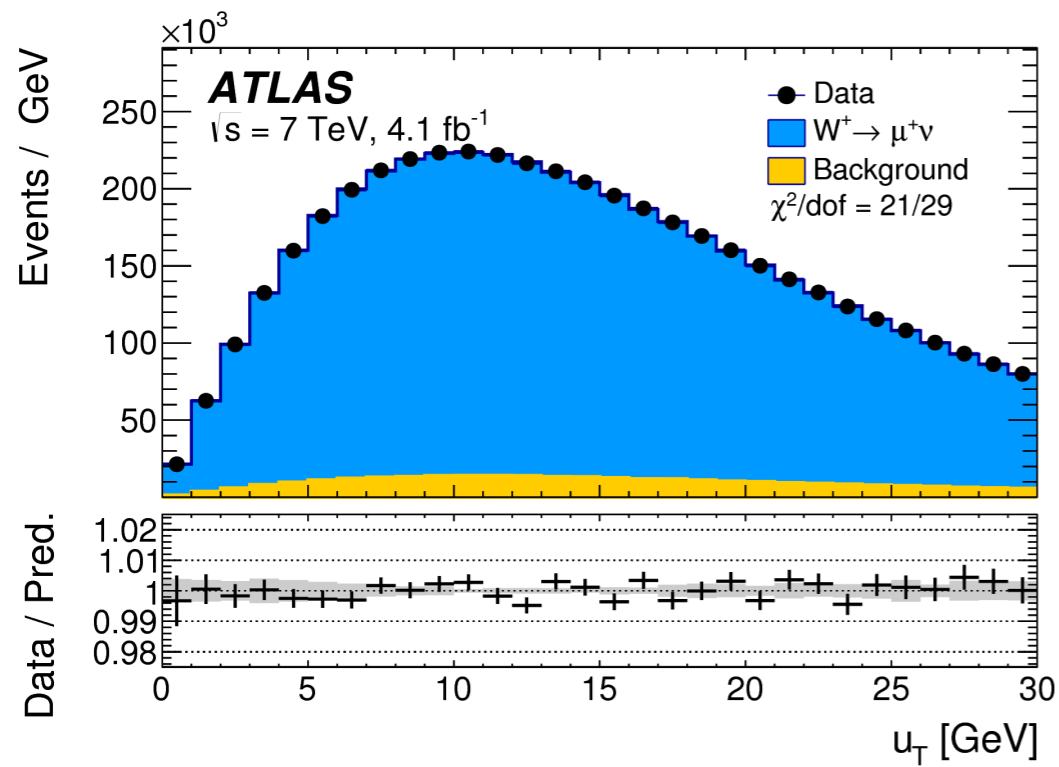


# Z mass measurement

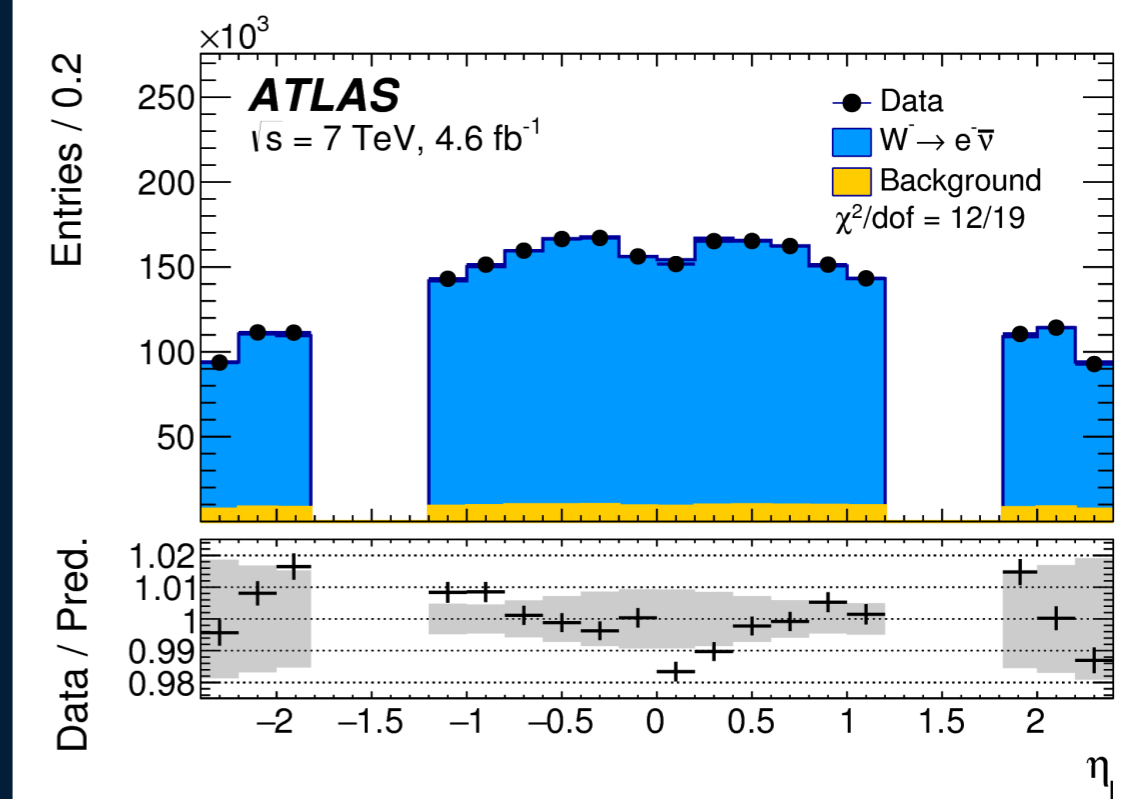
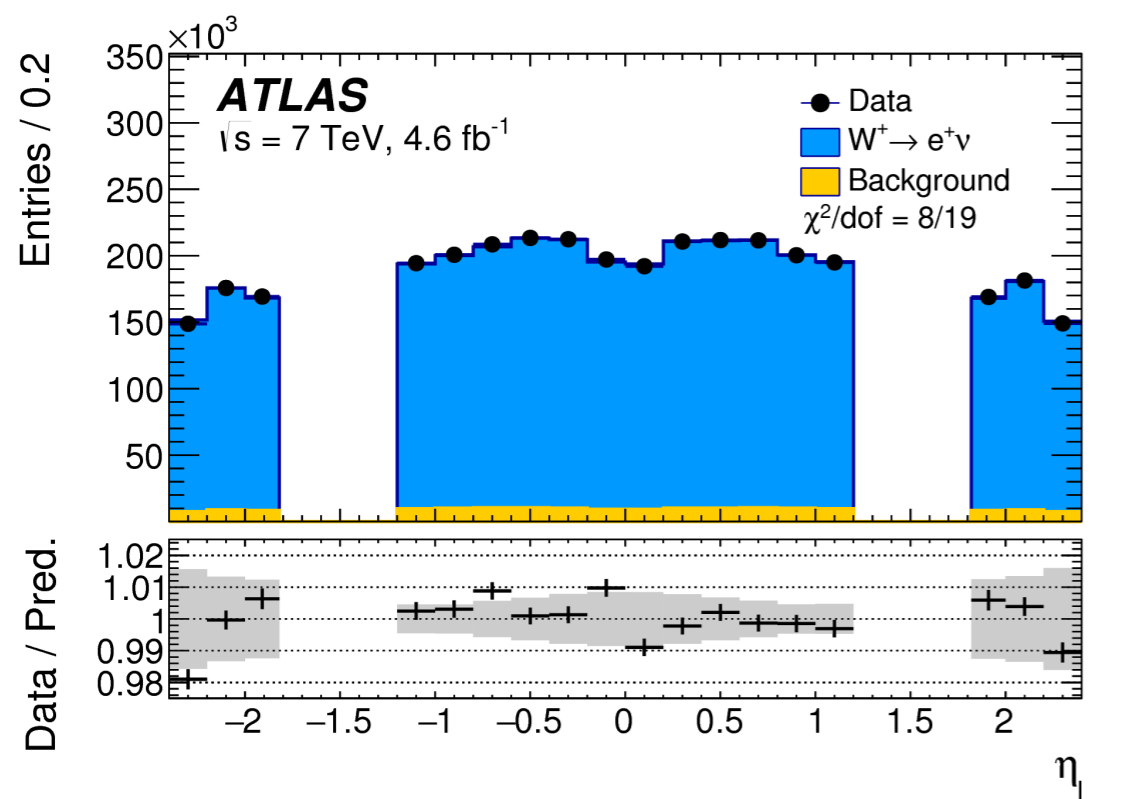
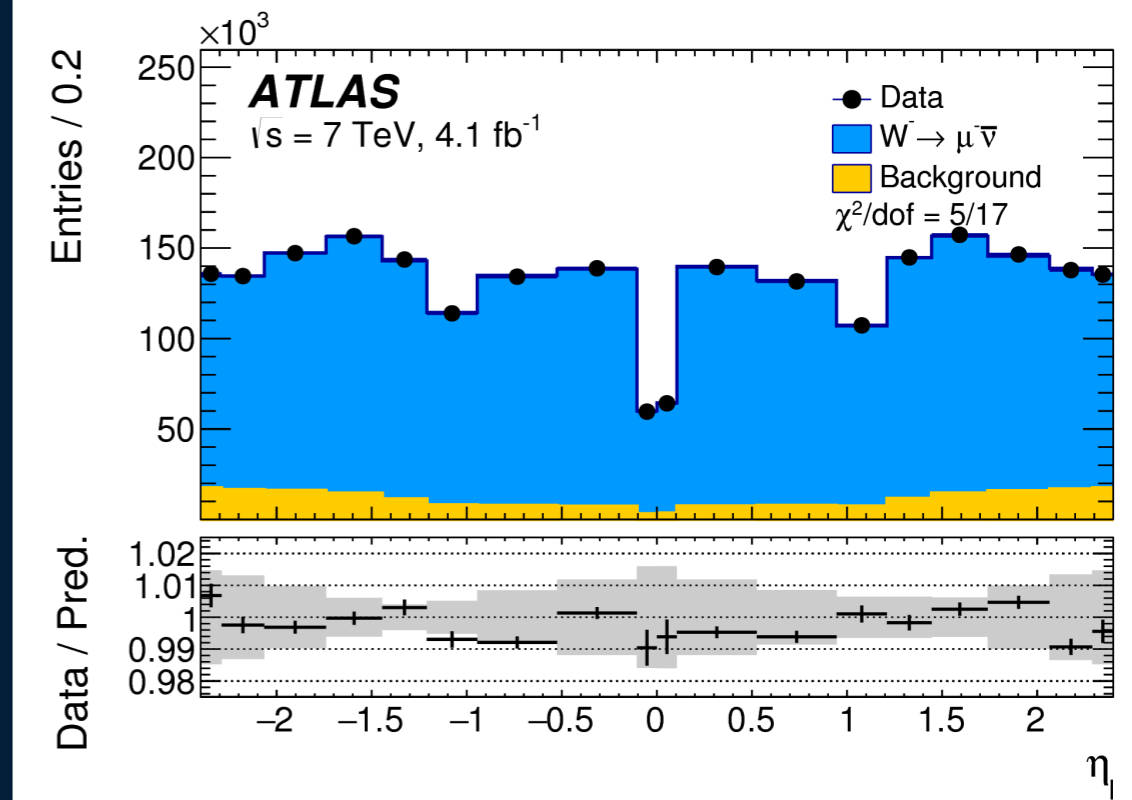
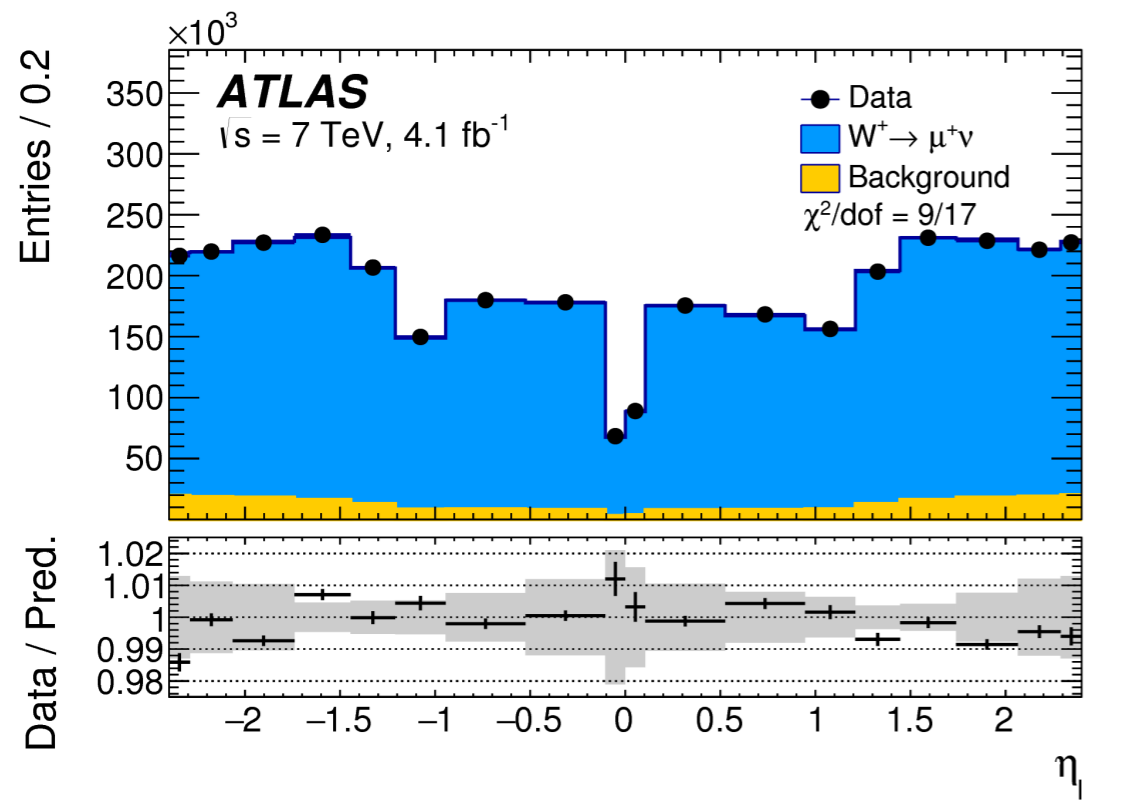




# Hadronic recoil

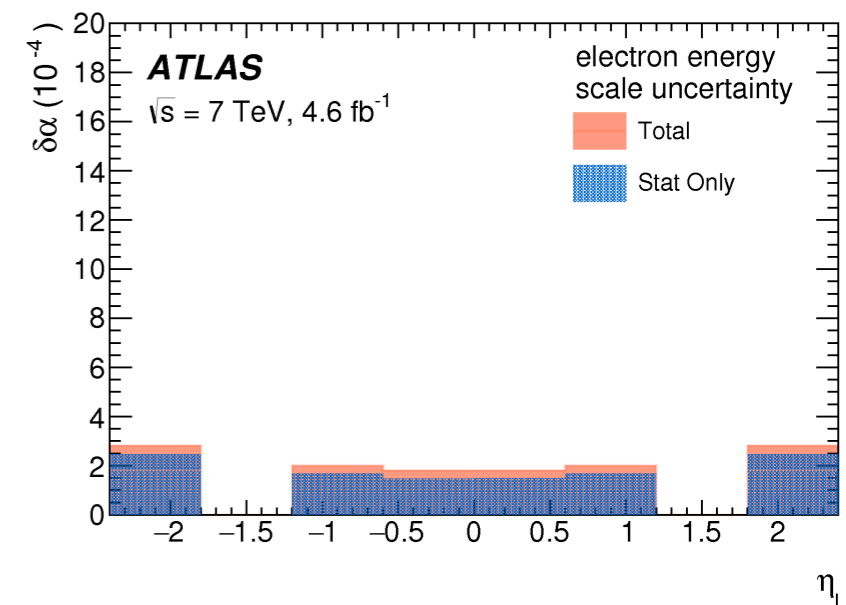
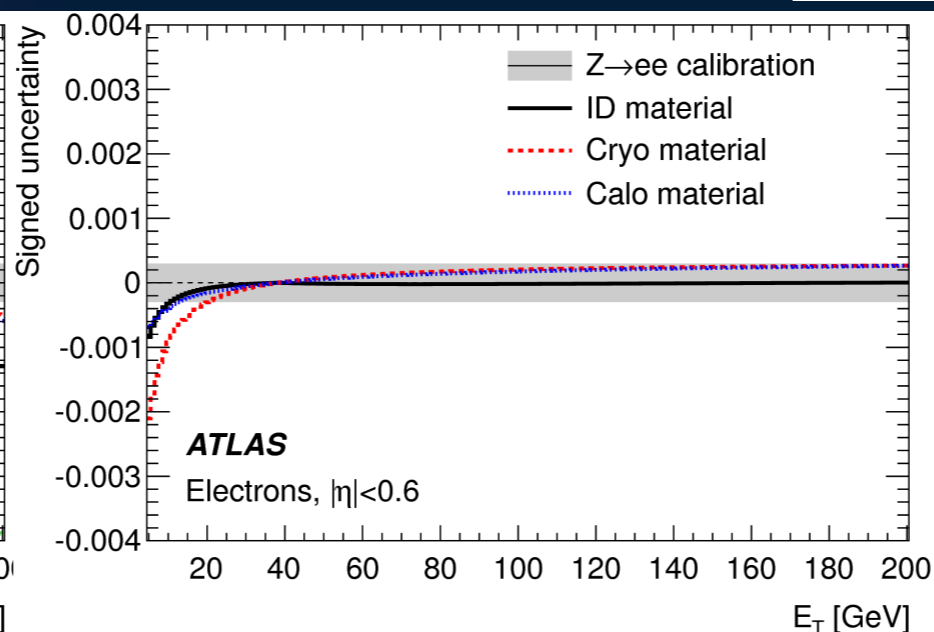
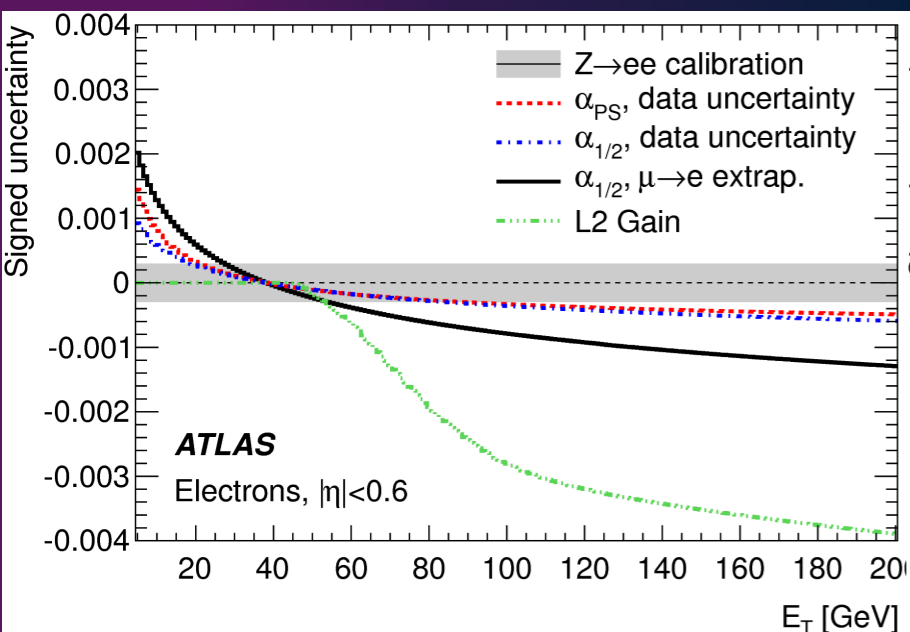
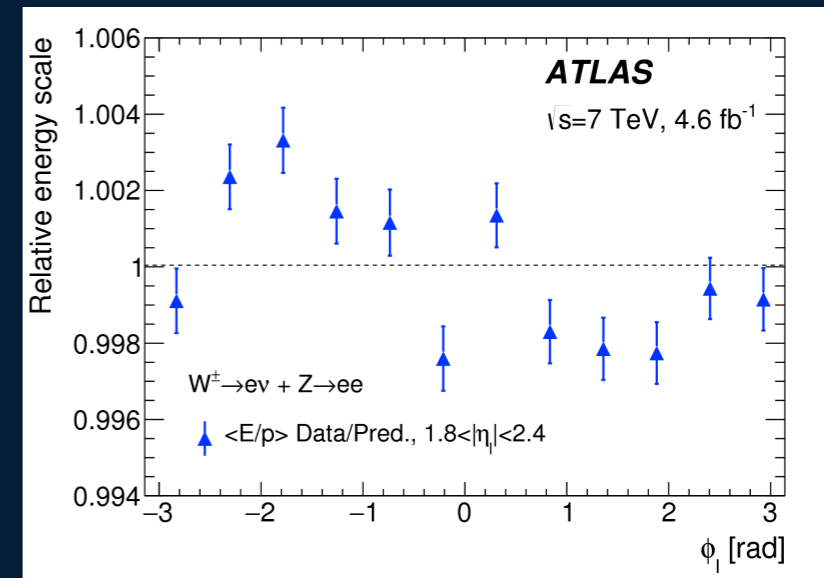


# Lepton eta

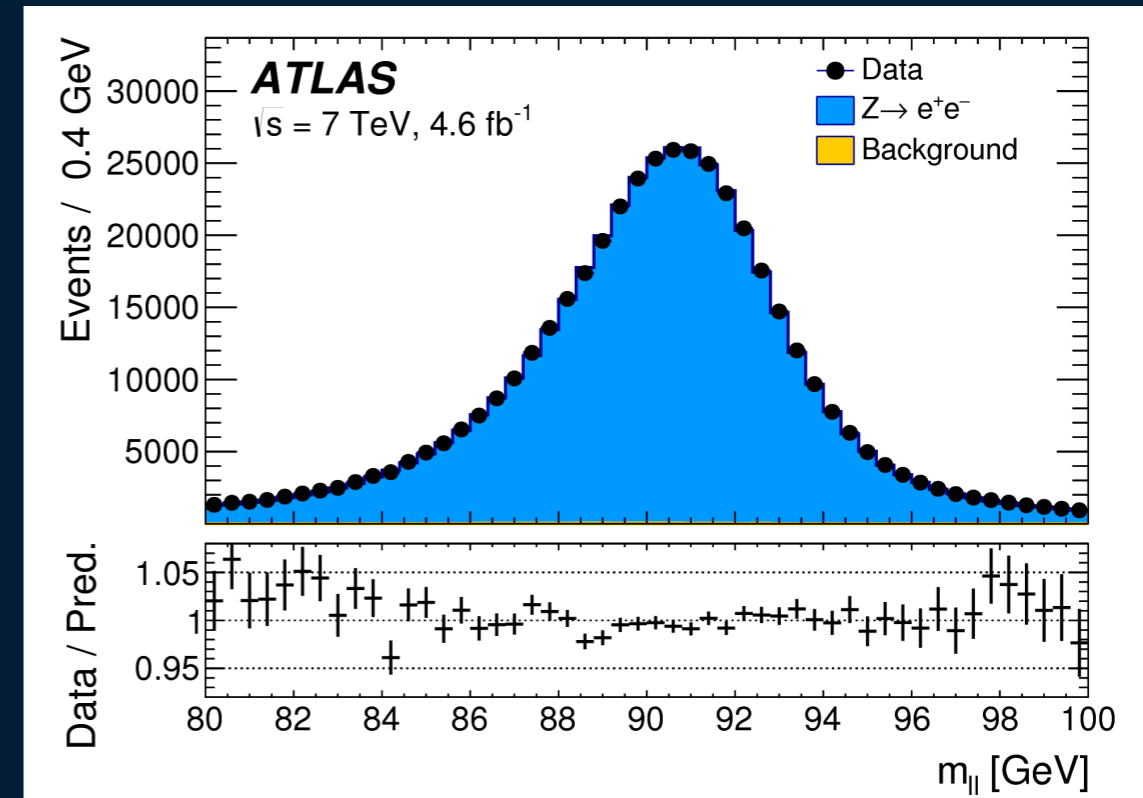
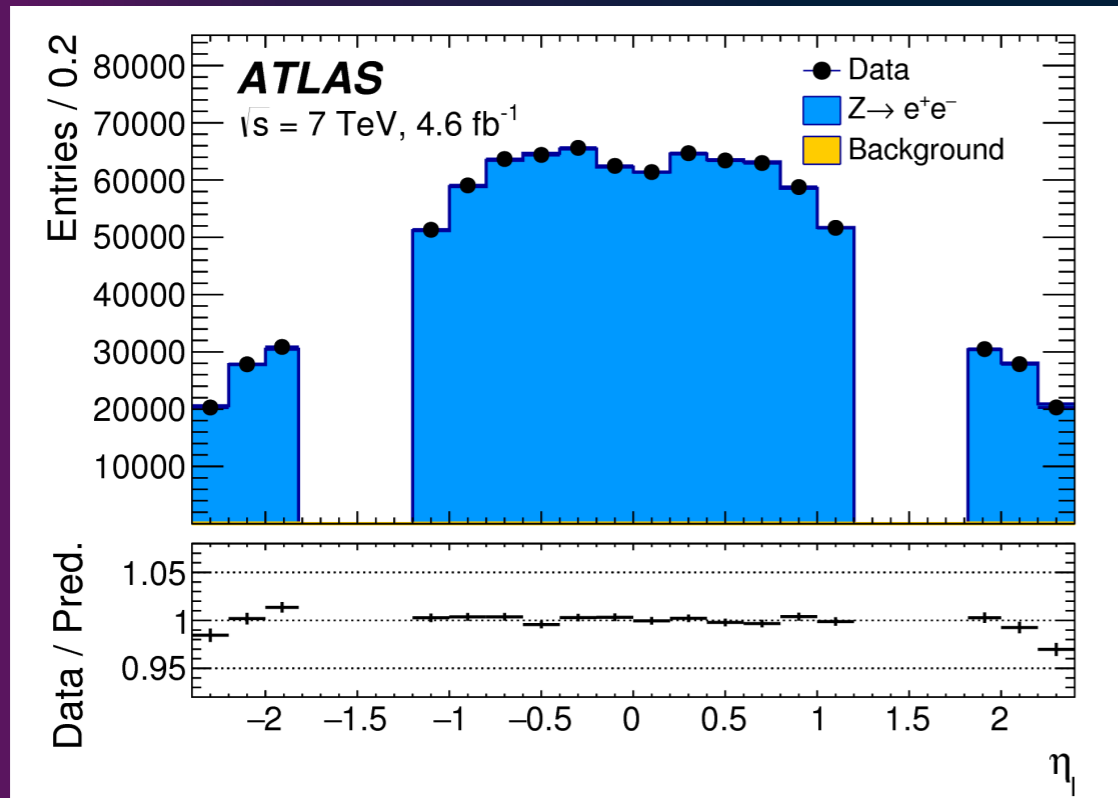


# Electron calibration

- Electron measurement : energy from the EM calorimeter; eta and phi from the ID
- Calibration sequence :
  - Calorimeter longitudinal intercalibration using muon energy deposits (  $Z \rightarrow \mu\mu$  events)
  - Passive material and presampler response corrections derived using longitudinal shower profiles of electrons and photons
  - Overall energy scale and resolution from Zee decays
- $\phi$  modulation due to mechanical deformation under gravity of the calorimeter ('pear-shape') corrected with W and Z events



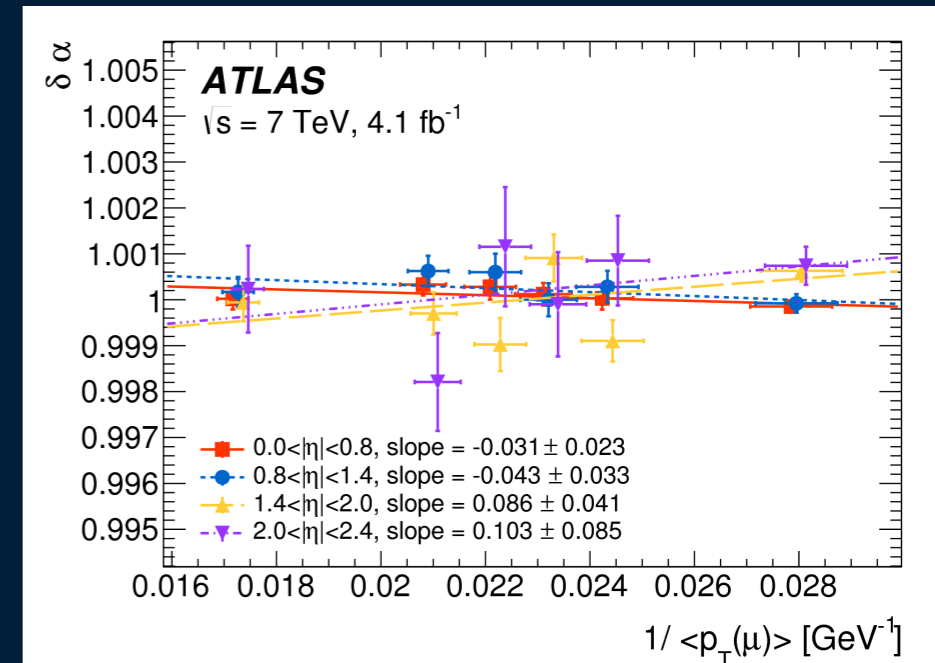
# Electron calibration



$\eta_e$   range	[0.0, 0.6]		[0.6, 1.2]		[1.82, 2.4]		Combined	
	$p_T^\ell$	$m_T$	$p_T^\ell$	$m_T$	$p_T^\ell$	$m_T$	$p_T^\ell$	$m_T$
Kinematic distribution								
$\delta m_W$ [MeV]								
Energy scale	10.4	10.3	10.8	10.1	16.1	17.1	8.1	8.0
Energy resolution	5.0	6.0	7.3	6.7	10.4	15.5	3.5	5.5
Energy linearity	2.2	4.2	5.8	8.9	8.6	10.6	3.4	5.5
Energy tails	2.3	3.3	2.3	3.3	2.3	3.3	2.3	3.3
Reconstruction efficiency	10.5	8.8	9.9	7.8	14.5	11.0	7.2	6.0
Identification efficiency	10.4	7.7	11.7	8.8	16.7	12.1	7.3	5.6
Trigger and isolation efficiencies	0.2	0.5	0.3	0.5	2.0	2.2	0.8	0.9
Charge mismeasurement	0.2	0.2	0.2	0.2	1.5	1.5	0.1	0.1
Total	19.0	17.5	21.1	19.4	30.7	30.5	14.2	14.3

# Muon calibration

- Kinematic parameters from inner tracker
  - radial and **longitudinal (sagitta)** biases
- muon momentum scale calibration using Z, extrapolation to W momentum range using  $p_{T\ell}(W)$  spectrum
- muon sagitta bias correction uses W events (E/p) and Z events



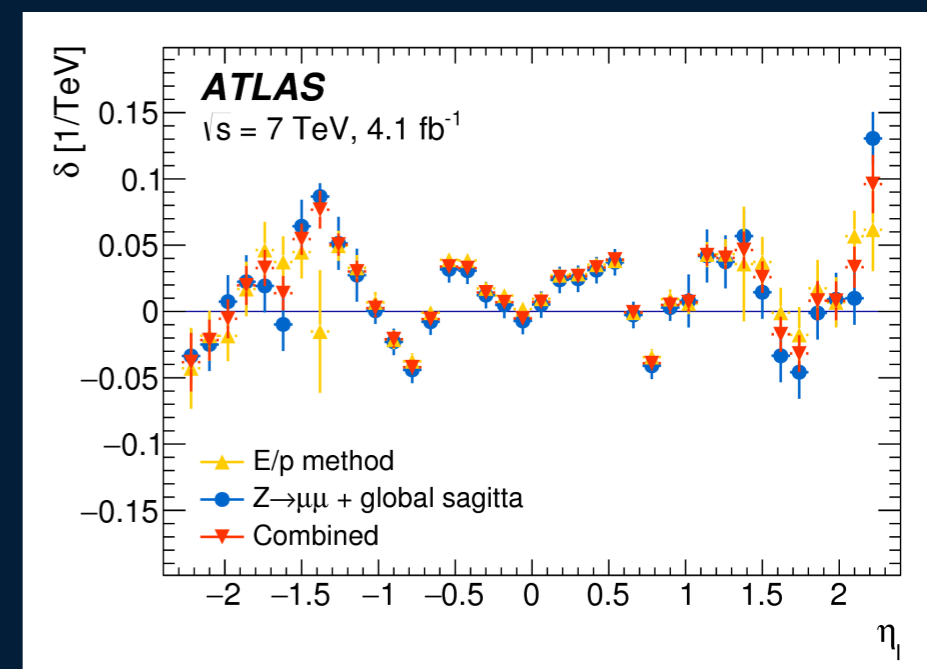
momentum scale

momentum resolution

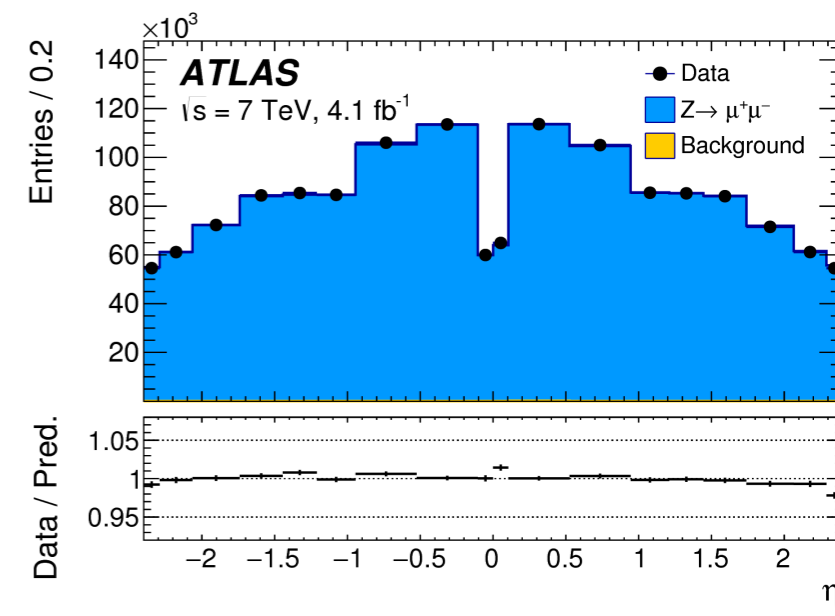
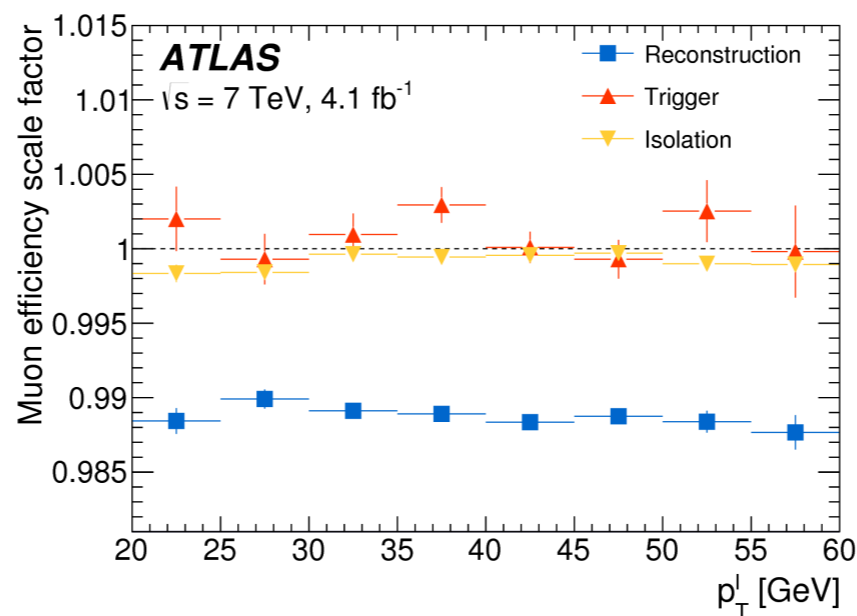
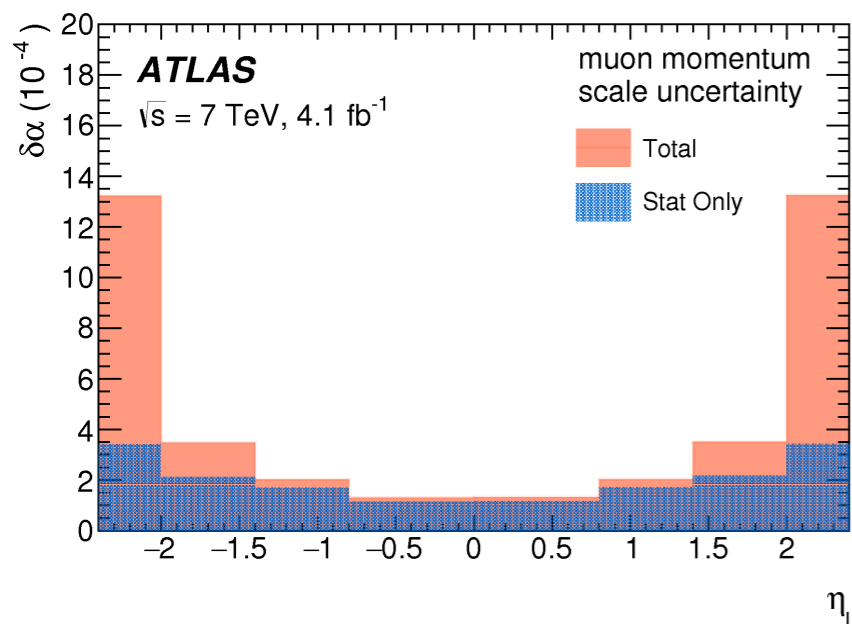
$$p_T^{\text{MC,corr}} = p_T^{\text{MC}} \times [1 + \alpha(\eta, \phi)] \times [1 + \beta_{\text{curv}}(\eta) \cdot G(0, 1) \cdot p_T^{\text{MC}}]$$

$$p_T^{\text{data,corr}} = \frac{p_T^{\text{data}}}{1 + q \cdot \delta(\eta, \phi) \cdot p_T^{\text{data}}}$$

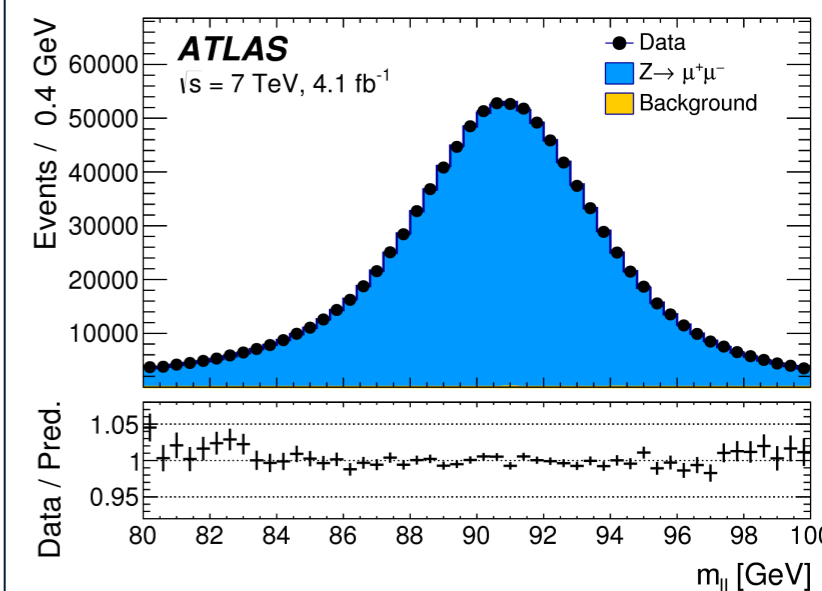
sagitta bias correction



# Muon calibration



$\eta_e$   range	[0.0, 0.8]		[0.8, 1.4]		[1.4, 2.0]		[2.0, 2.4]		Combined	
	$p_T^l$	$m_T$	$p_T^l$	$m_T$	$p_T^l$	$m_T$	$p_T^l$	$m_T$	$p_T^l$	$m_T$
$\delta m_W$ [MeV]										
Momentum scale	8.9	9.3	14.2	15.6	27.4	29.2	111.0	115.4	8.4	8.8
Momentum resolution	1.8	2.0	1.9	1.7	1.5	2.2	3.4	3.8	1.0	1.2
Sagitta bias	0.7	0.8	1.7	1.7	3.1	3.1	4.5	4.3	0.6	0.6
Reconstruction and isolation efficiencies	4.0	3.6	5.1	3.7	4.7	3.5	6.4	5.5	2.7	2.2
Trigger efficiency	5.6	5.0	7.1	5.0	11.8	9.1	12.1	9.9	4.1	3.2
Total	11.4	11.4	16.9	17.0	30.4	31.0	112.0	116.1	9.8	9.7



- As expected, uncertainties are smaller than for electron



# Background fractions

		$W \rightarrow \mu\nu$					
Category		$W \rightarrow \tau\nu$	$Z \rightarrow \mu\mu$	$Z \rightarrow \tau\tau$	Top	Dibosons	Multijet
$W^\pm$	$0.0 <  \eta  < 0.8$	1.04	2.83	0.12	0.16	0.08	0.72
$W^\pm$	$0.8 <  \eta  < 1.4$	1.01	4.44	0.11	0.12	0.07	0.57
$W^\pm$	$1.4 <  \eta  < 2.0$	0.99	6.78	0.11	0.07	0.06	0.51
$W^\pm$	$2.0 <  \eta  < 2.4$	1.00	8.50	0.10	0.04	0.05	0.50
$W^\pm$	all $\eta$ bins	1.01	5.41	0.11	0.10	0.06	0.58
$W^+$	all $\eta$ bins	0.99	4.80	0.10	0.09	0.06	0.51
$W^-$	all $\eta$ bins	1.04	6.28	0.14	0.12	0.08	0.68

		$W \rightarrow e\nu$					
Category		$W \rightarrow \tau\nu$	$Z \rightarrow ee$	$Z \rightarrow \tau\tau$	Top	Dibosons	Multijet
$W^\pm$	$0.0 <  \eta  < 0.6$	1.02	3.34	0.13	0.15	0.08	0.59
$W^\pm$	$0.6 <  \eta  < 1.2$	1.00	3.48	0.12	0.13	0.08	0.76
$W^\pm$	$1.8 <  \eta  < 2.4$	0.97	3.23	0.11	0.05	0.05	1.74
$W^\pm$	all $\eta$ bins	1.00	3.37	0.12	0.12	0.07	1.00
$W^+$	all $\eta$ bins	0.98	2.92	0.10	0.11	0.06	0.84
$W^-$	all $\eta$ bins	1.04	3.98	0.14	0.13	0.08	1.21

# Full uncertainty table

Combined categories	Value [MeV]	Stat. Unc.	Muon Unc.	Elec. Unc.	Recoil Unc.	Bckg. Unc.	QCD Unc.	EW Unc.	PDF Unc.	Total Unc.	$\chi^2/\text{dof}$ of Comb.
$m_T, W^+, e-\mu$	80370.0	12.3	8.3	6.7	14.5	9.7	9.4	3.4	16.9	30.9	2/6
$m_T, W^-, e-\mu$	80381.1	13.9	8.8	6.6	11.8	10.2	9.7	3.4	16.2	30.5	7/6
$m_T, W^\pm, e-\mu$	80375.7	9.6	7.8	5.5	13.0	8.3	9.6	3.4	10.2	25.1	11/13
$p_T^\ell, W^+, e-\mu$	80352.0	9.6	6.5	8.4	2.5	5.2	8.3	5.7	14.5	23.5	5/6
$p_T^\ell, W^-, e-\mu$	80383.4	10.8	7.0	8.1	2.5	6.1	8.1	5.7	13.5	23.6	10/6
$p_T^\ell, W^\pm, e-\mu$	80369.4	7.2	6.3	6.7	2.5	4.6	8.3	5.7	9.0	18.7	19/13
$p_T^\ell, W^\pm, e$	80347.2	9.9	0.0	14.8	2.6	5.7	8.2	5.3	8.9	23.1	4/5
$m_T, W^\pm, e$	80364.6	13.5	0.0	14.4	13.2	12.8	9.5	3.4	10.2	30.8	8/5
$m_T-p_T^\ell, W^+, e$	80345.4	11.7	0.0	16.0	3.8	7.4	8.3	5.0	13.7	27.4	1/5
$m_T-p_T^\ell, W^-, e$	80359.4	12.9	0.0	15.1	3.9	8.5	8.4	4.9	13.4	27.6	8/5
$m_T-p_T^\ell, W^\pm, e$	80349.8	9.0	0.0	14.7	3.3	6.1	8.3	5.1	9.0	22.9	12/11
$p_T^\ell, W^\pm, \mu$	80382.3	10.1	10.7	0.0	2.5	3.9	8.4	6.0	10.7	21.4	7/7
$m_T, W^\pm, \mu$	80381.5	13.0	11.6	0.0	13.0	6.0	9.6	3.4	11.2	27.2	3/7
$m_T-p_T^\ell, W^+, \mu$	80364.1	11.4	12.4	0.0	4.0	4.7	8.8	5.4	17.6	27.2	5/7
$m_T-p_T^\ell, W^-, \mu$	80398.6	12.0	13.0	0.0	4.1	5.7	8.4	5.3	16.8	27.4	3/7
$m_T-p_T^\ell, W^\pm, \mu$	80382.0	8.6	10.7	0.0	3.7	4.3	8.6	5.4	10.9	21.0	10/15
$m_T-p_T^\ell, W^+, e-\mu$	80352.7	8.9	6.6	8.2	3.1	5.5	8.4	5.4	14.6	23.4	7/13
$m_T-p_T^\ell, W^-, e-\mu$	80383.6	9.7	7.2	7.8	3.3	6.6	8.3	5.3	13.6	23.4	15/13
$m_T-p_T^\ell, W^\pm, e-\mu$	80369.5	6.8	6.6	6.4	2.9	4.5	8.3	5.5	9.2	18.5	29/27

# lepton uncertainty tables

$ \eta_e $ range	[0.0, 0.8]		[0.8, 1.4]		[1.4, 2.0]		[2.0, 2.4]		Combined	
	$p_T^\ell$	$m_T$	$p_T^\ell$	$m_T$	$p_T^\ell$	$m_T$	$p_T^\ell$	$m_T$	$p_T^\ell$	$m_T$
Kinematic distribution										
$\delta m_W$ [MeV]										
Momentum scale	8.9	9.3	14.2	15.6	27.4	29.2	111.0	115.4	8.4	8.8
Momentum resolution	1.8	2.0	1.9	1.7	1.5	2.2	3.4	3.8	1.0	1.2
Sagitta bias	0.7	0.8	1.7	1.7	3.1	3.1	4.5	4.3	0.6	0.6
Reconstruction and isolation efficiencies	4.0	3.6	5.1	3.7	4.7	3.5	6.4	5.5	2.7	2.2
Trigger efficiency	5.6	5.0	7.1	5.0	11.8	9.1	12.1	9.9	4.1	3.2
Total	11.4	11.4	16.9	17.0	30.4	31.0	112.0	116.1	9.8	9.7

$ \eta_e $ range	[0.0, 0.6]		[0.6, 1.2]		[1.82, 2.4]		Combined	
	$p_T^\ell$	$m_T$	$p_T^\ell$	$m_T$	$p_T^\ell$	$m_T$	$p_T^\ell$	$m_T$
Kinematic distribution								
$\delta m_W$ [MeV]								
Energy scale	10.4	10.3	10.8	10.1	16.1	17.1	8.1	8.0
Energy resolution	5.0	6.0	7.3	6.7	10.4	15.5	3.5	5.5
Energy linearity	2.2	4.2	5.8	8.9	8.6	10.6	3.4	5.5
Energy tails	2.3	3.3	2.3	3.3	2.3	3.3	2.3	3.3
Reconstruction efficiency	10.5	8.8	9.9	7.8	14.5	11.0	7.2	6.0
Identification efficiency	10.4	7.7	11.7	8.8	16.7	12.1	7.3	5.6
Trigger and isolation efficiencies	0.2	0.5	0.3	0.5	2.0	2.2	0.8	0.9
Charge mismeasurement	0.2	0.2	0.2	0.2	1.5	1.5	0.1	0.1
Total	19.0	17.5	21.1	19.4	30.7	30.5	14.2	14.3

## Weights of all categories

Observable	Channel	$\eta$ range	Weight
$m_T$	$W^+ \rightarrow \mu\nu$	$ \eta  < 0.8$	0.018
		$0.8 <  \eta  < 1.4$	0.022
		$1.4 <  \eta  < 2.0$	0.003
		$2.0 <  \eta  < 2.4$	0.006
	$W^- \rightarrow \mu\nu$	$ \eta  < 0.8$	0.020
		$0.8 <  \eta  < 1.4$	0.018
		$1.4 <  \eta  < 2.0$	0.022
		$2.0 <  \eta  < 2.4$	0.001
	$W^+ \rightarrow e\nu$	$ \eta  < 0.6$	0.013
		$0.6 <  \eta  < 1.2$	0.001
		$1.8 <  \eta  < 2.4$	0.010
	$W^- \rightarrow e\nu$	$ \eta  < 0.6$	0.008
$0.6 <  \eta  < 1.2$		0.000	
$1.8 <  \eta  < 2.4$		0.002	
$p_T^\ell$	$W^+ \rightarrow \mu\nu$	$ \eta  < 0.8$	0.101
		$0.8 <  \eta  < 1.4$	0.076
		$1.4 <  \eta  < 2.0$	0.050
		$2.0 <  \eta  < 2.4$	0.011
	$W^- \rightarrow \mu\nu$	$ \eta  < 0.8$	0.097
		$0.8 <  \eta  < 1.4$	0.071
		$1.4 <  \eta  < 2.0$	0.047
		$2.0 <  \eta  < 2.4$	0.010
	$W^+ \rightarrow e\nu$	$ \eta  < 0.6$	0.056
		$0.6 <  \eta  < 1.2$	0.071
		$1.8 <  \eta  < 2.4$	0.081
	$W^- \rightarrow e\nu$	$ \eta  < 0.6$	0.062
$0.6 <  \eta  < 1.2$		0.056	
$1.8 <  \eta  < 2.4$		0.067	

# Post-fit data-mc plots (W-, electron)

